UNIVERSITÀ DEGLI STUDI DI VERONA

DIPARTIMENTO DI BIOTECNOLOGIE

SCUOLA DI DOTTORATO IN SCIENZE DELLA VITA E DELLA SALUTE

DOTTORATO DI RICERCA IN BIOTECNOLOGIE MOLECOLARI, INDUSTRIALI ED AMBIENTALI

CICLO /ANNO XXIV /2009

RICERCA E DETERMINAZIONE QUANTITATIVA DI PROTEINE DI INTERESSE BIOMEDICO ATTRAVERSO TECNICHE DI PROTEOMICA DIFFERENZIALE E BIOSENSORI

DISCOVERY AND QUANTIFICATION OF PROTEINS OF BIOLOGICAL RELEVANCE THROUGH DIFFERENTIAL PROTEOMICS AND BIOSENSING

REALIZZATA IN COTUTELA CON L'UNIVERSITÀ DI CRANFIELD (UK) S.S.D. BIO/10

Coordinatori: Per l'Università di Verona
Prof. Roberto Bassi

Per l'Università di Cranfield
Prof. Naresh Magan

Tutori: Per l'Università di Verona
D.ssa Alessandra Maria Bossi
D.ssa Daniela Cecconi

Per l'Università di Cranfield
D.ssa Iva Chianella

Dottorando: Dott. Francesco Lonardoni

Riassunto

La linea generale su cui si sviluppa il mio progetto di dottorato è la ricerca e misurazione quantitativa di biomarcatori, ed è inserito nel più ampio campo della diagnostica medica.
Un biomarcatore è definito in modo chiaro dalla Food and Drug Administration statunitense come “una caratteristica che sia oggettivamente misurabile e valutabile come indicatore di processi fisiologici o patologici o di risposta a trattamento con farmaci”.
La ricerca moderna ha compiuto passi da gigante negli ultimi decenni, e ad un ritmo sempre crescente ha portato ad un’esplosione di metodiche e risultati scientifici impensabili anche solo due decenni fa. In particolare lo sviluppo di tecniche come la Risonanza Magnetica Nucleare, la Tomografia Assiale Computerizzata, la Spettroscopia di Massa oltre ai progressi della chimica e dell’informatica hanno accelerato il processo della conoscenza del corpo umano e di ciò che può minacciare il suo benessere.
La ricerca di un marcatore di patologia è in realtà un processo molto ampio, che parte dalla conoscenza approfondita iniziale della malattia, partendo dalla sua espressione esteriore per poi passare all’identificazione delle cause, su cui lavorare per prevenirne gli effetti, talora drammatici.
L’eziologia di una patologia può essere esteriore od interiore al nostro corpo, o addirittura alla loro interfaccia nella particolare fase di vita simbiotica che è la gestazione. Diverse concause possono in effetti alterare il delicato equilibrio di crescita intrauterino, con il risultato di minacciare il benessere di madre e/o feto. Uno di questi effetti può essere il ritardo di crescita intrauterino, patologia che nei paesi sviluppati colpisce da uno a tre neonati su mille compromettendone il benessere fisico e/o psichico alla nascita e/o nella vita futura. La ricerca ci ha fornito i mezzi per studiare questa condizione, in particolare nella scoperta dei meccanismi che la causano, spesso evidenziati da una presenza alterata di alcune proteine. La proteomica differenziale è la metodica per rilevare questo scostamento da una condizione fisiologica equilibrata, ed il primo progetto di ricerca di questo

periodo di dottorato è stato proprio rivolto a questo: un'analisi proteomica differenziale su siero di cordone ombelicale e fluido amniotico alla ricerca di biomarcatori di ritardo di crescita intrauterino, una patologia altrimenti detta IUGR (Intra Uterine Growth Restriction).

Nel progetto in questione sono stati analizzati campioni di siero di cordone ombelicale e fluido amniotico provenienti da madri al termine della gravidanza, per le quali sia stato diagnosticato (si parla di "casi") o meno ("controlli") un ritardo di crescita intrauterino. Con la tecnica della elettroforesi bidimensionale su gel di poliacrilammide (2D-PAGE) la moltitudine di proteine presenti nei suddetti campioni è stata dipanata, in modo da identificare separatamente le singole proteine sovra- o sottoespresse in caso di patologia. Il risultato è stato l'identificazione di 14 proteine uniche nel siero e 11 nel cordone ombelicale, concorrenti complessivamente a determinare un quadro d'insieme della patologia. Queste proteine sono coinvolte in processi alterati nel caso di ritardo di crescita intrauterino, in particolare: coagulazione del sangue, pressione sanguigna, difese immunitarie, omeostasi di ferro e rame, stress ossidativo. I risultati forniti dall'elettroforesi bidimensionale sono stati validati in modo incrociato con un'altra tecnica, il Western Blot, applicato su 5 proteine scelte per importanza fisiologica o livello di sovra- o sottoespressione. Di particolare spicco nel determinare il quadro complessivo di modulazione proteica sono state: transferrina (coinvolta nel trasporto di ossigeno nel sangue), kininogeno (coinvolta nei processi di coagulazione e di modulazione della pressione sanguigna), fibrinogeno (coinvolta nel processo di coagulazione del sangue), angiotensinogeno (uno dei soggetti implicati nella regolazione della pressione sanguigna) e componente C3 del complemento (complesso proteico implicato nella cosiddetta "immunità innata").

Ma se la ricerca applicata si avvale di potenti metodiche è perché a monte c'è stato un altrettanto importante lavoro di messa a punto delle stesse. Questo lavoro è svolto generalmente da équipe che si occupano di diversi aspetti del problema da affrontare. Diverse condizioni patologiche sono innescate da un' alterazione di un meccanismo fisiologico in particolare: la

comunicazione attraverso la fosforilazione delle proteine, facente parte del gruppo delle cosiddette modificazioni post-traslazionali (PTM, Post Translational Modifications). Queste sono modificazioni chimiche delle proteine nella fase successiva alla loro sintesi ribosomiale, che a valle di una serie di passaggi trasforma in una molecola effettiva l'informazione potenziale contenuta nel DNA. Alterazioni in questo processo biologico sono causa di gravi malattie come cancro, neurodegenerazione e diabete e l'avanzamento della tecnologia è lo strumento per approfondirne la conoscenza. In particolare gli studi degli scienziati hanno fatto emergere la necessità di nuovi materiali per la cattura delle fosfoproteine, soggetti rari in un mare di proteine non fosforilate. Allo scopo una tecnologia promettente è lo stampo molecolare di polimeri, che sfrutta la molecola oggetto di analisi per formare attorno a sé una tasca complementare ad essa, in grado di riconoscerla e legarla successivamente quando rimossa dalla matrice stessa. Data poi la dimensione nanometrica delle proteine, lavorare sulla stessa scala dimensionale favorisce l'efficacia del riconoscimento delle molecole, come avviene per l'interazione antigene-anticorpo. L'idea che nasce da questa premessa è quindi quella della sintesi e caratterizzazione di nanoparticelle stampate molecolarmente per il riconoscimento di fosfoproteine e fosfopeptidi: il secondo progetto seguito durante questo periodo di dottorato di ricerca.

La fase sperimentale ha portato a sintetizzare e caratterizzare fisicamente nanoparticelle (cioè particelle aventi almeno una dimensione al di sotto dei 100 nanometri) di copolimeri con 4 ricette diverse, in presenza o meno del templato: fosfotirosina protetta all'azoto terminale con fluorenilmetossicarbonile (Fmoc). La fase di verifica delle proprietà di legame è stata effettuata su una ricetta delle quattro, preparata stavolta con metodo standardizzato, ovvero non sotto forma di nanoparticelle. Si è valutata la capacità di legare fosfotirosina in sue soluzioni a concentrazione crescente.

I risultati vedono una tendenza di legame a saturazione nel polimero stampato, mentre un accumulo crescente di substrato nel caso del polimero non stampato.

Ma l'individuazione dei marcatori di patologie è solo una fase del processo della diagnosi medica: una volta individuato un marcatore di patologia è necessario mettere a punto un metodo di misura dello stesso. Questo metodo dovrà essere il più possibile sensibile alle concentrazioni dell'analita nel campione in esame e specifico per esso, in modo da non confondere un segnale derivante da un fondo di molecole con la sua presenza. Un grosso beneficio alla condizione del paziente può anche derivare dalla possibilità di misurare l'analita nel luogo dove si trova la persona, attuando così quella che si chiama "point of care diagnostics". A tale scopo esistono delle tecniche analitiche che più si prestano alla realizzazione di dispositivi portatili semplici: una di queste è la risonanza plasmonica superficiale (Surface Plasmon Resonance, SPR). La terza parte del mio periodo di dottorato è stata quindi dedicata alla messa a punto di un metodo di rilevazione di un ormone peptidico, l'epcidina, sfruttando la suddetta tecnica. L'analita in questione è il principale regolatore del metabolismo del ferro, e la realizzazione di una metodica analitica sensibile ed efficace per la sua misurazione è considerata essere effettivamente necessaria dalla comunità scientifica internazionale.

I risultati ottenuti in questa parte sperimentale sono stati la creazione di una curva di calibrazione per l'epcidina in concentrazioni nel range pato-fisiologico 1-100ng/mL, una verifica della scarsa interazione del nostro sistema di cattura dell'epcidina nei confronti di un suo competitore, una sua forma troncata, più la valutazione della costante di affinità dell'analita per il legante utilizzato nella cattura, risultata essere 50nM, quindi in linea con precedenti misurazioni in soluzione.

Date le premesse fin qui espresse ritengo che il lavoro da me svolto si inserisca in un panorama di grande interesse per il benessere di ognuno di noi. Spero solo di aver dato un contributo piccolo ma sensibile all'impulso della ricerca, in particolare in Italia.

Preface

The general outline of my 3 year PhD period work focuses on the discovery and quantification of proteins and peptides of biological relevance. This general aim is branched in different research subjects.

Medical diagnosis is the process of attempting to determine and/or identify a possible disease or disorder. Diagnostics has made many steps forward in the last decades with the advent and progress of powerful techniques, like imaging techniques (NMR, PET), mass spectrometry, bioinformatics and genomic tools. Big leaps have been done also specifically in the biochemical field, particularly in the identification and quantity evaluation of molecules whose presence in human body increases or decreases following a pathological condition.

The Food and Drug Administration (FDA) defines a biomarker as “a characteristic that is objectively measured and evaluated as an indicator of normal biologic processes, pathogenic processes, or pharmacologic responses to a therapeutic intervention”. Biomarker discovery is a long process which starts from the study of the characteristics of the organism of interest. The genomic approach reveals the potential characteristics of the organism, subsequently expressed in a protein pattern through the transcriptional and translational steps, eventually followed by the post-translational modifications.

The “proteome” is defined as the entire wealth of PROTEins expressed by the genOME. This is a very kaleidoscopic entity, different from subject to subject and different in different stages of life, or in different situations to which an organism can be exposed. Proteins are subjected to Post Translational Modifications (PTM, e.g. glycosylation, phosphorylation, deamydation, splicing) and these runaway modifications often correlate with alterations from the normal setup. A proteomic approach takes a picture of a particular stage of life of an organism, and permits to compare the different general protein patterns in different situations, e.g. from a normal to a disease state.

Due to the large number of different proteins (thousands in a single cell) and their high differential expression (it can span 10 orders of magnitude in human blood) a single stage of separation is not enough to analyze them singularly. First of all prefractionation techniques to separate different parts of a cell (membrane, citosol, nuclei, etc.) or different fractions of a liquid (blood, urine, CSF, synovial fluid) are needed to reduce the complexity. Then orthogonal techniques have to be applied. These techniques exploit the different physical-chemical characteristics of proteins, e.g. molecular mass, isoelectric point, hydrophilicity. Nowadays the most established technique to take a snapshot of this changing entity is 2D gel electrophoresis (2-DE). Other orthogonal techniques are being used as well. MudPIT (Multidimensional Protein Identification Technology), for example, combines Strong Cation Exchange chromatography (SCX) and Reversed Phase chromatography (RP) to separate proteins and peptides in liquid phase on-line, and has the advantage to be directly interfaced to a mass spectrometer (MS) improving sensitivity and resolution.

Particular fractions of the proteome can be separately analyzed. One important case is phosphorylation, the most widespread and studied PTM. Also in this case there are most established techniques to selectively catch and analyze phosphorylated proteins and peptides, with the aim of characterize phosphorylation pathways and find abnormalities in their regulation, frequent in many diseases like cancer or neurodegeneration. In order to improve our understanding of these networks, with the aim of finding new drug targets or biomarkers, improvements at all the analysis levels are needed. One critical step is the enrichment of phosphopeptides, not enough efficient for a comprehensive covering of this chemically heterogeneous class of molecules.

Once found a protein or peptide of biological value, its relevance as biomarker has to be validated on a wide group of subjects. Then its routine measurement can be needed in health screenings, possibly carried out with fast and cheap methods. Regarding this goal, biosensors can be particularly suitable. These are devices made of a bioreceptor molecule, able to bind to

or react with the analyte of interest, a transducing system that converts the biological event into an electric signal, and the data analysis system, that elaborates this signal to show the final parameter(s) to the operator.

My 3 years PhD period has evolved in this panorama, spanning from the biomarkers/drug targets discovery to assays/biosensors development.

The first project that I followed exploited proteomic techniques to find relevant protein markers for Intrauterine Growth Restriction (IUGR) in cordonal blood and amniotic fluid, to shed some light in the pathology mechanisms and furnishing a tool for an early diagnosis of the disease.

I moved then on the production of Molecularly Imprinted Polymers, with the final goal of selectively extract phosphopeptides from a peptide mixture and thus find alternatives for the grasp of the phosphoproteome.

Finally I stepped into the biosensors field, focusing my work on the detection of hepcidin peptide hormone, the major subject in iron homeostasis in vertebrates and marker of iron unbalance diseases.

All this work has been done keeping fix one idea in my mind: everybody that works in this field faces the challenge and has the inspiring aim of improve, maybe just a bit and in a not immediately clear way, the health of anybody of us.

The proteomics work discussed in this thesis was carried out in Mass Spectrometry and Proteomics lab at the Biotechnology Department of the University of Verona (Italy), in collaboration with the Department of Environmental Medicine and Public Health and the Department of Gynecological Sciences and Reproductive Medicine of Padova (Italy), that provided the biological samples. This study was approved by the Ethical Committee of Padova University Hospital, after obtaining written informed consent from the mothers of the foetuses.

The work on Molecularly Imprinted Polymers and the development of the SPR biosensor was performed in the Biochemical Methodologies and Molecular Imprinting Laboratory at the Biotechnology Department of University of Verona (Italy) and in Health Department of Cranfield University (Bedfordshire, UK). The results obtained are here discussed and evaluated.

Contents

List of abbreviations

2D-PAGE: Two Dimensional Polyacrylamide Gel Electrophoresis
AA: Acrylamide
AC: Abdominal Circumference
AF: Amniotic Fluid
AFM: Atomic Force Microscopy
AQUA: Absolute Quantification of proteins
BAP: 1,4-bis(acryloyl)piperazine
BIS: N,N'methylene-bis-acrylamide
BPD: Bipariethal Diameter
CHAPS: 3[(3-cholamidopropyl) dimethylammonium]-1-propanesulfonate
CID: Collision Induced Dissociation
CPP: Calcium Phosphate Precipitation
CRL: Crown-Rump Length
DAU: 1,3 diallylurea
DC: Detergent Compatible
DHB: Dihydroxybenzoic Acid
DLS: Dynamic Light Scattering
DPIC: Diphenyliodonium chloride
DTT: Dithiothreitol
ECD: Electron Capture Dissociation
ECL: Enhanced Chemiluminescence
EDC: 1-ethyl-3-(3-dimethylaminopropyl) carbodiimide
ELISA: Enzyme-Linked Immuno Sorbent Assay
ERLIC: Electrostatic Repulsion - Hydrophilic Interaction Chromatography
ESI: Electrospray Ionization
ETD: Electron Transfer Dissociation
Eth: Ethanolamine
FL: Femur Length
Fmoc-: Fluorenylmethyloxycarbonyl-
GO: Gene Ontology
HAMMOC: Hydroxy Acid Modified Metal Oxide Chromatography
HAP: hydroxyapathite
HBD: Hepcidin-Binding Domain
HC: Head Circumference
HEMA: 2-hydroxyethyl methacrylate
HH: Hereditary Haemocromatosis
HILIC: Hydrophilic Interaction Chromatography
HSA: Human Serum Albumin
ICPL: Isotope-Coded Protein Label
IDA: Iminodiacetic Acid
IEF: Isoelectric Focusing
IFC: Integrated Microfluidic Cartridge
IMAC: Immobilized Metal Affinity Chromatography
IP: Immunoaffinity Purification
IPG: Immobilized pH Gradient
IT: Ion Trap
iTRAQ: isotope Tags for Relative and Absolute Quantification
IUGR: Intra Uterine Growth Restriction
K_D: Equilibrium Dissociation constant
LCQ: Liquid Chromatography Quadrupole
LTQ: Linear Trap Quadrupole
MALDI: Matrix Assisted Laser Desorption Ionization
MB: Methylene blue
MIP: Molecularly Imprinted Polymer
MOAC: Metal Oxide Chromatography
MP: Multiplex Proteomics

MS: Mass Spectroscopy
MSA: Multi-Stage Activation
MW: Molecular Weight
M/Z: Mass/charge ratio
NHS: N-hydroxysuccinimide
NTA: Nitrilotriacetic Acid
OD: Optical Density
PAC: Phosphoramidate Chemistry
PAIs: Protein Abundance Indexes
pdMS3: phosphorylated directed fragmentation
pI: Isoelectric point
PVDF: Polyvinylidene Difluoride
QQQ: Triple Quadrupole
RAS: Renin-Angiotensin System
RP: Reversed Phase
SALDI: Surface Assisted Laser Desorption/Ionization
SAX: Strong Anion exchange chromatography
SCX: Strong Cation exchange chromatography
SDS: Sodium Dodecyl Sulphate
SEM: Scanning Electron Microscopy
SGA: Small for Gestational Age
SILAC: Stable Isotope Labeling with Aminoacids in Cell culture
SIMAC: Sequential elution from IMAC
SPM: Scanning Probe Microscopy
SSP: Standard Spot numbering
TBP: Tributylphosphine
TED: Tris(carboxymethyl)ethylenediamine
TEM: Transmission Electron Microscopy
TOF: Time-Of-Flight
TSIA: Toluensulphinic Acid
UC: Umbilical Cord
WCX: Weak Cation Exchange
XIC: Extracted Ion Chromatogram
XPS: X-ray Photoelectron Spectroscopy

Chapter 1

DISCOVERY OF NEW PROTEIN MARKERS FOR INTRAUTERINE GROWTH RESTRICTION

1 Introduction

Foetus growth is a complex process driven basically by four factors: maternal, placental, genetic and external (1). All these factors are intimately correlated in determining a harmonic growth of the foetus. An unbalance of one or more of them can determine little or bigger alterations in foetus' wellbeing. In modern hospitals foetus growth is monitored throughout the pregnancy with several exams at well determined periods of the expected 40 weeks of gestation. Ecography is the most renowned method, by which different metric parameters are measured: head circumference (HC), biparietal diameter (BPD), femur length (FL), abdominal circumference (AC), crown-rump length (CRL) and Humerus Length (HL) (figure 1) (2). Other routinary exams are cardiotocography (foetus heart beat), eco-doppler (evaluation of blood flux from mother to foetus and *vice-versa*) and mother's urine and blood analysis (biochemical analysis).

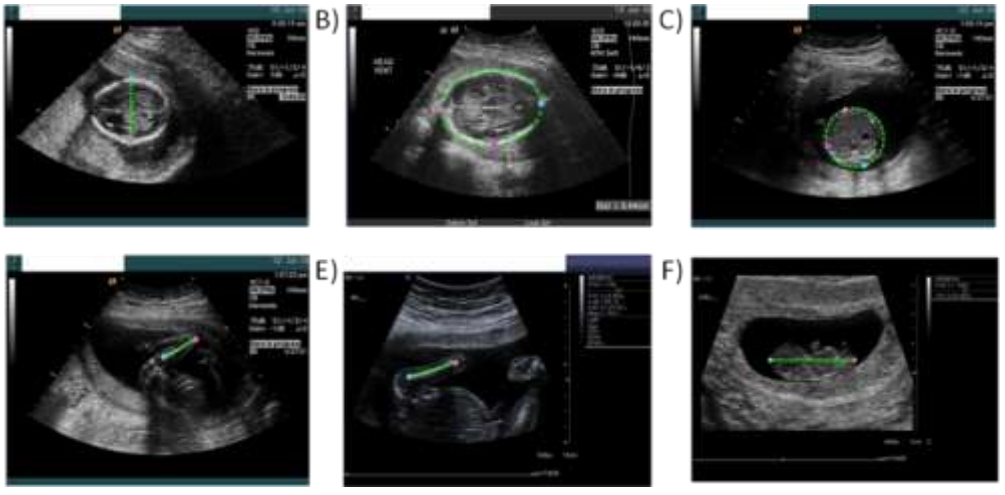

Figure 1. *Foetal segmentation measured through ecography: A) BPD, B) HC, C) AC, D) FL, E) HL, F) CRL (Pictures taken from: Carneiro G, Georgescu B, Good S, Comaniciu D, IEEE Transactions on Medical Imaging 2008, 27, 1342-1355).*

The foetus weight is normally estimated through ecographic measurements, e.g. AC as single parameter has a good correlation with the weight (2) and normally follows a sigmoidal trend, therefore it is more pronounced in the middle of the gestational period (figure 2). Customized growth charts made on homogeneous populations are available and are used in order to assess the normal increase of the foetus weight (3).

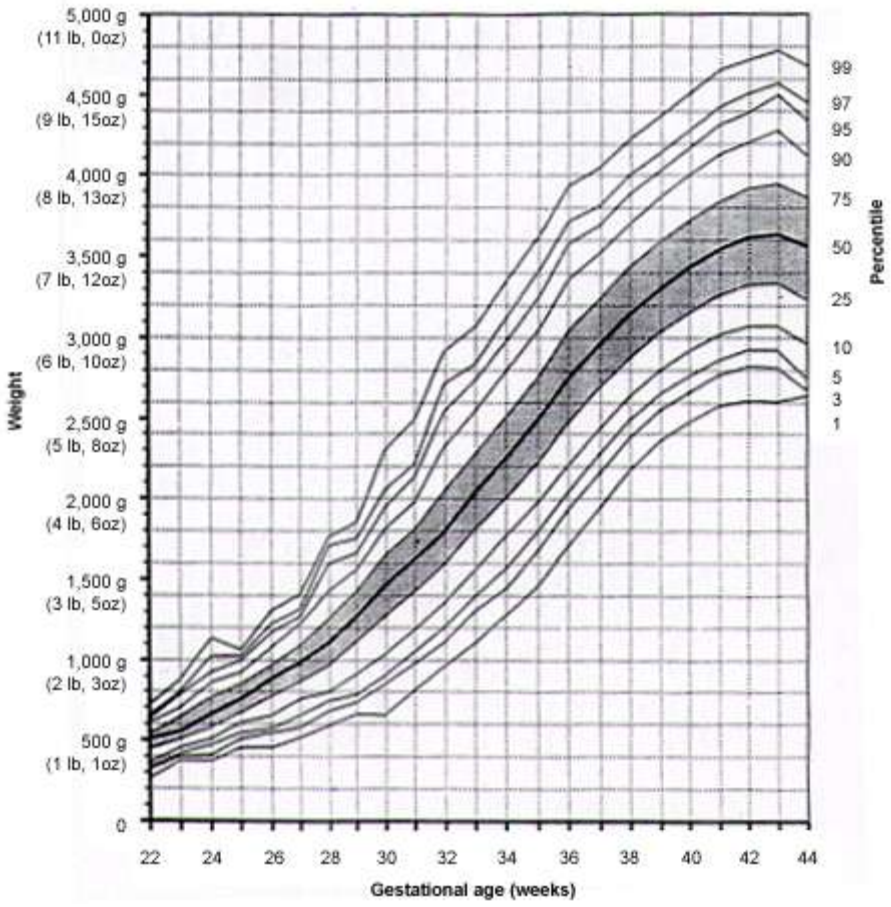

Figure 2. *Sigmoidal trend of foetus' weight increase during the gestational period (Picture taken from: Peleg D, Kennedy CM, Hunter SK. Am Fam Physician. 1998 Aug 1;58(2):453-460).*

When the weight is less than the 10th customized centile we speak about a small for gestational age foetus (SGA). This small size can be physiological, i.e. due to factors like parity or altitude that normally reduce the weight, otherwise a pathological condition can be present and it has to be carefully considered by ostetricians. In this case we speak about intrauterine growth restriction (IUGR).

The discrimination between SGA and IUGR is normally determined through a series of ecographic measurements with 2 weeks of delay: if the growth shows an accentuated slowdown a pathological condition is present, and actions have to be taken in order to secure the best health condition for the foetus and the mother. This condition is in fact related to serious problems for the foetus, both perinatally, carrying increased morbidity and mortality, and for the adult life bringing metabolic and cognitive deficits (4). Apart the cases where hormonal therapy is effective (5) no proven therapy in uterus is nowadays available, and a decision has to be taken in letting the foetus grow in adverse conditions or program the delivery. This decision is normally taken considering the gestational age, that has to be evaluated as more precisely as possible (2). Obstetrical management is therefore critical, and subjected to law regulation and juridical disputes. In this context legal medicine plays a role in ascertain when a not proper obstetrical management was present, having consequences as health problems of the foetus and/or the mother (6). The growing number of juridical disputes raises the need of a precise determination of the period when the pathological condition emerged (damage timing) and if it was not seen. This determination can be made *a posteriori*, evaluating the presence of biomarkers in cordonal blood serum or amniotic fluid.

Amniotic fluid (AF), routinely used for prenatal diagnosis, contains large amounts of proteins produced by the amnion epithelial cells, foetal tissues, foetal excretions, and placental tissues. Additionally, molecules originating from maternal circulation are released in the amniotic cavity. The biochemical composition of AF is modified throughout pregnancy and its protein profile reflects both physiological and pathological changes affecting the foetus and the mother (7), (8). Identification of changes in the balance of proteins, therefore, may be used to detect a particular type of pathology, or to identify a specific genetic disorder. Potential biomarkers in AF have already been identified in cases of inflammation and premature rupture of foetal membranes (9), (10).

Umbilical cord (UC) blood drawn from the doubly clamped umbilical cord at delivery reflects the foetal blood compartment. Along these lines, the cord blood levels of various growth factors and hormones have been related to size at birth by several groups (11), (12). Protein S100B is a recently identified UC blood protein able to assess newborn brain damage (13). Other established anoxy markers are umbilical cord blood pH, uric acid, cytokines and lactate levels in umbilical vein (14), (15).

The purpose of this project is to investigate the differential protein expression levels in UC serum (UCS) and amniotic fluid (AF) in IUGR, to produce information on the causes and mechanisms of prenatal disorders and reveal possible markers for postnatal complications and disease progression. Moreover, as said before, new markers for precision and accuracy improvement of damage timing are needed, in order to assess possible responsibilities of a not proper obstetrical treatment.

The chosen experimental technique is two-dimensional polyacrylamide gel electrophoresis (2D-PAGE), a well established tool for proteomic analysis that can be used to compare patterns of protein expression in various biological materials under physiological and pathological conditions. MS, in association with bioinformatics, provides the tool for the identification of protein spots on 2D-PAGE maps. In the next paragraph this technique will be explained in detail.

2 Two-dimensional gel electrophoresis (2D-PAGE)

In 2D-PAGE proteins in a sample are separated in two dimensions according respectively to their isoelectric point (pI) and molecular mass (MW). The technique includes sample preparation, protein separation through gel electrophoresis, protein detection, digestion of the differentially expressed proteins and their identification with MS and bioinformatic tools (figure 3).

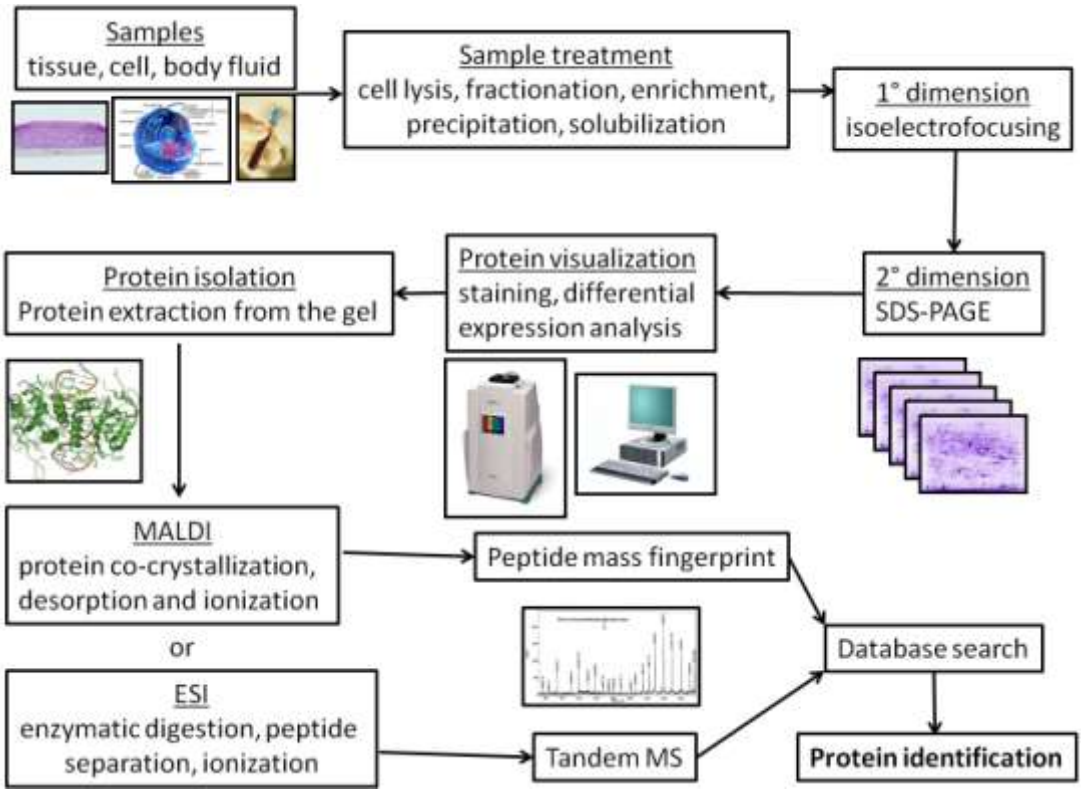

Figure 3. *Workflow of a clinical proteomics analysis, i.e. regarding clinical samples and molecular medicine studies. MALDI: Matrix Assisted Laser Desorption Ionization; ESI: Electrospray Ionization.*

2.1 Sample preparation

Normally proteins are in a first step extracted from a complex media, like a cell culture or a body fluid, and treated to remove impurities like nucleic acids, lipids, salts and sugars. This step can be done for example on serum samples through acetone precipitation and centrifugation: impurities will be mostly present in the supernatant and proteins can be isolated as pellet. These are subsequently solubilized in a highly dispersive media, like 7M urea, 2M thiourea plus 3% surfactant (e.g. 3[(3-cholamidopropyl) dimethylammonium]-1-propanesulfonate, “CHAPS”, a sulfobetainic zwitterionic detergent) Tris buffer. In order to remove nucleic acids a prolonged centrifugation at high speed (e.g.14000 x g x 40’) is usually effective, otherwise the use of ampholytes can suit the purpose of precipitate them, subsequently removed by centrifugation. In order to improve the solubilisation, sulfur bridges are broken by using a reducing agent like tributhylphosphine (TBP) and –SH groups are prevented to be re-formed

through iodoacetamide or acrylamide (AA) blocking. This operation also avoids the creation of fake omo and etero-oligomers due to –SH recombination (16).

2.2 Protein separation

The samples are then loaded onto polyacrylamide strips with an immobilized pH gradient (IPG strips) and the applied voltage induces proteins to migrate depending on their charge, variable along the strip. When they are in a region with pH corresponding to their pI they stop due to a null net charge. This first separation is furtherly amplified with a second dimension. The IPG strips are equilibrated in a solution containing sodium dodecyl sulphate (SDS), which binds to proteins proportionally to the number of aminoacidic residues (about 1 SDS molecule every 2 residues), conferring to every protein a negative charge proportional to its molecular weight. The strip is then interfaced on a side of a polyacrylamide gel slab through agarose gel bridging. A second electrophoretic migration along the gel matrix separates proteins with the same pI but different MW. More maps are produced with different samples to evaluate the statistical variation, both analytical and biological.

2.3 Detection of proteins

Protein spots in the gel are then stained to be visualised and therefore evaluate protein amounts. A common stain is colloidal Coomassie blue (17), while other stains are SyproRuby. RuBPS (both fluorescent) (18) and Silver staining (the most sensitive but at the same time difficult to control for not reaching an equilibrium in the staining process) (19). Each of these methods is compatible with the downstream MS analysis.

The gel images are then acquired and digitized, to be furtherly analysed with dedicated software like PDQuest, Melanie, Phoretic and Progenesis Gel images are superimposed to match protein spots, in order to compare quantities of the same protein between the gels and find modulations of expression between groups of samples. The level of appreciable differential

expression depends on the number of replicates, e.g. with 10 replicates a 1.5 times modulation is appreciable (20).

2.4 Protein digestion

Once found protein spots with a significant differential expression their identity needs to be inferred. MS methods are the most powerful and versatile available with this purpose. First of all the protein spots need to be cut out from the gel, then they are submitted to proteolytic digestion with an enzyme like trypsin, that cleaves peptide bonds in proximity of a C-terminal lysine or arginine and generates peptides of suitable length for MS analysis (figure 4).

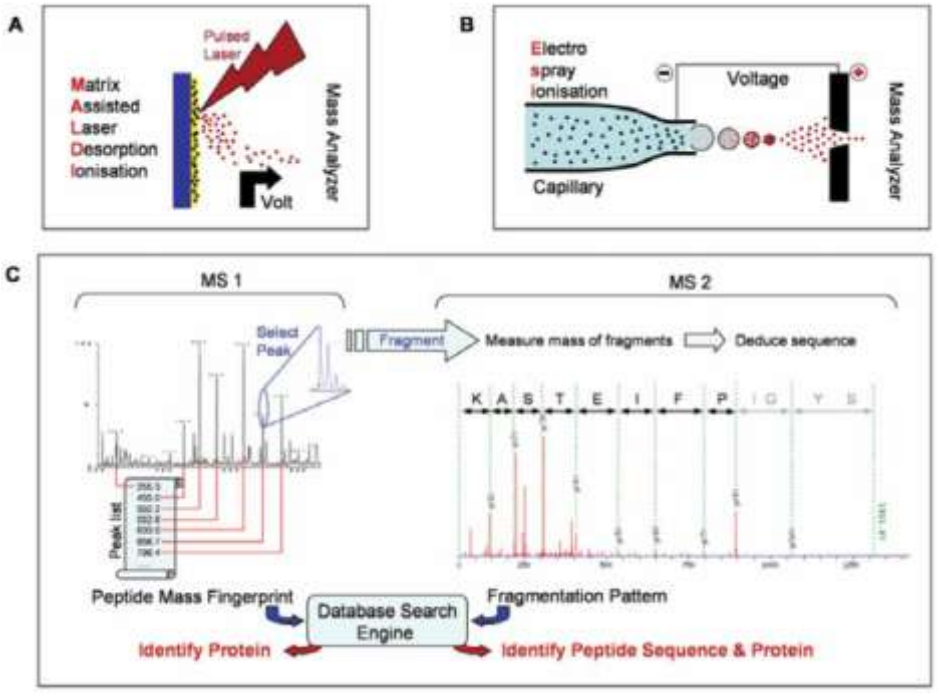

Figure 4. *Mass Spectroscopy methods. In proteomics mostly MALDI and ESI methods are used to ionise proteins and/or peptides, subsequently fragmented to give a* MS^1 *spectrum. A further fragmentation of the most abundant peptides gives the* MS^2 *spectrum.*

2.5 Protein identification

The identification of proteins through mass spectroscopy relies on the accurate measurement of protein and peptide masses.

A mass spectrometer is a device made essentially of three components:

1) an ionizing source, that in this case ionizes proteins and peptides;

2) a mass analyser, that resolves the ions in dependence of their mass/charge ratio (m/z);

3) a detector, that reveals the ions resolved by the mass analyser.

In proteomic studies two ionizing methods are generally employed: Matrix Assisted Laser Desorption Ionization (MALDI) and Electrospray Ionization (ESI) (21). In MALDI peptides are co-crystallized in a matrix with molecules like sinapinic acid or alpha-cyano-4-hydroxycinnamic acid. A laser impulse then softly desorbs and ionizes the peptides, whose m/z is measured, usually with Time-Of-Flight detectors (TOF). The combination of more peptide masses is associated with a specific protein (peptide fingerprint). In order to deepen the analysis a further fragmentation of peptides can be performed, via a second collision chamber and another TOF analyser (MALDI-TOF/TOF). The collision with helium atoms, electrons or other collision agents like electron transferring molecules induces the backbone fragmentation in correspondence of peptide bonds, permitting to infer the peptide sequence through calculation of mass difference of adjacent peaks (tandem MS/MS).

In ESI-MS, instead, peptides firstly separated with an HPLC column are ionised with an electrospray system. The preferred detectors for this system are Ion Trap (IT) and triple quadrupole (QQQ).

The peptide sequence is the first step in protein identification, and its reliability is expressed through a score, calculated as $S= -10Log_{10}(P)$. P is the probability that a sequence match between MS and database data is a random event, and is given by the ratio between the significance threshold of random match chosen E and the number of proteins in the database N.

For example, if during a search 500000 peptides fell within the window of mass tolerance chosen and the significance threshold chosen is 0.05 (1 in a 20 chance to to be a false positive) the corresponding score threshold would be $S= -10Log_{10}(E/N) -10Log_{10}(0.05/500000)= 70$. The protein score is given by the sum of the scores of individual peptides.

Other parameters to be included in mass spectrum analysis are mass tolerance, the presence of modifications (e.g. –SH blocking with AA) and the

N- or C-terminal aminoacid depending on the lysing enzyme used. The mass spectrum is a forest of peaks, and the highest are submitted to further fragmentation. The results of fragmentation are analysed with softwares like MASCOT (at the Matrix Science server) or SEQUEST to correlate the peptide sequences with the ones usually derived from genomic data. These data can be found in dedicated protein databases like SWISSPROT maintained by the Swiss Institute for Bioinformatics and the European Bioinformatics Institute, or the USA government-funded National Center for Biotechnology Information (NCBI).

A successful protein identification depends on many parameters, like the number of successfully identified peptides, their uniqueness for a protein and the sequence coverage. Nevertheless there can be ambiguities, and a 100% assignation is not always possible (that is why mass spectroscopists speak about “correlation” and not “identification”) (21). A MASCOT score for a peptide above 30 is usually considered enough to have a good correlation.

2.6 Bioinformatics

Once obtained a reasonable correlation between MS data and a protein, it becomes a potential candidate as marker of disease or of drug treatment. In order to have a complete understanding of its role, its molecular functions (e.g. enzyme), cellular or extracellular districts where it is present (e.g. cytoplasma) and biological processes in which it is involved (e.g. glucose oxidation) have to be known. This study, called Gene Ontology (GO) can be performed with one of the many softwares available, like SWISSPROT or GeneCards, curated by the Crown Human Genomic Centre at the Weizmann Institute of Science in Israel (22).

The next step is inserting the protein in the nets of processes in which it is involved, this time with the help of dedicated softwares like Kioto Encyclopedia of Genes and Genomes (KEGG, hosting more than 150000 pathway maps) or Reactome.

3 Materials and methods

3.1 Umbilical cord blood and amniotic fluid withdraw

The study, approved by the Ethical Committee of Padova University Hospital (Padova, Italy), was performed after obtaining written informed consent from the mothers of the foetuses. Ten IUGR and ten AGA full-term singleton neonates, all of Italian origin, were included in the study. Offspring of mothers with a birth weight below the 10th customized centile were characterized as IUGR. The Gestation Related Optimal Weight computer-generated program was used to calculate the customized centile for each pregnancy, taking into consideration significant determinants of birth weight, such as maternal height and booking weight, ethnic group, parity, gestational age and gender. The choice of the neonates excluded the cases where a chromosomal pathology, child-dependent disease or mother consumption of xenobiotics were present.

Umbilical cord blood samples (UCS) have been withdrawn from double clamped umbilical cord of singletons, from full-term deliveries performed with caesarean section. UCS was obtained after clotting for 30-45 min at room temperature followed by centrifugation at 3000g for 20 min in BD Vacutainer® glass serum tube, then samples were added of protease inhibitors (Roche) and frozen straightaway at -80°C until the analysis.

Amniotic fluid (AF) samples were obtained through withdrawing with syringe after amniotic sac resection, and treated with the same procedure as serum, avoiding the clotting step.

3.2 Protein sample preparation

The samples of UCS were albumin and IgG depleted (with ProteoPrep Blue Depletion kit, Sigma). Proteins, from UCS and AF, were precipitated with 4 volumes of acetone at -20°C for 2 h and then resuspended in a solubilising solution: 7 M urea (Sigma, Sigma-Aldrich Corporation, St. Louis, MO, USA), 2 M thiourea (Sigma), 3% CHAPS (Sigma), and 20 mM Tris (Sigma). Centrifugation at 14000 x g at 4°C for 40 min was performed to get rid of incidentally present nucleic acids.

The samples were then incubated with 5 mM tributylphosphine (Sigma) and 20 mM acrylamide (Sigma) for 60 minutes at room temperature to reduce protein disulphide bonds and alkylate the cysteine thiolic groups. The reaction was blocked by the addition of 10 mM ditiothreitol (DTT, Sigma). Protein concentration was evaluated by Detergent Compatible (DC) Protein assay (Bio-Rad Labs., Hercules, CA, USA) based on the Lowry method.

3.3 Two-dimensional gel electrophoresis and image analysis

UCS and AF protein fractionation by 2-DE were performed as reported by Cecconi el al. (23). Briefly, 450 µl of each sample (containing 3 mg/ml of protein) was separated by 17 cm pH 3-10 NL IPG strip, and the total product time x voltage applied was 70000 Vh for each strip. The second dimensional separation was done using 8-18%T gradient SDS-PAGE, applying 40 mA for each gel for 3 min, then 2 mA/gel for 1 h, and 20 mA/gel until the track dye, bromophenol-blue, reached the anodic end of the gels. After 2-DE, the proteins were detected by Sypro Ruby. The image analysis of the 2D gels replicates was performed by PDQuest software (Bio-Rad), version 7.3. Each gel was analysed for spot detection, background subtraction and protein spot optical density (OD) intensity quantification. The gel image showing the higher number of spots and the best protein pattern was chosen as a reference template, and spots in this standard gel were then matched across all gels. Spot quantity values were normalised in each gel dividing the raw quantity of each spot by the total quantity of all the spots included in the standard gel. Gels were divided in two groups (control and IUGR samples) and, for each protein spot, the average spot quantity value and its variance coefficient in each group were determined. Data were log transformed and analysed with Student’s t-test, then spots giving significant results ($P < 0.01$) were verified visually to exclude artefacts.

3.4 Mass spectrometry and protein identification

Spots showing a statistically significant differential expression were carefully cut out from 2-D Sypro Ruby stained gels and subjected to in-gel trypsin

digestion (17). Briefly, spots were destained with three washing steps: 50mM NH_4HCO_3, 50% 50mM NH_4HCO_3 (v/v), 50% acetonitrile, 100% acetonitrile, and dried at 37°C for 30 min. The gel pieces were then swollen in digestion buffer containing 50mM NH_4CO_3 and 12.5ng/ml of trypsin (modified porcine trypsin, Promega, Madison, WI) and the digestion proceded at 37°C overnight. The supernatants were collected and peptides were extracted in an ultrasonic bath (twice with 50% acetonitrile, 50% H_2O v/v with 1% formic acid, once with acetonitrile). Finally tryptic peptides were dried by vacuum centrifugation. Peptides from 8 µl of each sample were then separated by reversed phase (RP) nano-HPLC-Chip technology (Agilent Technologies, Palo Alto, CA, USA) online-coupled with a 3D ion trap mass spectrometer (model Esquire 6000, Bruker Daltonics, Bremen, Germany). The chip was composed of a Zorbax 300SB-C18 (150mm×75µm, with a 5µm particle size) analytical column and a Zorbax 300SB-C18 (40 nL, 5µm) enrichment column. The complete system was fully controlled by ChemStation (Agilent Technologies) and EsquireControl (Bruker Daltonics) softwares. The scan range used was from 300 to 1800 m/z. For tandem MS experiments, the system was operated with automatic switching between MS and MS/MS modes. The three most abundant peptides of each m/z were selected to be further isolated and fragmented. The MS/MS scanning was performed in the normal resolution mode at a scan rate of 13.000 m/z per second. A total of five scans were averaged to obtain an MS/MS spectrum. Database searches were conducted using the MS/MS ion search of Mascot against all entries of the non-redundant NCBI database with the following parameters: specific trypsin digestion, up to one missed cleavage; fixed and variable modifications: propionamide (Cys) and oxidation (Met), respectively; peptide and fragment tolerances: ± 0.9 Da and ± 0.9 Da, respectively, and peptide charges: +1, +2 and +3. For positive identification, the score of the result of $[- 10 \times \mathrm{Log}_{10}(P)]$ had to be over the significance threshold level ($P < 0.01$) and at least 2 different peptides ($p < 0.05$) had to be assigned.

3.5 Protein validation by Western Blot analysis

Protein samples were precipitated with cold acetone at -20°C for 2 hours and centrifuged at 14000xg for 10 min. The pellets obtained were dried and resuspended with Laemmli's sample buffer (62.5 mM Tris-HCl, pH 6.8, 25% glycerol, 2% SDS, 0.01% Bromophenol Blue, 5% ß-mercaptoethanol) through 5 min heating in boiling water. A 1-D SDS-PAGE separation on 10%T acrylamide gel in Tris/glycine/SDS buffer was then performed. The separated proteins were transferred to a PVDF membrane through electroblotting and equal protein loading in each lane (60 μg) was verified by Ponceau red staining. The membranes were treated with primary and secondary antibodies at the appropriate dilutions (see Table 1) and bound antibody was detected by Enhanced Chemiluminescence (ECL) Western blotting detection system (Millipore, USA). Western blots were scanned by a ChemiDoc instrument (Bio-Rad) and images were analyzed using Quantity One image processing software (Bio-Rad).

3.6 Classification of Proteins

Functional annotation was obtained by assignment of Gene Ontology (GO) terms for the identified proteins. GO analysis was performed with the help of GeneCards database (http://www.genecards.org), classifying each protein with respect to its molecular function and biological process in which it is involved.

4 Results

The typical high resolution 2-DE protein pattern of IUGR and control neonates, obtained from UCS and AF protein extracts, are reported in figure 5 and 6. By PDQuest analysis we measured differential protein expression by analyzing the 10 biological replica of 2-DE maps obtained for each group.

A total of 18 and 13 spots (matched across all the replica 2D maps) were found to be differentially expressed ($P < 0.01$) in UCS and AF respectively. Spots selected from the differential analysis were subjected to RP-HPLC-ESI-MS/MS analysis for protein identification.

The unique differentially expressed proteins identified were 14 in UCS, and 11 in AF samples. In Table 1, the successfully identified proteins corresponding to up- or down-regulated spots in UCS and AF are shown, together with the gene names, the standard spot number (SSP), the identification parameters and the indication of their gene ontology (GO) annotation (biological process and molecular function). Protein GO classification indicate that 21% of proteins are involved in inflammatory response, 20% in immune response, while a smaller proportion are related to transport, blood pressure, and coagulation. Figure 8 shows as a pie chart the distribution of the identified proteins catalogued according to the biological process in which they are involved.

Western Blot analysis, performed to determine the level of expression of five candidate proteins (complement C3-alpha chain (C3), serotransferrin (TF), kininogen light chain (KNG1), apolipoprotein J (CLU), and angiotensinogen (AGT) identified by 2-DE analysis are shown in figure 7. The relative protein expression in both samples was normalized through Ponceau Red staining, that permits to appreciate the total protein amount. Trends of changes in the same direction as those detected in the 2D gel analyses were detected for all the proteins. The quantitative difference between the results obtained by 2D electrophoresis and by Western Blot suggested that most changes detected by the former technique specifically involve post-translationally modified forms, which can be only separated in 2D maps (figure 5 and 6).

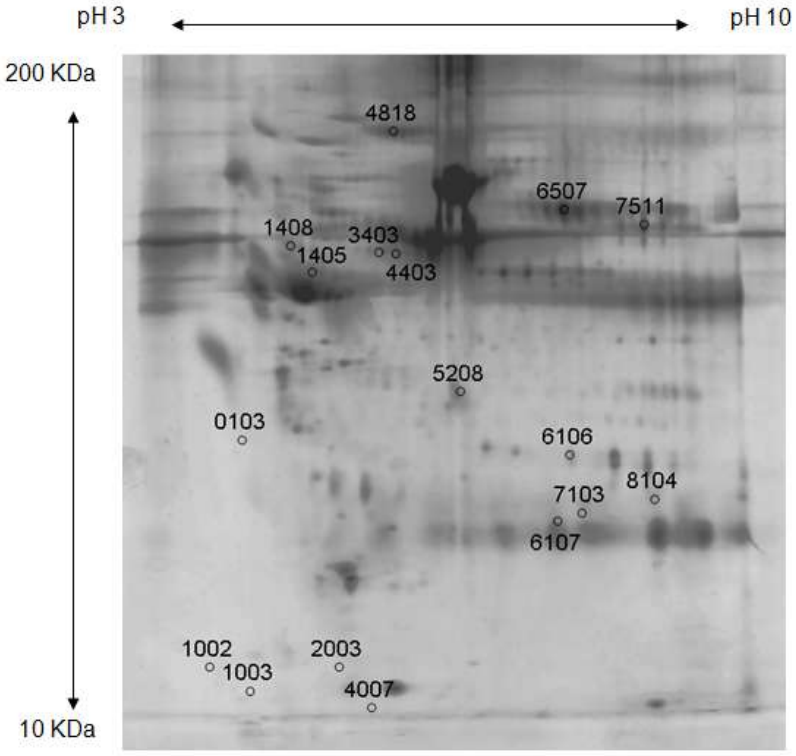

Figure 5. *2D-PAGE map of UCS with spots of differentially expressed proteins pinpointed with an SSP (Standard Spot numbering), assigned by PDQuest software).*

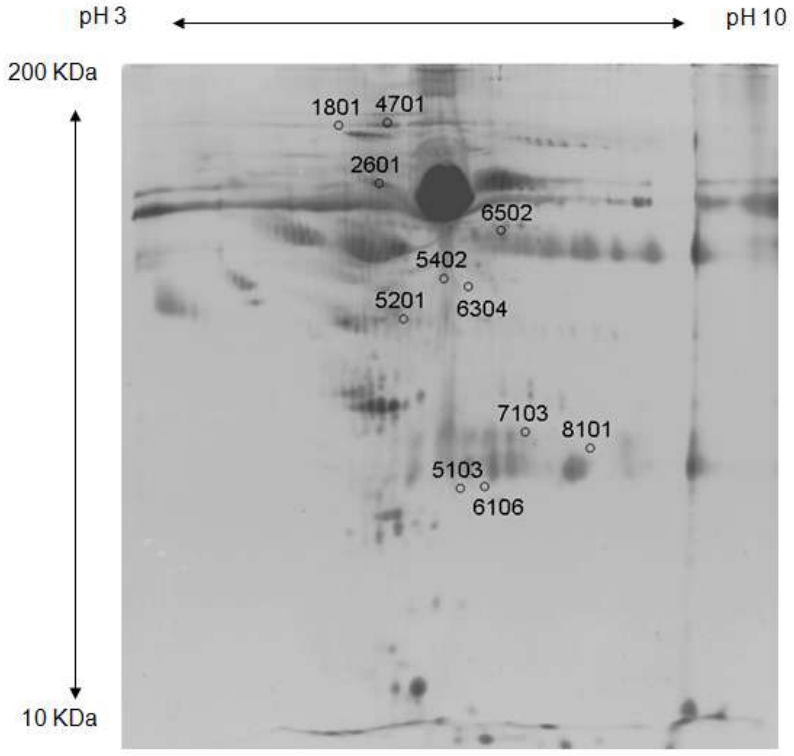

Figure 6. *2D-PAGE map of AF with spots of differentially expressed proteins pinpointed with an SSP (Standard Spot numbering), assigned by PDQuest software).*

Table 1. *Identified proteins that are differentially expressed in UCS and AF of IUGR newborns through 2-DE.*

Protein name	Gene name	IUGR sample	Spot no. [a]	NCBI acc. #	Mr. (kDa) exp/theor	pI exp/theor	No. of peptides identified	Mascot score [b]	Sequence Coverage (%) [c]	Molecular function GO term	Biological process GO term	Fold of variation IUGR/C [d]
Alpha-1-B-glycoprotein	A1BG	AF	2601	gi|69990	85/51.9	5.4/5.6	15	445	30	protein binding	crisp-3 binding	−2.0
Alpha-2-macroglobulin	A2M	UCS	4818	gi|177870	125/163.2	5.3/6.0	5	106	2	endopeptidase inhibitor	complement pathway	− 1.6
Angiotensinogen	AGT	UCS	1405	gi|532198	55/53.1	4.8/5.8	13	448	23	vasoconstrictor	Regulation of vasoconstriction	− 1.6
Apolipoprotein J	APOA1	UCS	0103	gi|178855	30/48.8	4.3/6.3	2	69	6	phospholipid binding	lipid transport	> 20
Carbonic anhydrase 1	CA1	AF	7103	gi|4502517	30/28.8	6.9/6.6	12	356	34	carbonate dehydratase activity	one-carbon metabolic process	+ 12.8
Ceruloplasmin	CP	AF	4701	gi|1620909	150/115.4	5.5/5.4	9	274	11	ferroxidase activity	ion transport	−1.8
Complement Component C3, Chain A	C3	UCS	7511	gi|78101267	60/71.1	7.2/6.8	14	730	30	endopeptidase inhibitor	inflammatory response	− 2.0
Complement Component C3b, Chain B	C3	UCS	3403	gi|118137965	55/103.9	5.2/5.2	3	122	4	endopeptidase inhibitor	inflammatory response	− 1.6
Complement Component C3b, Chain B	C3	UCS	4403	gi|118137965	55/103.9	5.2/5.2	18	509	19	endopeptidase inhibitor	inflammatory response	− 1.6
Complement Component C3c, Chain B	C3	UCS	8104	gi|78101270	25/21.5	7.3/5.8	7	172	31	endopeptidase inhibitor	inflammatory response	− 2.2
Complement component C4	C4A	UCS	1002	gi|179674	15/192.7	4.2/6.6	3	54	1	endopeptidase inhibitor	inflammatory response	− 2.6
Complement factor B	CFI	AF	6502	gi|291922	65/85.4	6.5/6.5	13	307	12	peptidase	inflammatory response	− 1.2
Fibrinogen beta chain	FGB	AF	5201	gi|2781208	45/37.6	5.8/5.8	7	206	15	protein binding	blood coagulation	>20
Fibrinogen beta chain	FGB	UCS	5208	gi|119625341	34/50.4	5.6/8.6	5	202	13	protein binding	blood coagulation	+ 8.5
Hemoglobin gamma-G	HBG2	UCS	1003	gi|31725	13/17.0	4.7/5.9	2	132	20	oxygen transporter activity	oxygen transport	> 20
Hemoglobin gamma-G	HBG2	UCS	2003	gi|183885	13/16.6	5.2/6.4	3	141	28	oxygen transporter activity	oxygen transport	> 20
Ig kappa 4 light chain	IGKV4-1	UCS	6107	gi|170684576	20/24.1	6.7/6.2	6	124	22	antigen binding	immune response	− 1.8
Ig lambda chain V-IV region	BCRL4	UCS	7103	gi|87901	20/15.5	6.8/7.7	3	123	25	antigen binding	immune response	− 1.7
Ig lambda chain V-IV region	BCRL4	UCS	8104	gi|87901	20/15.5	7.3/7.7	5	97	25	antigen binding	immune response	− 2.2
Ig light chain	IGKJ	AF	5103	gi|149673887	25/23.4	6.0/7.0	7	186	34	antigen binding	immune response	>20
Keratin, type II cytoskeletal 1	KRT1	UCS	4007	gi|11935049	12/66.0	5.5/8.2	5	141	6	protein binding	cytoskeleton organization	+ 2.1
Keratin, type II cytoskeletal 1	KRT1	UCS	6106	gi|119395750	27/66.0	6.8/8.2	13	398	17	protein binding	cytoskeleton organization	− 1.9
Kininogen-1 isoform 2	KNG1	UCS	1408	gi|4504893	55/47.9	4.6/6.3	11	333	21	endopeptidase inhibitor	regulation of vasoconstriction	− 1.8
Serotransferrin	TF	UCS	6507	gi|4557871	70/77.0	6.6/6.8	12	429	19	ferric iron binding	iron ion transport	− 1.5
Serum albumin	ALB	AF	1801	gi|28592	150/69.3	5.2/6.0	1	51	2	transport	carrier protein	>20
Serum albumin	ALB	AF	5402	gi|6013427	60/69.2	6.0/5.9	9	364	15	transport	carrier protein	>20
Serum albumin	ALB	AF	6106	gi|157830361	30/47.3	6.3/6.0	11	152	9	transport	carrier protein	>20
Serum albumin	ALB	AF	6304	gi|27692693	55/47.3	6.2/6.0	19	506	30	transport	carrier protein	−1.5
Serum albumin	ALB	AF	8101	gi|27692693	30/47.3	7.4/6.0	17	427	22	transport	carrier protein	>20

[a] Spot numbers refer to 2D gels of Figure 5 and 6.
[b] Score is $-10\log_{10}(p)$, where p is the probability that the observed match is a random event, based on the NCBI database using the MASCOT searching program as MS/MS data.
[c] Amino acid sequence coverage for the identified protein.
[d] Fold of variation in expression in IUGR/C ratio: increased protein (+), decreased protein (-).

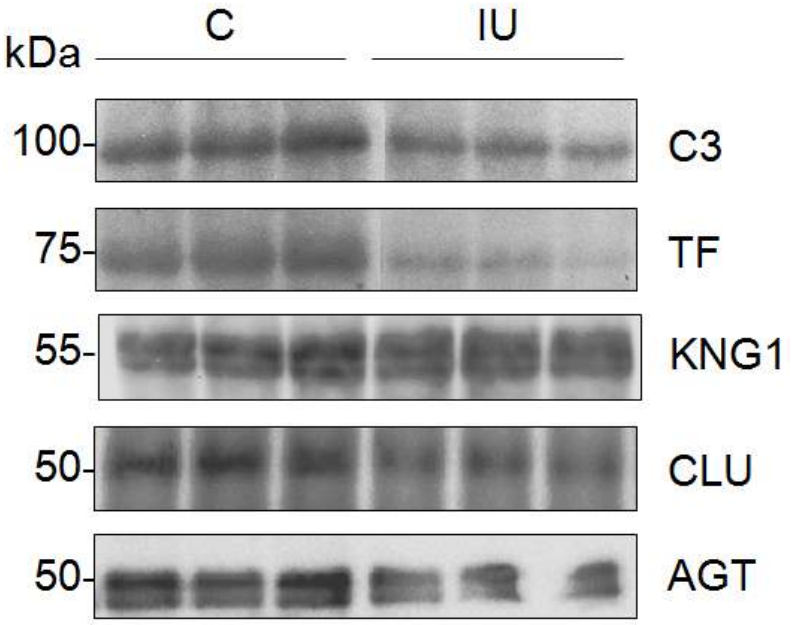

Figure 7. *Protein expression validation with Western blot analysis for five proteins. Film images with the relative protein expression were normalised by Ponceau red staining. Film images were captured with GS710 densitometer (Bio-Rad) and analysed with Quantity One software to calculate the band intensities (OD).*

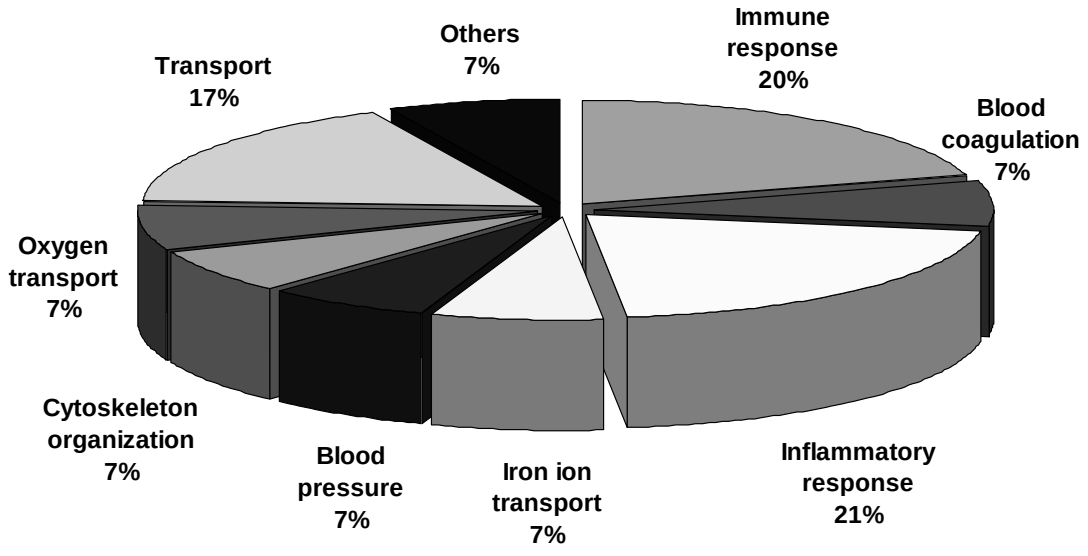

Figure 8. *Protein GO categorization. Distribution of the identified proteins according to the biological process(es) in which they are involved. GO analysis was performed by using GeneCards database.*

Table 2. *The different primary and secondary antibodies used for Western Blot analysis, with the corresponding dilutions.*

Primary antibody	**Dilution**
Mouse anti-complement C3B-alpha (Chemicon)	1:1000
Mouse anti- angiotensinogen (Abnova)	1:2000
Mouse anti-transferrin HTF-14 (GeneTex)	1:1000
Mouse anti-clusterin CLI-9 (GeneTex)	1:2000
Rabbit anti-kininogen1 (GeneTex)	1:2000
Secondary antibody	**Dilution**
Goat anti-mouse IgG, HRP conjugated (Millipore)	1:5000
Donkey anti-rabbit IgG, HRP conjugated (Amersham)	1:10000

5 Discussion

The differentially expressed proteins identified in both umbilical cord serum and amniotic fluid samples of IUGR and AGA neonates are described and discussed in the following paragraphs.

5.1 Coagulation and IUGR

The association between coagulation disorders and IUGR has already been demonstrated by several publications (24), (25), (26). A low grade activation of the coagulation system is in fact suggested as one possible factor in the pathogenesis of IUGR. Accordingly, it has been reported that heparin treatment significantly improved the growth of the growth-restricted foetus (27), (28), (29). Among the proteins that play pivotal role in coagulation there is fibrinogen, which is converted by thrombin into fibrin to form a clot. Interestingly, it has been demonstrated that the G/A polymorphism at position - 455 of the beta-fibrinogen gene may enhance the physiological increase in fibrinogen levels during pregnancy and thereby predispose to obstetric complications (30), (31). In line with these findings, we found that fibrinogen was up-regulated in UCS as well as in AF of IUGR samples.

Another protein related to coagulation is also alpha 2-macroglobulin (A2M) which is a protease inhibitor with both anticoagulant and procoagulant properties (it neutralizes alpha-thrombin, plasmin, and activates protein C) (32). In some studies A2M has been negatively correlated with birth weight: infants with lower birth weight had higher cord serum A2M concentrations as compared to those with higher birth weight (33), (34). Our data stand in contrast with these findings, indeed we reported a down-regulation of A2M in UCS of mothers of IUGR infants. An explanation of this discrepancy may depend on the modulation of different PTM-modified isoforms.

5.2 Immune mechanisms and IUGR

Another mechanism that seems involved in IUGR development is the inflammatory response, which interestingly has been linked to the coagulation process state (35), (36). Normal pregnancy is associated with increased maternal plasma complement components concentration. Complement activation may in fact compensate for the decreased adaptive immunity observed in normal pregnancy, and is aimed to protect the host (mother and/or foetus) from microorganisms and other potential antigens (37), (38).

The available data on the relationship between complement activation and growth retardation appear to be conflicting: some studies have reported that complement levels were significantly lower in mothers of SGA infants than in controls (39) suggesting that the immunological derangement leads to placental lesions and growth restriction. On the contrary, others indicate that complement activation is associated with IUGR and other pathologic pregnancy outcomes (such as preeclampsia and recurrent spontaneous abortions) (40). In particular, it has been reported that C5 (36), as well as C3a activation (41), are crucial intermediary events (in the first trimester of pregnancy) in the pathogenesis of IUGR. In this study we found that IUGR newborns are related to down-regulation of C3, C3b, C3c, C4 complement components in UCS, as well as down-regulation of complement factor B in AF samples respectively. Our findings emphasize the central role of

complement proteins modulation as a key process implicated in poor pregnancy outcomes.

5.3 Blood pressure alteration and IUGR

Pregnancy is a physiological condition characterised by a progressive increase of the different components of the renal renin-angiotensin system (RAS). RAS is involved not only in the regulation of blood pressure and fluid-electrolyte homeostasis, but has also a role in the human placenta development throughout gestation: angiotensin II for example inhibits human trophoblast invasion (42). Alterations in RAS have been already observed in IUGR offspring and may play a key role in the aetiology of IUGR hypertension (43), (44). Interestingly, it has been reported that maternal and foetal angiotensinogen Thr235 genotypes are associated with an increased risk of IUGR (45), (46), as well as of preeclampsia.

which is a medical condition in which hypertension arises in pregnancy (47). Here we reported that angiotensinogen is down-regulated in UCS of IUGR newborns. Further studies are needed to understand whether the decreased angiotensinogen we identified is the Thr235 variant or not, and to prove whether the data obtained are consistent with previous reported from other.

Another protein related to blood pressure control is kininogen, which belong to plasma kallikrein-kinin system (KKS) that plays a role not only in blood pressure (via modulation of RAS system), but also in inflammation, coagulation and pain. Kininogen is a thiol protease that circulate as two different isoforms produced by alternative splicing, high molecular weight (HK) and low molecular weight kininogen (LK). Cleavage of HK by plasma kallikrein results in kininogen heavy chain (63 kD), light chain (58 kD) and modified light chain (45 kD). It has been reported that downregulation of plasma HK precedes the onset of preeclampsia (20-week gestation) (48).

In agreement with these observation, we found that the kininogen modified light chain (45 kD) was down-regulated in UCS of IUGR newborns. Moreover, it has been reported that reduced levels of vasodilator substances, such as prostacyclin and kallikrein, may have a causal role in IUGR (49), (50).

5.4 Iron and copper homeostasis, oxidative stress and IUGR

Cu and Fe metabolism are known to be linked and to play a pivotal role during pregnancy: transferrin (Tf) is the main protein regulating Fe homeostasis, whereas ceruloplasmin (CP) is the major copper-carrying protein which acts as a circulating ferroxidase enzyme able to oxidize ferrous ions to less toxic ferric forms. Together ceruloplasmin and transferrin act as an antioxidative system. Fe deficiency during pregnancy is common and has serious consequences both in the short and the long term such as foetal growth retardation and cardiovascular problems in the adult offspring. Similarly, Cu deficiency, although not so common, also has deleterious effects (51), (52). Here we shown that serotransferrin was down-regulated in UCS, while ceruloplasmin was decreased in AF of IUGR newborns.

Several studies have shown a link between altered iron homeostasis and growth retardation: a decrease in transferrin receptor 1 has been reported in IUGR placentas (53); elevated maternal ferritin was related to an increased risk of IUGR (54), while a decrease of serum concentrations of total and highly sialylated serotransferrins was detected in severe preeclampsia (55). In addition, as concerning copper homeostasis it has been demonstrated that in IUGR placentas the level of Cu was significantly reduced (56), and that ceruloplasmin levels were decreased in small for dates babies (57), (58).

6 Conclusion

Our results support the conclusion that the IUGR condition alters the expression of proteins some of which are involved in the coagulation process, immune mechanisms, blood pressure and iron and copper homeostasis control. The identification of proteins, whose expression is altered by IUGR, may contribute to improve the understanding of this important clinical condition, leading to the individuation of candidate proteins that could be further investigated as biomarkers. The real importance of all of these candidates require further validation in vitro and in vivo; nevertheless, they could represent promising diagnostic targets, and shed a ray of hope for a target-oriented therapy of IUGR.

Chapter 2

MOLECULARLY IMPRINTED POLYMERS FOR PHOSPHOPROTEOMICS

1 Introduction

The present project is aimed at developing a pre-fractionation approach for proteomics based on selective polymeric materials, to be used prior to proteome analysis for selecting classes of proteins on the basis on homogeneous functional criteria.

2 A particular fraction of the proteome

Post-translational modifications (PTMs) are covalent processing events that change the properties of a protein by proteolytic cleavage or by addition of a modifying group to one or more aminoacids. Far from being mere "decorations", PTMs of a protein determine its activity state, localization, turnover, and interactions with other proteins. In signaling, for example, kinase cascades are turned on and off by the reversibile addition and removal of phosphate groups, and in the cell cycle ubiquitination marks cyclins for destruction at defined time points (59).

Other examples of the biological effects of protein modifications are attachment of fatty acids for membrane anchoring and association, glycosylation for protein half-life, targeting, "cell-cell" and "cell-matrix" interactions. Consequently, the analysis of proteins and their PTMs is particularly important for the study of the physio-pathology (60).

3 Phosphoproteomics

3.1 Introduction

Phosphorylation is the most widespread and studied Post Translational Modification (PTM) in proteins (61).

It is involved in almost all cell functions: metabolism, osmoregulation, transcription, translation, cell cycle progression, cytoskeletal rearrangement,

cell movement, apoptosis, differentiation, regulation of the signal transduction pathways, intercellular communication during the development and functioning of the nervous system (62), (63), (64).

The phosphorylation/dephosphorylation process is regulated by the switch kinases/phosphatases. Kinases add a phosphate group to a receptive side chain of an aminoacid; phosphatases catalyze instead the hydrolysis of a phosphoester bond (65), (66). The effect of the addition or subtraction of a phosphate group is the modification of enzymatic activity, protein-protein interaction and cellular localization.

Phosphorylation is not an unique process: often a single protein can display more than a single site suitable for the process, often catalyzed by different kinases. For example, glycogen synthase contains at least 9 phosphorylation sites, and its modulation is performed by at least 5 protein kinases acting on different sites of the protein (67). A misregulation of the phosphorylation processes can cause severe damage to the cells, leading to diseases like cancer, diabetes or neurodegeneration (68), (69).

The most common kind of phosphorylation in eukaryotes is O-phosphorylation, on serine, threonine and tyrosine with a ratio of 1800/200/1 (70), (71). Other sites of phosphorylation can be histidine, lysine, arginine, glutamic acid, aspartic acid and cysteine (64), even though are less studied due to the lability of the chemical bond and the subsequent necessity to use very special techniques to analyse them.

It is esteemed that 2-4% of eukaryotic genes are associated with kinases and phosphatases (there are about 500 kinase and 100 phosphatase genes in the human genome) (72), (73), (74). Around 100,000 phosphorylation sites may exist in the human proteome, the majority of which are presently unknown (75). The importance of studying the phosphorylation was marked by the success of the cancer drug *Gleevec*, the first to inhibit a specific kinase, which gave definitely an impulse to the research on kinases and their substrates as potential drug targets (72).

The comprehensive analysis of the protein phosphorylation should include: identification of phosphorylated proteins and of their sites of phosphorylation,

how these phosphorylations modify the biological activity of the protein and kinases and phosphatases involved in the process.

3.2. A delicate analysis

Working in phosphoproteomics presents a series of hurdles in the analytical strategy.

The first issue concerns the reversible nature of the phosphorylation. The study of the phosphoproteins necessitates their isolation from a cell extract or a sub-cellular compartment. Subsequently to the cell lysis, however, many enzymes like phosphatases become active, determining the degradation of the proteins and detachment of phosphate groups from their sites. Also kinases can express their action, confusing the picture of which phosphate groups are biologically relevant (65). Working at low temperature helps significantly in slowing down these processes, but it's not enough. In order to stop the action of these enzymes it is essential to add to the cell extracts a specific mix of inhibitors of proteases and phosphatases (76) while to inhibit kinases EDTA, EGTA or kinase inhibitors are added. It is also important to choose an inhibition mix that doesn't interfere with the downstream analytical methods, like the phospho-specific enrichment methods.

Another issue relates with phosphoproteins characterization, mostly performed through Mass Spectrometry (MS) methods after enzymatic digesting. The detection of phosphopeptides (FPs from now on) with MS is hampered by the presence of the non phosphorylated partners; moreover, the efficiency of ionization is higher for the latter ones, also generally more present in the sample (this fact is referred to as "low stoichiometry" of phosphorylation).

It follows that enrichment methods are necessary to extract the phosphoproteins or the FPs from the sample. There are various methods to choose from, depending to the kind of sample and the aims of the study.

3.3.Detection of phosphoproteins

The detection of phosphoproteins in a sample still relies on optimized "classical" methods.

3.3.1 Isotopic labeling of phosphoproteins

One of the oldest methods used to study phosphoproteins is the metabolic labeling with ^{32}P and ^{33}P. It consists in nourishing living cells or organisms with substances labeled with these radioactive isotopes which are incorporated in the synthesised proteins. Following lysis of the cells, the protein population is isolated through 1-DE or 2-DE, visualized on the gels with autoradiography or acquired digitally with Phosphorimager systems. This method is still largely employed, because of its simplicity and reliability when somebody works with alive systems in vitro or in vivo (77).

A comparison between the performances of ^{32}P and ^{33}P in labeling the proteins was made (78), indicating that ^{33}P gives more neat image and higher resolution, even though after a longer exposition time, respect ^{32}P.

Apart from the safety and environmental implications in using radioactive isotopes, this method has other drawbacks. First of all it is not compatible with some downstream methods, like MS. Furthermore it can only be applied on viable cells, since the radioactive isotopes have to be taken from the media and metabolized: it cannot be therefore applied on post-mortem tissues or biopsies.

In in vivo studies, cells are incubated with ^{32}P, however the presence of ATP reservoirs inside the cells can interfere with the labeling, reducing the efficiency of the method (79). Furthermore, ^{32}P is toxic for the cells, and over time can cause damages (80).

In in vitro studies, proteins are incubated with specific kinases in the presence of [γ-^{32}P]-ATP and, under specific conditions, the radioactive atom is incorporated into aminoacidic residues. Due to the unnatural presence of kinase respect the target protein, however, it is frequent the phosphorylation of a different target instead of the natural one (promiscuity) (81).

3.3.2 Western Blotting employing phosphospecific antibodies

Western blotting is a quite old technique. It is based on the selective binding of an antibody to a protein, transferred from a 1D or 2D gel to a nitrocellulose or polyvinylidene difluoride (PVDF) membrane support, and the subsequent revealing of the antibody marked spot with some visual method (82). The key role is played by the antibody, that should be specific for the protein epitope of interest: in this case epitopes are phosphoserine, phosphothreonine and phosphotyrosine. The selectivity and affinity characteristics of the antibody are of major importance, to perform specific recognition and limit false positives. While excellent anti-phosphotyrosine antibodies have been developed (e.g. (PY)20, (PY)100 and 4G10 hybridoma clones), better antibodies are still needed for phosphoserine and phosphothreonine. Antibodies generated against pSer and pThr, in fact, very often necessitate of a consensus sequence flanking the phosphoaminoacid; this might be due to the lower immunogenicity of pSer/pThr compared to pTyr (83).

Grønborg et al. performed a test for specificity and reliability of anti-phosphoserine and anti-phosphothreonine antibodies (70). They made a large scale differential analysis of phosphorylated proteins, succeeding in identifying phosphorylation sites and FPs not identified with dedicated prediction software. The combination of high resolution 2-DE techniques and the Enhanced ChemiLuminescence (ECL) system give improved sensitivity to the method, i.e. intensification of around 1000 times of the light emitted from a spot (84).

Although Western blotting is an efficient technique to reveal even small amount of protein (10^{-10} mol), its use in quantitative analysis is limited by the variability of the amount of proteins that can be transferred to the membrane.

3.3.3 Direct staining of phosphoproteins

The easiest way to detect phosphoproteins in a sample is the direct staining with a phosphospecific dye after a SDS-PAGE gel. Many attempts have been done from the 1970's (85), but all these methods face problems in terms of sensibility and of non specificity, e.g. the inability to discriminate between

phosphorylated and non phosphorylated proteins or to detect phosphotyrosine. Quite recently a novel fluorescent dye has been introduced: Pro-Q Diamond. This dye selectively binds to phosphoproteins requiring a very simple experimental protocol. The sensitivity of the stain depends on the number of phosphorylated residues of the proteins: the detection limit was 16 ng for pepsin (1 phosphorylated residue) and 2 ng for casein (8 phosphorylated residues) (86). Thus, the method is very useful for a preliminary screening, but still not sufficient for a comprehensive analysis of the phosphoproteome.

The dye is also compatible with MS and with Multiplex Proteomics (MP), i.e. detecting simultaneously phosphoproteins and total proteins (e.g. these latter stained with SYPRO Ruby dye) on the same 2D gel. The combination of the two staining methods permits to distinguish low represented but highly phosphorylated proteins from highly represented but poorly phosphorylated ones, comparing the results from the two different colorations.

3.3.4 Detection of phosphoproteins employing protein phosphatases

The presence or absence of a phosphate group on a protein is enough to change its pI and subsequently its position in the 1st dimension of a 2D gel. That's why, by employing a phosphatase enzyme, it is possible to modify the position of a protein spot on a map and thus determine its nature comparing the maps before and after the treatment. Softwares have been also developed that can predict the pI shift due to the addition/removal of a phosphate group, that can be of 1-2 pH units (87). As an example, Yamagata et al. exploited the specific enzymatic activity of k-phosphatase (kPPase) on phosphoserine, phosphothreonine, phosphotyrosine and phosphohistidine residues to identify novel phosphoproteins in cultured rat fibroblasts (88).

The methods employing phosphatases, however, are not suitable for quantitative analysis, mainly because of the complexity of the analysis and the variable efficacy of the enzymatic action.

3.4. Selective enrichment of phosphoproteins and FPs

The identification of the PTM sites on a protein is generally performed by using MS approaches. On most occasions, the only enrichment of the sample in phosphoproteins followed by protease-specific digestion and MS analysis is not sufficient to identify the sites of phosphorylation present (due to the general low stoichiometry of the phosphorylation), thus a second enrichment step at the FP level is often also required.

Some commercial kits for phosphoprotein and FP enrichment are available, offering ease of use and reproducibility; nevertheless it has been clearly demonstrated that the different methods available differ in the specificity of isolation and in the set of phosphoproteins and FPs isolated (89), strongly suggesting that no single method is sufficient for a comprehensive phosphoproteome analysis. Strategies for phospho-specific enrichment are shown in fig.1.

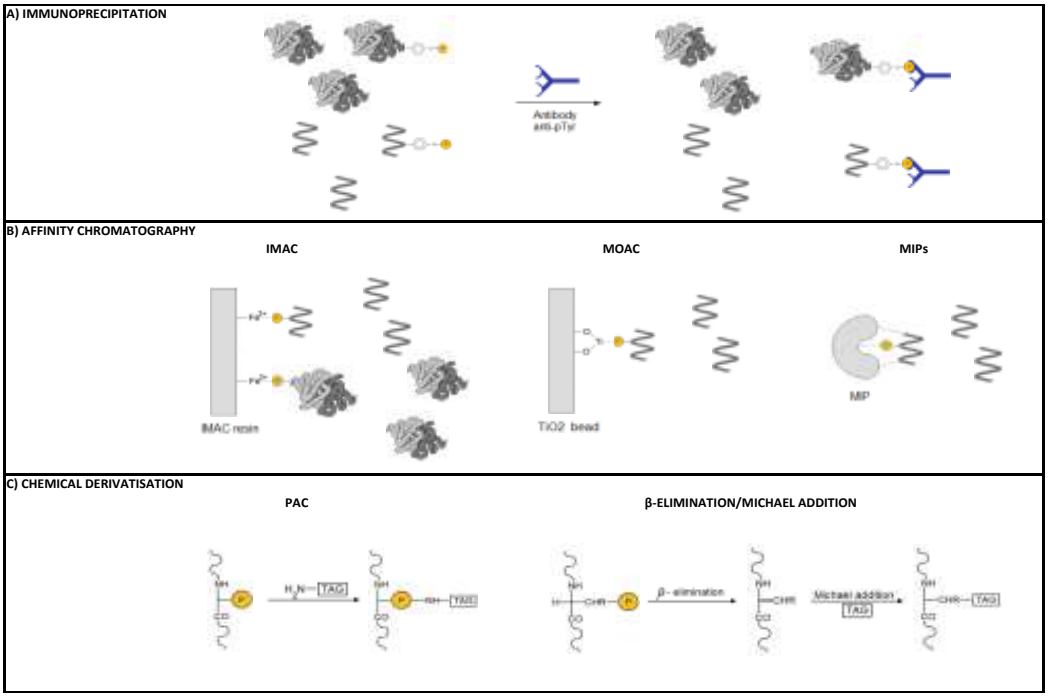

Figure 1. *Selective enrichment of phosphoproteins and phosphopeptides.*

A) Immunoprecipitation: phosphoproteins or phosphopeptides are selectively precipitated through the use of appropriate anti-phospho antibodies; at the moment only the use of anti-pTyr antibodies has proven to be robust.

B) Affinity chromatography: a resin with immobilized chelated metal or TiO_2 can selectively bind the phosphoric group of peptides and also proteins in IMAC (par. 4.2). A combined approach is SIMAC (IMAC + TiO_2). An alternative technique could be the use of Molecularly Imprinted Polymers (MIPs, par.4.10).
C) Chemical derivatization: the phosphoric group reacts with the aminogroup of a tag in PAC or can be subdued to β-elimination and linking of a suitable tag through Michael addition (par. 4.11).

3.4.1 Phosphoprotein enrichment by Immunoprecipitation

Phospho-specific antibodies can be used to selectively immunoprecipitate phosphorylated proteins depending on the specificity of the antibody. As for Western blotting (see above) anti-phosphotyrosine antibodies are the most reliably and widely used in order to enrich tyrosine-phosphorylated proteins from complex mixtures.
After immunoprecipitation (IP) the phosphotyrosine enriched sample can be analyzed with different analytical methods such as 1-DE and 2-DE (90).
Also in this case, variations of protein phosphorylation levels are very difficult to characterize unless in combination with a particular protein labeling (Stable Isotope Labeling with Aminoacids in Cell culture: SILAC, see par.6.1) with stable isotopes (^{13}C or ^{15}N) is used (91). This strategy allowed a quantitative and temporal investigation of tyrosine phosphorylation events of proteins involved in signaling pathways after stimulation with Epidermal Growth Factor (EGF) (92).

3.4.2 Phosphopeptide and phosphoprotein enrichment using Immobilized Metal Affinity Chromatography (IMAC)

IMAC exploits the material formed through chelation of a di-, tri- or tetravalent metal by nitrilotriacetic acid (NTA), iminodiacetic acid (IDA) or Tris(carboxymethyl)ethylenediamine (TED) immobilized on a solid support, like porous silica beads (93). The most commonly used resins make use of Fe^{3+},Ga^{3+} and Al^{3+}, even though Zn^{2+} and Zr^{4+} are used as well (94).

This method is routinary employed in FPs enrichment prior to MS analysis, nevertheless it has some limits; the most evident is its undesired ability to bind acidic peptides. This limitation has been largely surpassed by the acidification of the media (to protonate the carboxylic groups) (95) and esterification of the carboxylic moieties with methanolic HCl before the enrichment step, even if this method introduces complexity due to the variable yield of methylation.

A second limitation is the net bias of the method towards monophosphorylated peptides (96).

The method is particularly effective when used in combination with an enrichment step at the protein level. This operation can be carried out with methods like IMAC itself, exploiting however a more suitable solid support, like sepharose beads. Moreover, secondary interactions have to be reduced, e.g. with the use of denaturing conditions (6M urea). The detachment of the potentially many phosphate groups from the column imposes instead the use of strong eluting buffer as 0.1-0.2 M EDTA (97).

Other phosphoprotein enrichment methods are phosphotyrosine IP (98), Strong Anion eXchange chromatography (SAX) (99), Strong Cation eXchange chromatography (SCX) (100) and SDS-PAGE (101).

3.4.3 Metal Oxide Affinity Chromatography (MOAC)

Metal oxide chromatography (MOAC) employs mainly Ti, Zr or Al oxides, in the form of solid or coated beads, as chromatographic media to sequestrate FPs. Many different crystalline forms and nanostructured materials have been devised (102).

The first report about the potentialities of these materials regarded the use of TiO_2-based columns to sequestrate phosphate ions from the water (103).

In 2004, Pinkse et al. published a paper on the use of this material to bind FPs. They devised a 2D-LC-MS online strategy with TiO_2 beads (Titansphere) as first dimension and RP as second one (104).

Acidic conditions (pH 2.9) promoted the adhesion of FPs to the first column, leaving the non-phosphorylated ones to flow through and to be analysed with

nano-LC-RP- MS/MS. Basic conditions (pH 9.0) eluted FPs in a second step. The method was tested on a 153kDa homo-dimeric cGMP-dependent kinase, promoting the discovery a total of 8 phosphosites, 2 of which were novel.

Larsen's group then devised an off-line strategy to bind FPs to a TiO_2 material. The use of additives as 2,5-dihydroxybenzoic acid (DHB), phthalic acid or glycolic acid largely reduced the aspecific attachment of acidic peptides (105). This technique has been named HAMMOC, for hydroxy acid modified metal oxide chromatography.

A significative advantage of TiO_2 is its tolerance towards most buffers and salts used in biochemistry and cell biology laboratories. This is one of the reasons which made TiO_2 so common in large scale phosphoproteomics studies (106). Not only titania has been employed as metal oxide for FPs enrichment. Natural substitutes can be oxides belonging to the same group. For example, ZrO_2 microtips have been recently introduced as mean for FPs enrichment. This oxide shows a preference towards singly phosphorylated FPs, while TiO_2 preferentially retains multiply phosphorylated ones (107). However, subsequent large-scale studies demonstrated also a lower selectivity versus acidic peptides (108), suggesting the necessity of further improvements.

3.4.4 Sequential elution from IMAC (SIMAC)

The identification of multiply phosphorylated peptides has proven to be a hard task, mostly because of their difficult ionization and subsequent low signal compared to singly- and not-FPs, so to be not selected for the subsequent fragmentation in the mass spectrometer.

To address this issue, in 2007 Martin Larsen's group presented an analytical strategy for sequential elution of mono- and multiphosphorylated peptides. The sequential elution from IMAC (SIMAC) exploits the complementary characteristics of IMAC and TiO_2 in enriching the sample respectively in multiply and singly phosphorylated peptides (76).

In particular, the elution from IMAC in acidic conditions (pH 1.0) enriches the sample in mono-FPs, while the basic conditions (pH 11.3) elute subsequently

the multi-FPs (109) A further enrichment with TiO_2 chromatography is needed only in the acidic fraction, because the basic one is enough depleted of non-FPs.

The separation of singly and multiply FPs permits then their analysis with $pdMS^3$ (phosphorylated directed fragmentation) in optimized settings for each group (76). The method was tested on a 120µg whole-cell extract from human mesenchimal stem cells (hMSCs) and the results compared with those from TiO_2 enrichment alone. A total of 716 phosphosites was identified with SIMAC, while 350 with TiO_2. Moreover the number of multiply phosphorylated peptides was significantly increased (74).

Recently, a new intriguing method for multiply phosphorylated peptides enrichment based on polyarginine-coated diamond nanoparticles was presented, however it has still to be tested on large scale samples and where a low amount of starting material (micrograms) is available (110).

3.4.5 Magnetic beads

Starting from the TiO_2-based chemistry with the idea to find an easier way to perform the extraction of FPs, Chen and Chen (111) thought to conjugate the properties of magnetic materials with those of TiO_2, coating Fe_3O_4 nanoparticles with TiO_2 through a silanic bridge. The nanobeads are mixed with a tryptic digest, vortexed and captured with a magnet. The captured FPs are subsequently analysed through a laser desorption/ionization from the inorganic particles and a run in MS. The method was named SALDI-MS, from Surface Assisted Laser Desorption/Ionization Mass Spectrometry (112). There were subsequent improvements of the method, using for example Fe_3O_4@C@SnO_2 core-shell microspheres (the symbol @ means “coated by”), with which scientists were able to detect 77 phosphorylation sites in rat liver cells (113).

3.4.6 Calcium phosphate precipitation (CPP)

In 1994, Reynolds et al. presented a strategy for FPs enrichment through Ca^{2+} ions and 50% ethanol precipitation. The precipitated peptides from a tryptic digest of casein mostly contained multiple phosphoserines (114).

Zhang et al. tested the strategy by using calcium chloride ($CaCl_2$), ammonia solution ($NH_3 \cdot H_2O$) and disodium phosphate (Na_2HPO_4) on a rice embryo preparation (46). The dissolved and desalted pellet was then enriched through IMAC. In total, 227 non-redundant phosphorylation sites were identified, of which 213 on serine residues and 14 on threonine.

Through phosphate precipitation directly coupled to LC-MS/MS, Qiangwei Xia et al. identified 466 unique phosphorylation sites (379 on serine and 87 on threonine) in post-mortem Alzheimer disease brain tissue, 70% of which were not reported in Phospho.ELM database (115).

In both studies no tyrosine phosphorylated peptides were identified: it is not clear if this is due to the low abundance of these or to the poor selectivity of the method. Anyway the method offers the advantage of being rather simple, column-free and straightforward.

Method	Target	Sample type and amount	Strategy	Results	Reference	Comments
IMAC (Immobilized Metal Affinity Chromatography) IDA or NTA on a polymer matrix or magnetic beads with chelated Fe^{3+}, Ga^{3+}, Al^{3+} or other metal cations. Binding through electrostatic interaction between phosphate groups and metal cations.	protein, peptide	H1 stem cells proteins, 10 mg *D.melanogaster* lysate Kc167,10 mg	SCX-IMAC-RPLC-MS^2 (ETD-OT) SCX-IMAC-RPLC-MS^2 (LTQ-OT)	10844 phosphosites at1% FDR 13720 phosphosites at 0.63% FDR	(116) (117)	Proven to be effective in large scale analysis. Limited capacity and specificity, directed towards multiply phosphorylated peptides, affinity for acidic peptides
MOAC (Metal Oxide Affinity Chromatography) TiO_2, ZrO_2 or Nb_2O_5 as particles or layered on a Fe_3O_4 magnetic core. Bidentate binding between metal and phosphoric group oxigens.	peptide	HeLa lysate (amount not given) K562 lysate, 400 µg	SCX-TiO_2-RP-MS^2 &MS^3 (LIT-FT-ICR) SCX-TiO_2/Nb_2O_5-RP-MS^2 (MALDI-TOF)	6600 phosphosites, 2244 proteins at<1%FPR 622/642/834 phosphopeptides (Ti/Nb/all*) at 4%FPR	(118) (119)	Robust and chemically inert material, high capacity and fast absorption. Slow flow desorption, most effective for singly phosphorylated peptides.
SCX (Strong Cation Exchange) Ion Exchange Chromatography. Phosphopeptides less retained by stationary phase due to their higher negative charge	peptide	HeLa cell lysate, 300 µg HEK 293 cell lysate, 1 mg	SCX-RP-LC-MS^2&MS^3 (IT) SCX-RP-LC-MS^2 (ETD,LIT)	2002 phosphosites >5000 unique phosphopeptides 1%FDR	(119) (120)	Coelution with other acidic peptides. Useful as pre-enrichment technique
SAX (Strong Anion Exchange) Ion Exchange Chromatography. Phosphopeptides more retained by stationary phase due to their higher negative charge	peptide	Human liver protein digest, 100 µg *A.thaliana* membrane proteins digest, 500 µg	SAX-RPLC-MS2&MS3 (LTQ) SAX-IMAC-RPLC-MS^2 (Q-TOF)	274 Phosphosites at 0.96% FDR 299 Phosphopeptides	(122) (100)	Useful for peptide fractionation. Useful as pre-enrichment technique
HILIC (Hydrophilic Interaction Chromatography) Phosphopeptides more retained by stationary phase due to their higher polarity	peptide	HeLa cell lysate, 1 mg *S.cerevisiae* total protein, 6 mg	HILIC-RP-MS & S2 (IT) IMAC-HILIC-RP-HPLC-MS^2 (LTQ)	1004 phosphosites 8764 unique phosphopeptides, 2278 proteins	(121) (122)	Coelution with other acidic peptides. Useful as pre-enrichment technique

Method	Target	Sample type and amount	Strategy	Results	Reference	Comments
Chemical derivatisation Phosphoric group directly bound to a tag through phosphoramidate chemistry, diazo chemistry or oxidation-reduction and condensation. Alternatively β-elimination /Michael addition can be performed.	peptide	*D.melanogaster* Kc 167 tryptic digest, 1.5 mg Jurkat T cells lysate (amount not reported)	PAC-RP-LC-MS^2 PAC-RP-LC-MS^2 (LTQ)	535 phosphosites 79 tyrosine phosphoproteins	(123) (124)	Modulation of peptide properties for MS purposes. Reaction yield, side reactions, large amount of sample required.
Immunoprecipitation Affinity of the phosphosite to the antibody	protein, peptide	Jurkat T cells lysate (amount not reported) HME Cells lysate, 4mg	IP(pY-100 antibody)-RP-LC-MS^2 (LCQ-IT) IP(pY-100 antibody)-RP-LC-MS^2 (LTQ-OT)	194 phosphotyrosine sites 481 phosphotyrosine sites at FDR 1%	(125) (126)	Mostly directed to p-Tyr phosphosites

Table 1. *Comparation of enrichment and fractionation methods for phosphopeptides.*

**superimposition without redundancies of Ti and Zr detected phosphosites.*
Abbreviations: CID, Collision-Induced Dissociation; DHB, Dihydroxybenzoic acid; ECD, Electron Capture Dissociation; ETD, Electron Transfer Dissociation; FDR, False Discovery Rate; FPR, False positive rate; FT-ICR, Fourier Transform Ion Cyclotron Resonance; b-HPA, b-hydroxypropanoic acid; LIT, Linear Ion Trap; OT, Orbitrap; Q-TOF, Quadrupole-Time-Of-Flight; RP, Reversed Phase; SCX, Strong Cation Exchange; LTQ, Linear Trap Quadrupole; LCQ, Liquid Chromatography Quadrupole; IP, Immunoaffinity Purification.

3.4.7 Ion exchange chromatography (IC)

The simple enrichment of FPs with IMAC, TiO_2 or SIMAC has generally proven to be not enough productive when a deep knowledge of the phosphoproteome is required (127).

A fractionation step is also needed. Chromatography techniques based on charge interaction, hydrophilic interaction or a combination of both have been employed for this purpose (128).

Anion exchange chromatography exploits the generally higher affinity of FPs for the positively charged stationary phase due to the intrinsic high negative charge carried by the phosphate group. Strong anion chromatography (SAX) has been employed both as fractionating technique before a FPs enrichment

step (e.g. with IMAC or TiO_2) (129) and also as sole fractionating technique before LC-MS/MS.

Nühse et al. for example identified more than 300 phosphorylation sites in the plasma membrane fractions of Arabidopsis thaliana using a SAX + IMAC approach (130), while Han and co-workers identified 274 phosphorylation sites in human liver tissue extract without the enrichment step.

A drawback of this method has been reported by Thingholm et al. (66), who noted a strong attachment of FPs to the SAX resin, from which they are difficultly recovered.

Its counterpart, strong cation chromatography (SCX), has been largely employed as prefractioning technique for proteins and peptides. The pioneering work on FPs was carried out by Beausoleil et al. in 2004 (119). Tryptic peptides were acidified at pH 2.7, where most of the peptides carry a +2 charge due to C-terminal lysine or arginine and the N-terminal aminogroup. FPs, instead, carry a reduced charge due to the phosphate group, e.g. +1 in monoFPs. The reduced affinity of the resin should therefore leaving FPs to flow more easily through the column. This idea was confirmed by the results, which brought to the identification of 2000 phosphosites in 8mg of nuclear extract of HeLa cells lysate.

Trinidad and co-workers evaluated the efficiency of SCX as prefractionation method prior to IMAC to the efficiency of IMAC and SCX alone, finding a three-fold increased FPs identification in the combined approach respect both methods (99).

The strength of SCX as prefractioning system was further confirmed by Olsen et al., who identified 6600 phosphosites in 2244 proteins in EGF-stimulated HeLa cells through SCX + TiO_2 (118). In more recent reports 23000 and 36000 phosphorylation sites have been identified respectively with SCX followed by IMAC and TiO_2 respectively (131), (127). This remarkable increase in number of detected phosphosites is mainly due to instrumental and software improvements (128).

It remains to be assessed if the fractionation/enrichment approach can be suitable in samples where a small amount of starting material is available.

3.4.8 Hydrophilic Interaction Chromatography

Hydrophilic interaction chromatography (HILIC) is a separation technique for biomolecules (132). The method relies on the interaction of the analytes, e.g. peptides, with a neutral stationary phase through hydrogen bonding. They are eluted from the column with a decreasingly organic mobile phase according to their polarities (hydrophilicity).

McNulty and Annan introduced this method as prefractionation step before IMAC (121). They tested the FPs enrichment capacity of HILIC compared to SCX and IMAC alone, as well as the fractionation ability of HILIC before and after IMAC treatment. The analysis of 1 mg of tryptic digest of HeLa cells evidenced the prefractionation vocation of the method. The use of IMAC prior to HILIC gave in fact a high level of nonspecific binding due to not FPs, while the reversed approach improved the selectivity for FPs to more than 99%.

ERLIC (Electrostatic Repulsion - Hydrophilic Interaction Chromatography), or Ion Pair normal phase, is a newly developed chromatographic method able to enrich and fractionate FPs in a single step (135).

At pH 2.0 the C-termini and the carboxylic side chains of Asp and Glu are neutral, thus the peptides are generally positively charged and are not retained by a positively charged stationary phase. The presence of a phosphate group, however, reduces the net charge of FPs; this is not enough to overcome the overall repulsion for the stationary phase due to the basic residues, however an organic mobile phase, e.g. acetonitrile 70%, promotes their hydrophilic interaction within the column. The attraction for the column is enhanced in multiply phosphorylated peptides.

Zarei et al. evidenced in fact a higher efficiency of ERLIC compared to SCX and HILIC in fractionating multiply phosphorylated peptides (128) more retained by the stationary phase.

In a recent article (134) Xi Chen et al. compared the FPs profiles obtained from a HeLa cell lysate by using 4 HPLC methods after a phosphor-enrichment with IMAC. Even though with any of the four methods (SCX, HILIC, ERLIC with volatile and not volatile solvent) 4-5000 peptides could be identified, the combination of all the methods gave a total number of 9069

unique FPs, with a considerable amount of non-overlapping unique FPs. The four methods are thus complementary to get a full coverage of the phosphoproteome.

3.4.9 Hydroxyapathite (HAP)

Firstly introduced by Tiselius and co-workers in 1956 (135), hydroxyapathite (HAP) chromatography has been very popular until the 1980s, when new matrices have been introduced. HAP is a crystalline form of calcium phosphate with formula $Ca_{10}(PO_4)_6(OH)_2$, which binds FPs in virtue of both anionic and cathionic interactions. In particular Ca^{2+} binds phosphoric groups, and more strongly than it does with other acidic groups. The binding to the matrix is thus proportional to the number of phosphogroups on the peptides and can be exploited for a sequential elution of them according to their degree of phosphorylation. Mamone et al. (136) exploited this material to analyse a tryptic digest of standard proteins. The advantages of HAP are the low cost of the material and the possibility to elute stepwise the peptides according to the degree of phosphorylation. Yet the system has to be tested on more complex biological samples.

3.4.10 Molecularly Imprinted Polymers (MIPs)

Recently (137), Borje Sellergren's group has proposed a method for the depletion of phosphotyrosine containing peptides based on Molecularly Imprinted Polymers (MIPs). FPs imprinting was performed by an epitope approach (138), i.e. using a part of the analyte of interest (in this case the N- and C-protected phosphotyrosine) as a template to prepare a MIP able to fish FPs. The Solid Phase Extraction analysis showed a 18-fold preferential retention for phosphorylated angiotensin II respect the non phosphorylated one, preference not shown in the not imprinted polymer. Moreover, the material showed a preference for a triply phosphorylated peptide over a monophosphorylated one, showing opposite behaviour comparing to TiO_2 material. Of course a more extensive analysis and improvements are needed in order to tackle more complex samples.

3.4.11 Chemical derivatisation strategies

The chemical derivatisation strategies exploit the typical properties of the phosphate groups in the peptides, like the lability of the phosphoesteric bond and the subsequent easy substitution of the phosphate with a nucleophilic tag.

A different widely used approach is the methyl esterification of the carboxylic groups, notoriously competitive with the phosphate groups due to their negative charge (Fig.2).

3.4.11.1 Methyl esterification of carboxyl-groups

In IMAC strategy carboxylic groups influence the elution of FPs, due to their charge attracted by the positively charged metal of the resin. For this reason their esterification could prove useful. Ficarro et al. first applied this strategy for the analysis of the cell extract from *S.cerevisiae* (96) through IMAC approach: 383 sites of phosphorylation were detected with this method. Some characteristics of this approach have already been depicted in par.4.2 and will be no further analysed.

Methyl esterification can be also exploited as a mean of isotopic labeling (with CH_3OH and CD_3OH for two different cellular states) for quantification purposes (98).

3.4.11.2 Biotin tagging by β-elimination and Michael addition

Many chemical derivatisation strategies have been devised to displace the phosphoryl group and binding a tag to the “naked” peptide. One of these methods (139) relies on the β-elimination of the phosphate from phosphoserine and phosphothreonine producing dehydroanaline and β-aminobutyric acid respectively. These products can be directly detected using tandem MS or derivatised, for example by Michael addition of a reactive thiol and subsequent binding of a tag.

One common tag is biotin, notoriously having great affinity for avidin, liable of immobilization to an affinity column (140).

This technique shows the limits of not being applicable to phosphotyrosine containing peptides and of the occurrence of side reactions like tagging of non phosphorylated serine.

Zhou et al. (141) proposed another method of derivatisation applicable to all residues, even if it involves many steps and it has not been tested on complex samples yet.

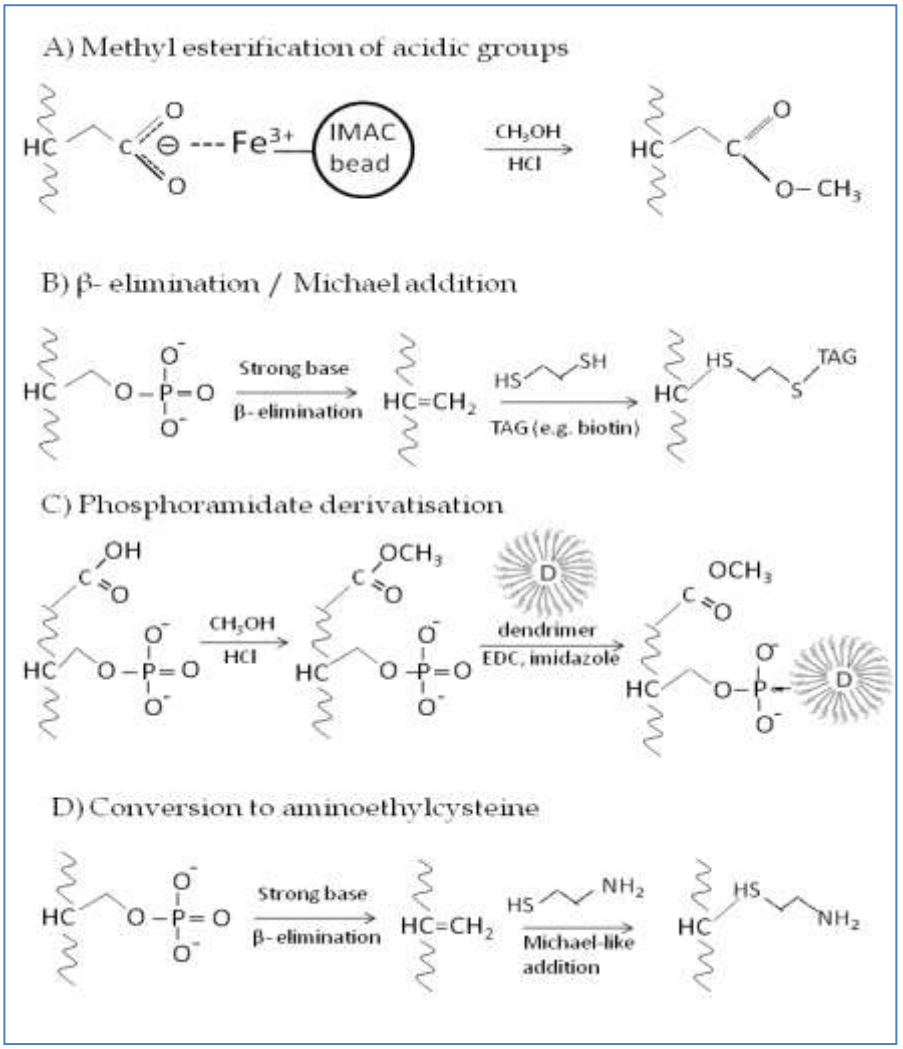

Figure 2. *Chemical derivatisation methods for phosphorylation capture and analysis.*

A) IMAC suffers of aspecific binding of acidic peptides to the resin. Esterification of carboxylic groups with Methanol/HCl is a strategy to overcome this problem.

B) In presence of a strong base the β-elimination at phosphoserine and phosphothreonine produces dehydroanaline and β-aminobutyric acid. These can be derivatised with a thiol through a Michael-like addition and a tag can be added. If the tag is biotin, its affinity with avidin can be exploited.

C) FPs can be derivatised to phosphoramidates after esterification of carboxylic groups. If a dendrimer is employed the derivatised peptides can be separated through size-selective methods.

D) β-elimination and Michael-like addition of cysteamine converts phosphoserine and phosphothreonine in lysine analogues that specific enzymes leave in the C-terminus.

3.4.11.3 Phosphoramidate conversion

In 2005 Aebersold's group proposed a derivatisation procedure based on the carboxyl protection through methyl esterification followed by conjugation to a soluble polymer with phosphoramidate chemistry (PAC) (124).

The mixture of peptides is first converted to the corresponding methyl esters. In this step two cellular states can also be differentially labeled for quantitative analysis. Subsequently, the methylated peptides are combined and put to react with EDC, imidazole and a polyamine dendrimer. Phosphopeptides are converted in the corresponding phosphoramidates, easily separated from the non FPs through size selective methods. FPs are recovered with a brief acid hydrolysis and sent to the MS analysis.

When coupled with pervanadate stimulation and an initial antiphosphotyrosine protein precipitation step, this method allowed the identification and quantification of all known plus previously unknown phosphorylation sites in 97 tyrosine proteins in Jurkat T cells.

A modification of this method was proposed (123), exploiting the reaction of the phosphate groups with cystamine and a reducing agent instead of the dendrimer. The –SH group of cystamine reacts with maleimide-activated glass beads, immobilizing the FPs on a solid phase. This method allowed the identification of 229 FPs in the cytosolic proteome of *Drosophila melanogaster* Kc167 cells without any pre-enrichment step.

3.4.11.4 Conversion to aminoethylcysteine

Even after a good preconcentration step it is difficult the exact assignation of a phosphorylation site, due to the lability of the phosphate group, often lost during the backbone fragmentation in a MS collision, and to the intrinsic low abundance of phosphorylated peptides.

To address this problem, Knight et al. (142) devised a derivatisation method based on β-elimination and Michael addition of cysteamine to convert phosphoserine and phosphothreonine in aminoethylcysteine (Aec) and β-methylaminoethylcysteine respectively. Due to the resemblance of Aec to lysine, the use of proteases that recognize this aminoacid (e.g. Lys-C and

lysyl endopeptidase) cleaves proteins leaving it in the C-terminus. The system works also with β-methylaminoethylcysteine and permits to identify the exact site of phosphorylation.

The limit of the method is the racemization in the addition step, converting only 50% of the phosphoaminoacids in the appropriate enzyme substrate. In the case of multiply phosphorylated peptides this fact greatly increases the complexity of the peptidic mix arising from the protein.

3.4.12 Comparison of enrichment methods

From this survey of enrichment methods emerges that no single technique is able to tackle the entire phosphoproteome. Some methods work in the direction of enriching only some species, like the antibodies for phosphotyrosine or the combination β-elimination/ Michael addition selective for phosphoserine and phosphothreonine. Other methods, like calcium precipitation, SAX, SCX and HILIC, work better as preseparation techniques to reduce sample complexity before more specific enrichment methods like IMAC, MOAC, SIMAC and PAC.

Every enrichment technique presents advantages and disadvantages, but also different specificities. Usually, MOAC is more specific for monophosphorylated peptides, due to the strong affinity for the multiply phosphorylated ones, not enough eluted. On the contrary, IMAC is more specific for multiply phosphorylated peptides, but has a low capacity and selectivity when used with highly complex samples. The combined approaches, like SIMAC, seem to be promising but revelate the necessity of a pre-enrichment step (143).

A systematic comparison of methods was made by Bodenmiller and co-workers (fig.3). They examined the reproducibility, specificity and efficiency of IMAC, PAC and two protocols for TiO_2 chromatography: $pTiO_2$ (phthalic acid in the loading buffer to quench nonspecific binding) and $dhbTiO_2$ (2,5-dihydrobenzoic acid, quencher too) (89). Each method was tested through the injection of 1.5 mg of tryptic digest from cytosolic fractions from *Drosophila melanogaster* cells. The authors found a very good reproducibility

of all the methods, making them suitable for quantitative analysis. Moreover, none of the methods was able to reveal the entire phosphoproteome, but they show partial overlapping results between each other.

In general a simple and straightforward strategy is desired, with few preparation steps and little sample handling in order to avoid loss of FPs. It is of course critical also the amount of starting material and the expertise of the people performing the extractions. For this reason detailed protocols are needed (144), (66).

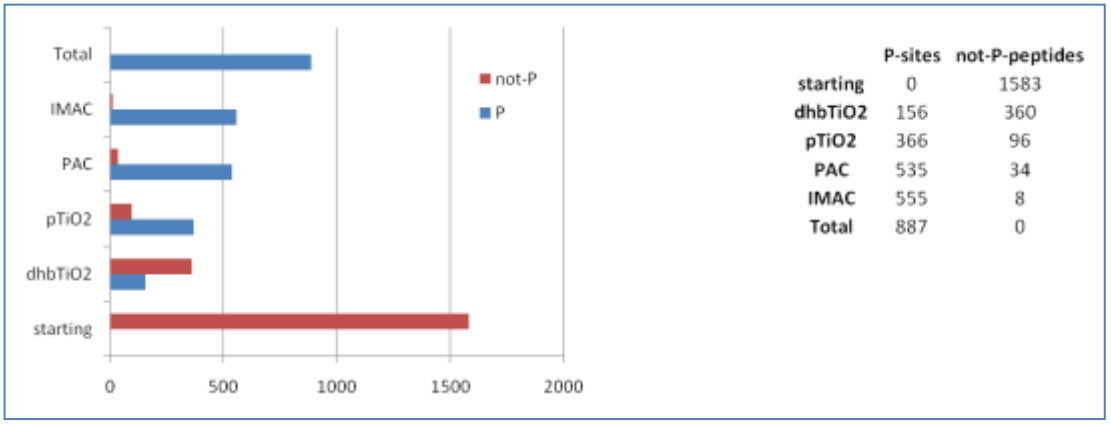

	P-sites	not-P-peptides
starting	0	1583
dhbTiO2	156	360
pTiO2	366	96
PAC	535	34
IMAC	555	8
Total	887	0

Figure 3. *Comparison of phosphorylation enrichment methods. The graph shows the efficiency and selectivity of IMAC, PAC and TiO_2, applied on a tryptic digest of a cytosolic protein extract of D.melanogaster cells [Bodenmiller et al., 2007]. In the starting material no FPs were detected, while the best selectivity in terms of P vs. not-P sites was IMAC.*

3.5 MS-based strategies for phosphoproteome analysis

Mass spectrometry has become the preferential method for peptide and protein identification following the separation steps, also in the PTM analysis (145).

The first step of a typical MS analysis consists in the cleavage of a single protein or a mixture by using a dedicated enzyme, usually trypsin, which preferentially cleaves the peptide bonds after arginin or lysine. Moreover, the tryptic fragments' weight is 700-3500 Da, a size suitable for MS analysis.

The peptides are thus separated by nanoLC and vaporized/ionized through an ESI source. Their mass is evaluated and a second fragmentation, generating MS/MS spectra, permits to evaluate also their aminoacidic sequence. This is possible because of the higher lability of the bonds between aminoacids. Depending on the position of the cleavage along the

peptide chain, the MS/MS fragments are classified in a,b,c (starting from the N-terminal) or x,y,z (starting from the C-terminal) according to Roepstorff and Fohlman (146), (147) (Fig.4). Only the highest abundance peptides are submitted to MS/MS. This creates a hurdle in phosphoproteomics, because of the lower abundance and difficult ionization of FPs compared to the co-present not-FPs, thus introducing the need of an enrichment step, as explained in section 4.

The information about the peptide sequence is submitted to database-digging softwares as MASCOT (148) or SEQUEST (149), which explore protein databases to find a sequence match with previously annotated proteins and rank the correlations through a probability score.

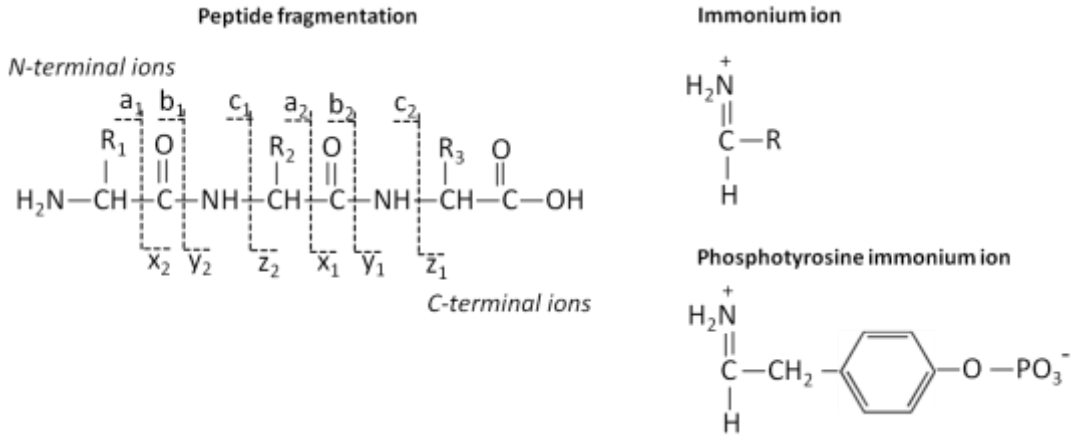

Figure 4. *Common nomenclature of peptide fragment ions. The peptide fragmentation in MS/MS mostly breaks the inter-residue bonds to generate fragment series. CID generates preferentially y and b ions, while mostly z and c ions are originated by ECD and ETD. Phosphotyrosine immonium ion is diagnostic of tyrosine phosphorylation.*

3.5.1 Collision Induced Dissociation (CID)

The most established method to induce a secondary fragmentation in peptides is the collision induced dissociation (CID). Basically, the peptide ion collides with an inert gas (He or Ar) which transfers its kinetic energy, subsequently redistributed between the atoms bringing to the breaking of the bonds. When a phosphoserine or phosphothreonine is present in the peptide sequence, the phosphoesteric bond is by far the most labile, thus a neutral loss of phosphoric acid H_3PO_4 (98 Da) takes place, originating respectively dehydroalanine and dehydroaminobutiric acid. Given that most part of the

energy is employed to break the phosphoesteric bond, far less energy is available for the subsequent fragmentation of the peptide chain (150).

This drains information when the identification of the phosphate group position is needed: only the bare presence or absence of a phosphate is assessed.

To overcome this issue several strategies have been applied. The first one is the introduction of a tertiary fragmentation, specifically directed towards peptides where a phosphate loss is detected. This strategy is named pdMS^3 (phosphorylation directed MS^3) (151). The information due to the alternative fragmentations of the precursor ion are in this case lost, but they can be kept through another approach, named Multi-Stage Activation (MSA) (152). In this case the ion trap, filled with the selected ion coming from neutral loss, is filled again with the original peptide and both are fragmented at the same time, originating a superimposed MS^2 / MS^3 spectra more information-rich.

Partial neutral loss happens also on phosphotyrosine residues, which leave a HPO_3 group (80Da) originating a characteristic phosphotyrosine immonium ion at m/z 216 (fig.4). The phosphoesteric bond is however in this case more stable, thus not compromising the information collection. Steen et al., for example, used the diagnostic fragment at m/z 216 for the selective detection of phosphotyrosine-containing peptides in chicken ovalbumin and murine MAP-kinase 2 (79).

3.5.2 Electron capture dissociation (ECD)

The limit of the peptide backbone poor fragmentation in the presence of a phosphate group was overcome in 1998 with a new fragmentation strategy. Electron Capture Dissociation (ECD) is a method developed by Zubarev and colleagues to improve the fragmentation of multiply charged protein and peptide ions (153). These ions capture easily a thermal electron (<0.2 eV), which induces a non ergodic fragmentation, i.e. without vibrational energy redistribution like in CID. The result is a fragmentation mostly at S-S and N-C_α backbone bonds, leaving intact the PTM bonds. The generated ions are c and z type (fig.4) (154). The method has some drawbacks, like a bigger

affinity for disulphide bonds and a difficult fragmentation of N-terminal proline, which has two bonds to break. Moreover it can be carried out only with expensive FT-ICR instruments (up to 1$ million) to generate the static magnetic field for the electrons, which reduces its wide scale diffusion.

3.5.3 Electron transfer dissociation (ETD)

The efforts to find an ECD-like method without the need of expensive instruments brought to the advent of ETD (Electron Transfer Dissociation). In this approach the electron is transferred to multiply charged peptides (charge >2+) through a radical anion with low electron affinity, like anthracene or azobenzene (155). The method can be implemented on linear quadrupole ITs, with the natural drawback of a reduced resolution and accuracy (156). Molina et al. (158) carried out a large scale analysis of human embryonic kidney 293T cells, identifying 1435 phosphosites, 80% of which were novel. Moreover, they identified 60% more FPs with ETD compared to CID, mainly due to the 40% more fragment ions . It has to be remarked the little overlap between the two fragmentation techniques, that was exploited to develop an integrated approach. Since ETD works better with high charge peptides, Lys-C was thought to give better results than trypsin, cleaving the peptides only at C-terminal lysine. Surprisingly the results did not match the expectations, probably due to the high number of missed cleavages in the tryptic lysate (157). Another way to generate highly charged peptides was attempted by Larsen et al, who added 0.1% m-nitrobenzyl alcohol (m-NBA) to the LC-MS solvent (158). This approach increased the predominant charge from 2+ to 3+, improving the ETD results. The approach is currently being tested on more complex samples. Another fact to remark is the evolution of the software, born for the CID approach, in the direction of meeting the features of spectra generated by new enzymes and fragmentations (159), (http://www.matrixscience.com).

Table 2. *Comparison of fragmentation methods. All the methods show good results with a class of peptides, suggesting that an integrated approach CID/ECD or CID/ETD could be more effective [Molina et al., 2007].*

	Fragmentation agent	**Generated ions**	**Instruments**	**Pros**	**Cons**
CID	Inert gas (He, Ar)	y, b	ESI-MS	Better fragmentation of low charge peptides (2+)	Fragmentation mostly at the phosphogroup
ECD	Thermal electron	z, c	FT-ICR	Fragmentation only along the peptide bond	Need of expensive FT-ICR
ETD	Low electron affinity anion (e.g.anthracene)	z, c	IT, Q-TOF	Fragmentation only along the peptide bond	Less sensitive than CID

3.6 Quantitative approaches for phosphoproteome analysis

In order to take a dynamic picture of the phosphorylation events in a particular pathway, it is desirable monitoring which sites are phosphorylated and to which extent following a stimulus. To achieve this goal some quantification methods are available and can be classified on the basis of the analysis step in which the quantitative information is generated: a differential isotopic label can be introduced in the cell culture, e.g. with labeled aminoacids (SILAC), in the protein mixture (ICAT), in the enzymatic digestion (^{18}O labeled water), or in the peptide mixture (iTRAQ), otherwise, in label-free experiments, the quantitative information is extracted at the MS level (Fig.7). A thorough review about quantitation strategies has been published by Bantscheff et al. (160).

		LEVEL			
		CELL	PROTEINS	PEPTIDES	MS
METHOD	SILAC	X			
	^{18}O		X		
	ICAT		X	X	
	iTRAQ			X	
	LABEL-free				X

Figure 7. *Strategies for quantitative analysis of protein phosphorylation. An isotopic label can be introduced in different moments of the analysis or not at all, in label-free experiments.*

3.6.1 Metabolic labeling

Metabolic labeling was first described in 1999 (161). In 2002 Mann and coworkers introduced the term Stable Isotope Labeling by Aminoacids in Cell culture (SILAC) and used it for quantitative analysis of protein phosphorylation in 2003 (162). The typical experiment consists of growing a cell population in a medium containing an essential aminoacid labeled with a stable isotope (^{15}N or ^{13}C), and growing in parallel another cell population in a medium on non-labeled aminoacid. Usually labeled arginine and lysine are used, in order to ensure that every peptide from one culture contains a label after tryptic digestion. After several doublings, the cells are harvested from both cultures, and the protein extracts mixed together. After proteolysis, peptides can be analysed by MS and differences in the abundance of a peptide in the two cell extracts are shown through the different heights of two mass shifted peaks.

Recently, with this method Olsen et al. (118) reported the most comprehensive analysis of the effects of EGF stimulation on phosphoproteome dynamics in HeLa cells. This strategy has allowed the drawing of some detailed maps of time-resolved signaling pathways (163), (164). The major limitation of SILAC stays in the cost of labeled aminoacids.

3.6.2 Protein and peptide labeling

Post-biosynthetic labeling of proteins and peptides is performed by chemical or enzymatic derivatization in vitro.

Enzymatic labeling exploits the incorporation of ^{18}O atoms from marked water during protein digestion. Trypsin and Glu-C introduce two heavy oxygen atoms, resulting in a 4 Da mass shift, generally sufficient for the differentiation of isotopomers. This method has been applied for quantitative proteomic purposes (165), but complete labeling is difficult to obtain.

Chemical modification can be carried out at protein or peptide level introducing a tag on a chemically reactive side chain of an aminoacid [Ong et al., 2005], in practice only cysteine and lysine are used for this purpose. A group of labeling reagents targets the N-terminus and the ε-aminogroup in the lysine side chain. They mostly exploit the N-hydroxysuccinimide (NHS) chemistry or other active esters and acid anhydrides, like in the Isotope-Coded Protein Label (ICPL) (166), isotope Tags for Relative and Absolute Quantification (iTRAQ) (167), Tandem Mass Tags (TMT) (168) and acetic/succinic anhydride (169).

iTRAQ is a commercially available reagent, allowing to follow the evolution of biological systems over multiple time points. It was used, for example, to quantify 222 tyrosine phosphorylation sites across seven time points following EGF stimulation (170).

Carboxylic groups of side chains of aspartic and glutamic acid as well as of the C-termini of peptidic chains can be isotopically labeled by esterification using deuterated alcohols, for example d_0 and d_3 methanolic HCl (171).

This reaction is particularly interesting, because the methylation is also a step used in the IMAC enrichment method to reduce aspecific binding of acidic peptides to the resin (par. 4.2).

General drawbacks of the chemical derivatization methods are the production of not desired side products, that negatively influence the quantification results and the cost of some of the mentioned reagents.

3.6.3 Absolute quantification using internal standards

The use of isotope-labeled internal standards in the field of proteomics is known with the name AQUA: Absolute QUAntification of proteins (172).

The simplest protocol requires adding a known amount of a stable isotope-labeled peptide to the protein digest and in comparing the signal of it in the mass spectra respect the other peak areas (173).

There are some drawbacks with this approach. First of all the high dynamic range of concentrations of peptides makes difficult to find an appropriate concentration of standard for every analyte; second, it's likely to find an isobaric peptide to our standard in the peptide mixture, therefore limiting its specificity. These problems, however, have been addressed with the approach called Multiple Reaction Monitoring (MRM) (174) , in which the triple quadrupole MS monitors both peptide and its fragments mass during the experiment. The combination of retention time, peptide mass and fragment mass practically eliminates the ambiguities, extending the dynamic range to 4-5 orders of magnitude (175). The real value of the quantification through the AQUA approach is naturally biased by the manipulation of sample before adding the standard: the amount of protein determined may therefore not reflect its actual expression level in the cell.

3.6.4 Label-free quantification

There are two approaches for label-free quantification of proteins. The first one relies on the measure of the area of a MS peak of a peptide related to a protein: the increase of this area means also an increased amount of the protein. This approach is called eXtracted Ion Chromatogram (XIC), because a single ion peak area is extracted from a plot of signal intensities against time in the chromatogram (176). Signal intensities of the same peptide in different experiments is then compared to extract quantitative information, for example the stoichiometry of phosphorylation (177).

The other approach measures the amount of peptides generated from a protein: the more is the amount of a protein the more are the tandem-MS generated peptides. Relative quantification is thus achieved by comparing the

number of spectra generated from a protein in different experiments. It is necessary a normalization, for example depending from the protein mass, creating therefore Protein Abundance Indexes (PAIs) (178). The relationship between number of peptides observed and protein amount had been found to be logarithmic (emPAI), (179).

3.7 Non-MS approaches to elucidate cellular signaling networks

3.7.1 Antibody-based approaches

In order to monitor previously identified phosphorylation sites, arrays employing phosphospecific antibodies have been used to investigate dozens of phosphorylation sites simultaneously (180). The general hurdle of these techniques is the limited availability of dedicated antibodies, however further improvements could extend the use of microarray technology in phosphoprotein studies (181).

Methods were developed to monitor the phosphorylation status of tyrosine (182) and the kinetics of phosphorylation (183) proteins in a multiplex format.

In order to evaluate the phosphorylation dynamics on a cellular scale, flow citometry approaches have been also devised to monitor up to 11 phosphorylation events in parallel; (184). Again, the main limit of this approach is the availability of suitable fluorescent-labeled antibodies.

3.7.2 Interaction of phosphoproteins and phosphorylated sites

The phosphorylation-related events include also protein-protein interactions in the cell signaling network. To investigate these phenomena, Jones et al. (185) devised a protein array to study the binary interactions between 61 fluorescent-labeled, tyrosine phosphorylated peptides from EGFR receptors with approximately 150 SH2 and PTB domains. By measuring the fluorescence at different titration points they determined the K_D values for every peptide-receptor couple.

Another approach was followed by Yaoi et al. (186), that immobilized SH2 domains on microspheres to extract interacting proteins and phosphoproteins from a complex mixture of different cell lines.

Both approaches revealed new insights in the cellular signaling networks.

3.7.3 Kinase screening on peptide and protein arrays

Peptide microarrays consist of synthetic peptide sequences deposited onto glass slides or attached to a derivatised surface, usually in triplicate, with peptides having substitutions in the phosphorylation sites as controls. The *in vitro* phosphorylation reaction is performed in the presence of radiolabeled ATP, the array exposed to a film and the image captured. The method assumes that phosphorylation of peptides should be in most of the cases similar to that of the same sequence in the intact protein, due to the fact that many phosphorylation sites are in accessible and flexible regions of the protein structure (130). Collins et al. used this approach for phosphorylation investigation of synaptic proteins, finding 28 unique phosphorylation sites (97).

The *in vitro* phosphorylation can naturally be different from the *in vivo* action, but the screening can select and give priority to some phosphorylation sites for further investigation.

The same approach can be used for immobilized proteins or protein domains. Ptacek et al. (187) immobilized yeast proteins on high density (4400 proteins in duplicate) arrays on glass slides. They screened 87 kinases, finding that each kinase recognized up to 256 substrates, with a media of 47 substrates per kinase. These data allowed the construction of a global kinase-substrate interaction network. There is of course a concern about non specific phosphorylation, but also the perspective of a high throughput analysis for mapping phosphorylation networks.

3.8 Bioinformatics

The knowledge discovery process in proteomics has been greatly boosted in the last years by the introduction of new bioinformatic tools.

Widely developed phosphoproteomics databases are for example PhosphoSite (188) containing around 100,000 non-redundant phosphorylation sites (as well as other modifications, given that the cell

signaling is not exclusively phosphocentric), and Phosida (189), containing temporal phosphorylation data from cell stimulation in time-course experiments.

These databases permit not only the data mining, but also the interpretation of the data in the context of biological regulation, diseases, tissues, subcellular localization, protein domains, sequences, motifs, etc. (http://www.phosphosite.org)

3.9 Conclusion about phosphoproteomics

Phosphoproteomics is a rapidly growing field, owing this evolution to the importance of the protein phosphorylation in many biological processes and its alteration in many diseases.

The analysis is usually performed with MS-based methods, supported by enrichment steps at the protein or peptide level. The improvement of MS has been enormous, with increase in resolution, mass accuracy, larger dynamic range and more sensitivity and speed, driving the progress in this field.

Of course it must be mentioned also the evolution in bioinformatics, with the developing of adequate software for literature mining, prediction algorithms, post-analysis annotation and so on. The aim of phosphoproteomics is not only to find phosphorylation sites, but also monitor the dynamic of phosphorylation following stimuli to characterize completely signaling networks.

Nowadays the phosphoproteome of highly complex samples has been tackled (99), (101), but further development of the methods, including of the bioinformatic tools to integrate complex databases, is needed for a more thorough knowledge of the mechanisms of phosphorylation networks.

4 Molecularly Imprinted Polymers

A relatively recent technique to develop affinity receptors that could find interesting applications in prefractionation is the molecular imprinting of polymers (MIPs). MIP permits to synthesise materials with entailed recognition properties, by exploiting a “template” mediated synthesis, where the “template” is a molecule of interest. During the polymerisation functional monomers assemble around the template either via reversible covalent bonds (190). or via non-covalent interactions such as hydrogen bonds, ionic bonds, hydrophobic interactions, van der Waals forces, etc. (191), (192).

The pre-assembly is further blocked by crosslinking, forming a polymer with embedded molecular depressions, or clefts, complementary to the template in size, shape and functionality.

Molecular imprinting of small molecules such as herbicides, metal ions or amino acids has been successfully accomplished and numerous papers express the potential of such materials as sensors (193), (194), chromatography beds (195), (196), synthetic antibodies (197), (198), synthetic enzymes (199), (200) or systems for controlled drug release (201), (202). These studies demonstrate that imprinted materials might exhibit very high selectivity and even enantioselectivity (199).

4.1 MIPs for proteins and peptides

A particular challenge concerns the development of MIPs to recognize large target molecules such as peptides and proteins. The complexity of such a process has been attributed to several reasons (203). First of all, large molecules are not able to diffuse through the polymeric network, limiting the use of crosslinking that proved to be successful in preserving the imprints. Second, the relative non-rigidity of proteins and the ease of unfolding may lead to the formation of poorly-defined recognition sites. Third, the poor solubility of most proteins in organic solvents limits the synthesis conditions.

Plus, large molecules possess a number of potential binding groups and the choice of the functional monomers plays a crucial role to the quality of the imprints. In the case of large biomolecules, it was suggested to exploit the

biochemical information on the natural receptors of the target proteins, as a starting point in the decisional process towards the definition of the monomer composition (204).

To overcome the limitations posed by the complexity of protein structure, it has been proposed to imprint only part of the protein. The short peptide sequences selected are called epitopes (205).

Regarding peptides imprinting, Kempe and Mosbach (206) demonstrated chiral separation of small peptide sequences with highly cross-linked MIPs. In another study, Kempe (207) developed a MIP able to recognize Z-oxytocin peptide, despite the selectivity of rebinding was not remarkable. In a more systematic study, carried out by Klein et al. (208), imprinting of tripeptide sequences was assayed, with specific binding of approximately 30% for the print sequence and much lower binding of other similar sequences. Finally, Hart and Shea (209) proposed metal affinity (Ni^{2+}) to histidine terminal groups and obtained a quite successful peptide imprinting.

A different strategy to address the issue of protein imprinting consists of surface aided imprinting, which attempts to produce successful imprints by depositing the proteins onto a support, thus taking advantages; 1) of the orientation of the template, and 2) of the problems linked to template entrapment. Proteins have been at first deposited on / immobilised to a solid surface and subsequently the polymer has been grown (210), (211), (212).

A wide choice of supports and materials have been used: polysiloxanes in the very early study of Glad et al. (213) demonstrated a successful imprinting of glycoprotein transferrin and later Lulka et al. (214) created a MIP for ricin onto silica particles. Fluoro-polymer films were prepared by Ratner and co-workers (215) by radio frequency glow discharge plasma deposition to form films around proteins deposited on a mica surface and subsequently coated with disaccharide molecules. Bossi et al. (216) coated polystyrene microtiter plates with a thin layer of a stable conjugated polymer (aminophenyl boronic acid) polymerized in the presence of various protein templates. Rick and Chou (217) imprinted proteins in thin layers of aminophenylboronic acid and

used micro-calorimetry measurements to assess the enthalpy changes associated with the rebinding and the imprinting efficiency.

To address the issue of the non compatibility of protein to organic solvents, some research groups have been working at the imprinting in aqueous conditions, thus with water compatible polymers, which ensures solubility and conformational stability of the proteins. Despite of the advantages, results are still limited. Hjerten and co-workers (218) pioneered the use of lightly crosslinked polyacrylamide hydrogels as the polymeric matrix. Hirayama et al. (219) incorporated charged functional groups (either positives or negatives) in polyacrylamide gels in the attempts to achieve a better recognition. Ou et al. (220) combined polyacrylamide simultaneously with two functional monomers, methacrylic acid and 2-(dimethylamino)ethyl methacrylate.

As drawback of hydrogel protein imprinting, the amount of protein template that remains entrapped in the MIP is generally high, due to diffusional limitations and of the collapse of local polymeric environments. In an attempt to ameliorate the rigidity of the hydrogel architecture, Gou et al. (221) developed a composite material, by insertion of imprinted polyacrylamide gel into the pores of chitosan or modified chitosan beads. The results achieved on protein and peptide imprinting still need amelioration, if the final goal of these materials is to compete with natural receptor systems. MIP methods for the selective recognition of specific peptide sequences and/or proteins remain a significant challenge.

4.2 MIPs for proteome with particular attention to phosphopeptides

Of particular interest in the proteome era becomes the MIP for phosphopeptide (FP) enrichment prior to proteomic MS analysis.

The works published deal quite exclusively with the preparation of MIPs for inorganic phosphates, and are mostly targeted to agricultural/waste water subject (222), (223). Against all odds, recently Sellergren’s group tried to develop a MIP-based method for FP enrichment, achieving positive indication on its feasibility, but still limited results (224). Most of the papers dealing with

phospho-groups converge in assessing the effectiveness of urea and thiourea monomers for the capture.

5 Synthesis and characterization of MIP nanoparticles selective for peptides containing phosphotyrosine

The purpose of this research line is to develop a selective material for pTyr-containing peptides. The application of such material will be primarily as alternative to antibodies, largely employed in phosphoproteome analysis to selectively enrich in phosphoproteins and/or phosphopeptides a protein or peptide mixture. The advantage of MIPs “plastic antibodies” respect to the natural ones is their potential much lower cost of production plus resistance to harsch conditions (pressure, temperature, basic or acidic pH) and in general a higher stability: they can be used in both aqueous and organic solvents (190). In perspective, the nano size of MIPs (nanoMIPs) further points out their use *in vivo* to selectively target a phosphorylated epitope, for which a suitable plastic antibody has been devised. This opens the exciting scenario of diagnostic and therapeutic molecules specifically tailored on the target by using itself as a model template. It remains as remarkable example of biomimicry the recent report of Kenneth Shea and colleagues, that devised a plastic antibody specifically directed against the peptide mellitin, a component of the bee venom. These MIP nanoparticles worked *in vivo,* by removing a lethal amount of toxin from the circulation of mice and significantly reduce their mortality (191). The first step of the nanoMIP synthesis process consists in the optimization of the production method for nanoparticles, that should be of suitable size and polydispersity. Their use *in vivo* requires for example an ideal size less than 100nm (similar in size to viruses) to penetrate living cells and translocate within the body (192) moreover a Polydispersity Index, associated with an homogeneous population (see next paragraph), should be ideally less than 0.2 (193), (www.malvern.com). In any case a particle size similar to the size of the proteins greatly facilitates the diffusion of the protein itself through the matrix, reducing the time of analysis (194), (195). The same method of synthesis is

subsequently used in presence of the template molecule to create its print in the nanoparticle. The molecule is then removed and the left cavities maintain the ability to rebind the same molecule due to their size and chemistry (functional groups of monomers oriented to compatible groups of the template during the polymer synthesis). The imprinted and not imprinted nanoparticles are then tested for specificity, selectivity and capacity (see Par.5.4).

Between the different ways of nanoparticles synthesis, photopolymerization seemed to be a valuable choice. This method employs a starter triad composed of a coloured antenna, a reducer and an oxidizer, that in this case were methylene blue (MB), toluensulphinic acid (TSIA) and diphenyliodonium chloride (DPIC), as suggested by Righetti et al. (196) (Fig. 8). The described mechanism employs MB, activated by the light, to form an excimer with TSIA, by which it is reduced. TSIA radical is an active one, while MB radical is passive, thus terminates the polymerization chain reaction. The scope of DPI is to boost the reaction through $MB^{\cdot}$ oxidation to form an active radical $Ph^{\cdot}$ while regenerating MB* (Fig. 8) (197). This method permits to control the polymer growth through a light-switch-like mechanism.

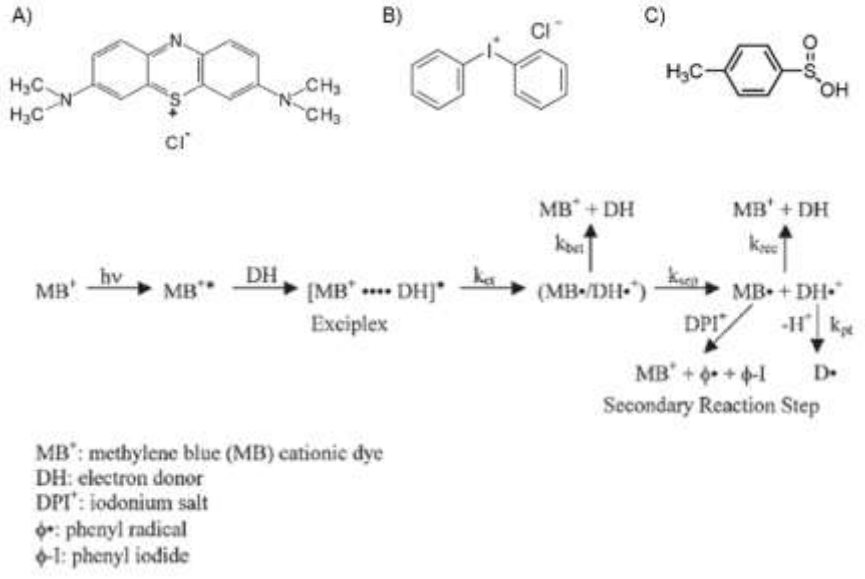

Figure 8. *Chemical structures of the three compounds employed as starter triad for the photopolymerization process: A) Methylene blue (MB), B) Diphenyliodonium chloride (DPI), C) Toluensulphinic acid (TSIA), plus the mechanism of activation: a visible-light-induced electron transfer initiation process (197).*

5.1 Techniques for nanoparticles physical characterization

The physical characterization of the nanoparticles can be made with a variety of different techniques, addressed to understand and control their synthesis and applications. Some widely used techniques are Transmission Electron Microscopy (TEM), Scanning Electron Microscopy (SEM) and Atomic Force Microscopy (AFM), mainly devoted to visualize the particles and thus explore their morphology plus other chatracteristics like aggregation. Other techniques like X-ray Photoelectron Spectroscopy (XPS) evaluate instead surface characteristics like chemical composition or electronic state (198). Dynamic Light Scattering (DLS) is another widely used technique that permits to assess particle size, particle number and tendence to aggregation (199).
In this project AFM and DLS were used.

5.1.1 Dynamic Light Scattering

Dynamic Light Scattering (DLS) is a physical technique employed to determine size distribution of particles in solution. The physical phenomenon at the basis is Rayleigh scattering, i.e. the diffusion of light in all the directions from particles smaller than the wavelength (200). When the light is coherent and monochromatic, like a laser, constructive and destructive interference happen between the light emitted by the scatterers. This interference changes continuously with the time due to Brownian motion of the particles. By detecting the light intensity at a certain angle (usually 173° respect to the light source) an intensity fluctuation can thus be observed. This fluctuation is faster for fast-moving particles, thus depends on the size of the particles, on their shape and on temperature and viscosity of the medium. The fluctuation is mathematically expressed by the autocorrelation function (Eq. 1):

$$1) \qquad g^2(q;\tau) = \frac{\langle I(t)I(t+\tau)\rangle}{\langle I(t)\rangle^2}$$

where $g^2(q;\tau)$ is the autocorrelation function at a particular wave vector q, and delay time τ, and I is the intensity. At short time delays τ the correlation is high, meaning that intensity changed very little due to the little motion of the particles. At longer time delays the correlation between intensities instead

decreases exponentially and depends essentially on the diffusion coefficient of the particles (Fig.9).

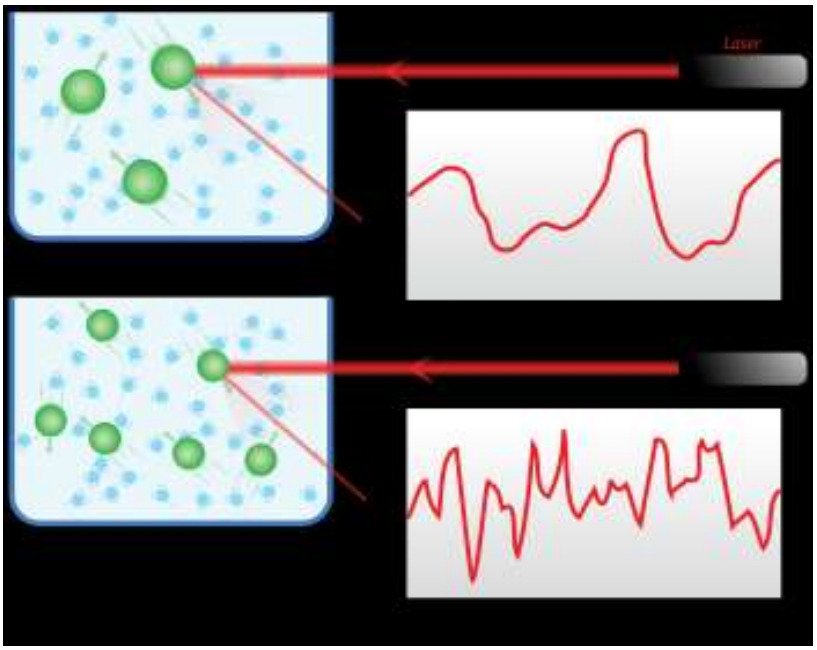

Figure 9. *Representation of the principle of Dynamic Light Scattering. Smaller particles give quicker fluctuations of a scattered laser light, as evidenced by the correlation function (picture taken from: Wikipedia).*

Information about the particles can be extracted by fitting the decay of the autocorrelation function. Numerical methods are employed for the purpose and they are essentially based on assumed size distribution. For example, if the sample is monodisperse the decay is fitted well by a simple exponential (Eq.2):

2) $$g^1(q;\tau) = \exp(-\Gamma\tau)$$

where Γ is the decay rate. The translational diffusion coefficient can be derived from the wave vector q and Γ according to Eq.3:

3) $$\Gamma = q^2 D$$

where q is:

4) $$q = \frac{4\pi n_0}{\lambda} \sin\left(\frac{\theta}{2}\right)$$

where λ is the incident laser wavelength, n_0 is the refractive index of the sample and θ is the angle at which the detector is positioned respect to the light source.

Through the Stokes-Einstein equation (Eq.5) is therefore possible to derive the hydrodynamic radius of the particles.

5) $$D = \frac{k_B T}{6\pi \eta r}$$

In this equation D is the diffusion coefficient, k_B the Boltzmann's constant, T the temperature, η the viscosity of the medium and r the radius of the spherical particle.

In most cases, however, the sample is polydisperse and the autocorrelation function is the sum of exponential decays of all the species in solution (Eq.6).

6) $$g^1(q;\tau) = \sum_{i=1}^{n} G_i(\Gamma_i)\exp(-\Gamma_i\tau) = \int G(\Gamma)\exp(-\Gamma\tau)\,d\Gamma$$

In this case a commonly used mathematical model to describe the system is the cumulant method. This model introduces the variance of the system as Polydispersity Index (Eq. 7).

7) $$g^1(q,\tau) = \exp\left(-\bar{\Gamma}\tau\right)\left(1 + \frac{\mu_2}{2!}\tau^2 - \frac{\mu_3}{3!}\tau^3 + \cdots\right)$$

where $\bar{\Gamma}$ is the average decay rate and $\mu_2/\bar{\Gamma}^2$ is the second order Polydispersity Index.

It should be noted that DLS gives information on the hydrodynamic diameter of spheric particles, meaning that it models the behavior of irregular shape ojects as they were spheres. Moreover the measured size considers also the layer of solvent or ions around the particles. This information is therefore generally different from what can be measured for example with electronic microscopy like TEM, that "sees" the naked particles (201).

5.1.2 Atomic Force Microscopy

Atomic Force Microscopy (AFM) is an instrument belonging to the class of the Scanning Probe Microscopies (SPM). Its resolution power of the order of nanometers make it particularly useful in studying nanoparticles, both for morphology and interactions with partners.

It consists of a silicon or silicon nitride cantilever, with a tip of the radius of curvature of the order of nanometers (Fig.10). The tip moves along the surface to sample all the relievs and depressions. Interactions of the probe with the surface are: mechanical contact force, van der Waals forces, capillary forces, chemical bonding, electrostatic forces, magnetic forces, Casimir forces, solvation forces, etc (202).

The scanned area is typically in the order of microns. A laser beam impinges above the cantilever being reflected and detected by a diode microarray. The detected ray of light raises an electric signal, digitized, elaborated and transformed in a reconstructed image of the surface (topography) by a dedicated software.

There are basically three ways of profiling a surface: contact mode, non-contact mode and tapping mode.

In contact mode the tip passes close to the surface keeping constant the interaction between them. The force must be in this case repulsive, in order to avoid the snapping in of the tip.

In non-contact mode there is not contact between the surface and the tip: the cantilever oscillates at a frequency slightly higher than its resonance frequency with an amplitude of few nanometers (<10nm). The interaction with the surface tends to decrease the frequency of oscillation, but a feedback loop system keeps it constant by modifying the average distance between tip and surface.

In intermittent contact, or tapping mode, the oscillation has a higher amplitude (100-200nm) and the tip intermittently touches the surface. This technique is well suited for soft matter, like lipid bilayers.

With AFM it is also possible to evaluate interaction forces by binding a ligand to the tip and scanning its interaction with a receptor immobilized to the surface (203).

AFM measurements in liquid samples are also possible, thus preserving the nature of labile molecules like proteins (204).

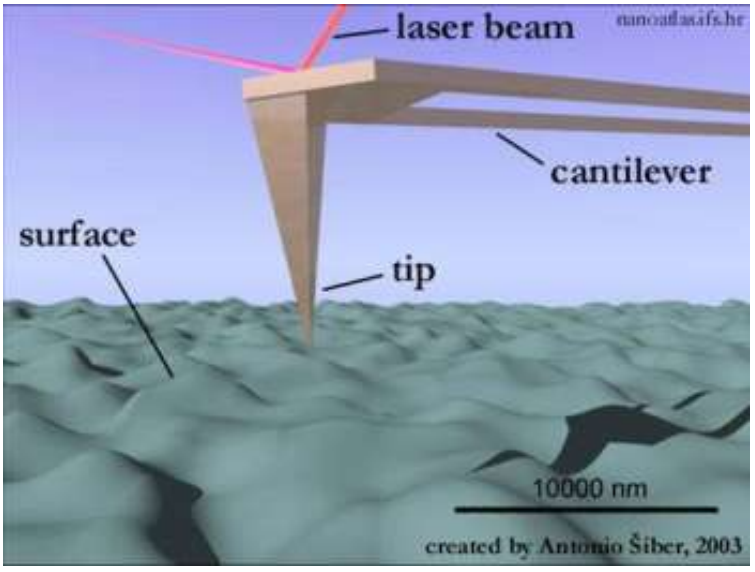

***Figure 10**. Representation of how Atomic Force Microscopy works. A nanometric size tip moves along a surface surveying relieves and depressions. A laser beam is reflected by the upper part of a cantilever that bears the tip and impinges to a detector. This information is interpreted by a software that reconstructs the surface topology (picture taken from: http://www.nanoatlas.ifs.hr).*

5.2 Nanoparticles synthesis

Different recipes were followed to find the best approach to produce nanoparticles of suitable size (diameter ideally less than 100nm) with low PDI and high yield in their production.

A Fmoc-protected phosphotyrosine (Fmoc-pTyr) was used as template, as suggested by Sellergren et al. (240).

Regarding the choice of functional monomers, positively charged monomers could be thought as effective for the phosphate group. Their choice is however unadviceable because of the bias introduced in imprinting: charged monomers are attracted by the charges independently of the molecule structure, i.e. the sequence of aminoacids in the case of peptides and/or proteins (240).

Instead, the functional monomers chosen were 2-hydroxyethyl methacrylate (HEMA) and 1,3-diallylurea (DAU), while crosslinkers were N,N'methylene-bis-acrylamide (BIS) and 1,4-bis(acryloyl)piperazine (BAP).

HEMA showed good properties in producing hydrogels, and is extensively used in commercial products, like contact lenses, for its swelling properties (205). The production of a soft polymer like a hydrogel is necessary when working with proteins, to permit their internalization in the polymer matrix (206). Dyallylurea has similar properties to the suggested monomers for phosphotyrosine imprinting, as recently reported by Sellergren et al. (240). BIS is a commonly used crosslinker for protein/peptide imprinting and for gel electrophoresis matrixes (207), (208). BAP shows instead more mechanical characteristics (keeping the shape) respect to BIS, and this is the reason for its choice in protein imprinting (209). The synthesis was carried out in two solvents. The aqueous solvent was 100mM, pH 8.20 Tris buffer, that does not show interference with the binding with pTyr (like a more "physiological" PBS) but at the same time largely employed in proteomics (210).

5.3 Bulk synthesis

Finally, the bulk synthesis (211) out of two recipes, chosen according to AFM and DLS results, was carried out. Rebinding experiments were performed on this material in order to collect preliminary information in standardized conditions before using nanoparticles. The method consists in preparing a solid polymer subsequently crushed and sieved to give micron-sized particles.

5.4 Functional characterization of MIPs

Functional characterization of MIPs consists in the assessment of the following characteristics:

capacity: amount of template that can be bound from 1 mg of polymer;

specificity: affinity of the template for MIP, expressed by the equilibrium dissociation constant K_D;

selectivity: ability of MIP to discriminate between the template and other substrates;

imprinting factor: ratio between the amount of substrate bound from MIP and from its not imprinted counterpart (Not Imprinted Polymer, NIP).

MIPs ability to rebind the template from its solutions can be evaluated as follows. A fixed amount of MIP and of NIP is put in contact with increasing concentrations of template molecule. After incubation the amount of free substrate [A] is evaluated in solution, therefore assessing its amount bound to the resin [AB] by subtracting it from the initial amount of substrate [A]i (Eq.4). A graph of substrate bound [AB] respect to the ratio [AB]/[A] (Scatchard plot, fig.11) permits to evaluate the affinity constant (K_D) of the substrate for the polymer (Eq.2) and the maxium amount of guest bound (the capacity, or the apparent maximum number of binding sites [B]max) given respectively by the slope and the intercept of the Scatchard equation (Eq.3). In an ideal 1:1 interaction between substrate and homogeneous binding sites of the polymer (Eq. 1), K_D is defined as follows:

1) $$A + B \rightleftharpoons AB$$

2) $$K_D = \frac{[A]\,[B]}{[AB]}$$

3) $$\frac{[AB]}{[A]} = \frac{[B]_{max} - [AB]}{K_D}$$

4) $$[A] = [A]_i - [AB]$$

The nature of the binding sites is never uniform and more kinds of guest-binding sites exist (212). This characteristic is evidenced by a not linear graph like fig.11, whose slopes give the value of two K_Ds.

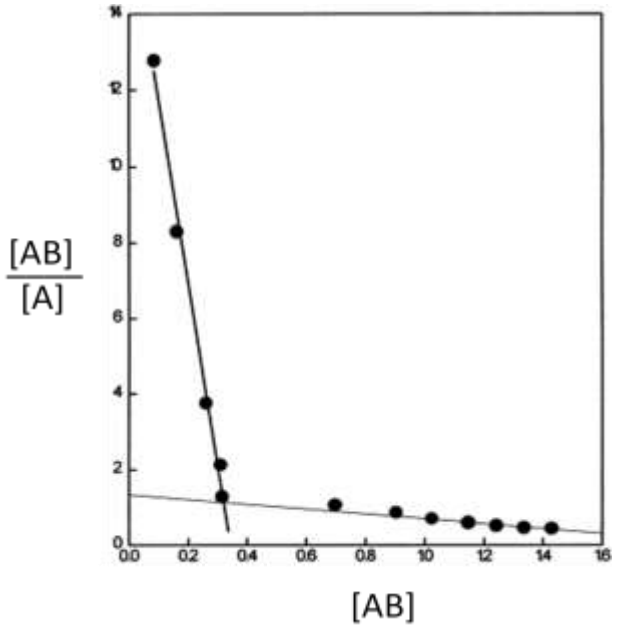

Figure 11. *Scatchard plot to estimate the binding nature of the polymer. Two kinds of binding sites are evidenced by two different slopes in the graph.*

5.5 Materials and methods

5.5.1 Materials

Reagents 2-hydroxyethyl methacrylate (HEMA), 1,4-bis(acryloyl)piperazine (BAP), toluensulphinic acid (TSIA), diphenyliodonium chloride (DPI) and methylene blue (MB) were purchased by Fluka (Steinheim, DE); 1,3 diallylurea (DAU) was an Aldrich product obtained from Sigma-Aldrich (St.Louis, MO, USA); N,N'methylene-bis-acrylamide (BIS) was a BioRad product (Hercules, CA, USA).

5.5.2 Small-scale synthesis of the nanoparticles

The list of recipes related to the synthesised polymers is reported in Table 5 (Par.5.6.1). Fmoc-protected phosphotyrosine was added in some samples with the ratio 1:2 respect to the functional monomer, as suggested by Sellergren et al. (240).

Synthesis was carried out either in 100mM Tris buffer pH 8.20 or in acetonitrile/water 9:1 v/v. All synthesis were made in a final volume of 3 mL and in 6 mL HPLC vials with silicon reversible cap. Samples were treated with an argon flow for 10 min prior to illumination. Irradiation was performed with a VIS transilluminator lamp (40W).

5.5.3 Dialysis of the nanoparticles

After the synthesis samples were dialysed straightaway by using a dialysis tubing cellulose membrane (Sigma) with cut-off 12000 Da. MilliQ water was used as receptor medium. Dialysis took place for 48h with 3 changes of solvent. The sample volume/receptor medium ratio was 1:400.

5.5.4 Size analysis of the nanoparticles

The size of the synthesized nanoparticles was determined by using Dynamic Light Scattering (DLS) technique on a Zetasizer Nano ZS instrument equipped with 633nm laser light and DTS Ver. 4.10 software package (Malvern Instruments Ltd., Worcestershire, UK). All the samples were sonicated for 20min prior to analysis and filtered on a 0.45 μm filter to eliminate large sedimenting particles. A 180sec equilibration time was needed for the sample to reach ambient temperature (25°C) after sonication. The mean value of the particle size was calculated from the results of three measurements on each sample. The light was collected at a 173° angle respect to the incident laser light. Size measurement results are reported in table 6 (Par.5.6.2).

5.5.5 Yield of the nanoparticles

The yield of the synthesis was calculated for the samples, as reported in table 3. Ten ml of solution containing nanoparticles were dialysed and freeze dried in pre-weighted Falcon polypropylene tubes. Yields were calculated respect to the initial amount of monomers.

5.5.6 Atomic force microscopy of the nanoparticles

AFM measurements were made on four samples produced with four different recipes, chosen according to DLS measurements. The best for size and PdI recipes were chosen, considering however to not exclude monomers, crosslinkers or solvents that could furnish interesting morphological or aggregation characteristics. The instrument was an NT-MDT Solver P47H-PRO AFM. Mica dishes (Ted Pella) were freshly peeled with cellotape before

sample deposition. Samples (not dialysed) were sonicated for 5 min, diluted 1:1 (v:v) with ethanol and 50µl of the mixture was deposited on mica dishes. After 5min the dishes were washed through dipping in 0.20µm filtered MilliQ water and dried for 20 sec with an air flow. Images were collected at room temperature (20°C) in semi-contact mode using NT-MDT NSG11 silicon cantilevers with Au backside coating, with a minimal applied force at a scan frequency of 0.5-2 Hz with 512 pixel resolution.

5.5.7 Large-scale synthesis of the nanoparticles

Eight recipes were produced on a larger scale. The recipes were chosen according to DLS measurements as explained in paragraph 5.5.6. Moreover a choice of variety in monomers, crosslinkers and solvents could offer interesting characteristics of rebinding. The recipes chosen are listed in table 3. The reaction was carried out in borosilicate glass bottles in a final volume of 100 mL after argon bubbling for 10 min. Irradiation was performed with a VIS transilluminator lamp (40W) under gentle stirring (250rpm).

Table 3. *Samples produced on large scale (W=Tris 100mM, pH8.2; A/W=ACN/Water 9:1 v/v).*

Recipe	Monomers	% T	% Cm	Time poly m.	mmol (mg) Cross linker	mmol (mg) monomer	mmol (mg) Fmoc-pTyr	solvent
F	HEMA/BIS	1	80	5'	6.30 (974)	1.58 (206)		W
F+pTyr	HEMA/BIS	1	80	5'	6.30 (974)	1.58 (206)	0.79 (382)	W
H1	HEMA/BAP	1	67	5'	4.55 (884)	2.27 (148)		W
H1+pTyr	HEMA/BAP	1	67	5'	4.55 (884)	2.27 (148)	1.13 (532)	W
L3	HEMA/BIS	0.2	80	18h	1.26 (195)	0.32 (41)		A/W
L3+pTyr	HEMA/BIS	0.2	80	18h	1.26 (195)	0.32 (41)	0.16 (77)	A/W
M3	DAU/BIS	0.2	80	18h	1.26 (195)	0.32 (45)		A/W
M3+pTyr	DAU/BIS	0.2	80	18h	1.26 (195)	0.32 (45)	0.16 (77)	A/W

5.5.8 Dialysis of the nanoparticles

After the synthesis the samples were dialysed straightaway by using a dialysis tubing cellulose membrane (Sigma) with cut-off 12000 Da. MilliQ water was used as dialysate. Dialysis took place for 96 hours with 12 changes of solvent. The sample volume/dialysate ratio was 1:50.

5.5.9 Electrodialysis of the nanoparticles

Dialysed nanoparticles were electrodialysed for 4h with a set current of 500V, 5.0mA, 1W. Samples were put in a 3500KDa cut-off SpectraPor membrane and added of 10mM histidine (Sigma). Anodic buffer was 1L of a 10mM histidine solution. After electrodialysis samples were dialysed again for 4h against 1L of MilliQ water with the same membrane.

5.5.10 Concentration of the nanoparticles

Electrodialysed samples were concentrated with Centriprep YM30 centrifugal filter devices (30kDa cut-off, Millipore). The applied centrifugal force was 1500xg for 15min, according to builder instructions. An initial volume of 100mL was reduced to 10mL.

5.5.11 Yield evaluation of the nanoparticles

One mL of every concentrated solution, corresponding to 10mL of initial nanoparticles solution, was put in previously weighted 6ml HPLC vials to quantify the presence of particles. Samples were freeze-dried for 24h and the weight measured with a Ohaus Explorer balance.

5.5.12 Standard bulk synthesis

Two recipes were chosen to produce bulk polymers and perform rebinding experiments. This operation was made to have an idea of the binding properties of the material in standardized conditions.

Solvents acetonitrile, methanol and hydrochloric acid, used to clean the synthesized polymers from Fmoc-pTyr, unreacted species and pTyr after rebinding, were purchased from Carlo Erba (Milano, Italy).

A 500 mg of HEMA/BIS 80%C and DAU/BIS 80%C were dissolved in 8mL Tris buffer 20mM, pH 8.20 (final total monomers content 6%T) and divided in two 6mL HPLC vials to prepare the not imprinted polymers (NIPs, controls).
A second aliquot was furtherly added of Fmoc-pTyr with a molar ratio 1:2 respect to the functional monomer to prepare the molecularly imprinted polymers (MIPs, see table 4). All the aliquots were subsequently added of 100µM methylene blue, 50µM diphenyliodonium chloride and 1 mM toluensulphinic acid and treated with an argon flow for 5 min prior to illumination. Irradiation was performed with a VIS transilluminator lamp (40W). An aluminium foil was used to wrap the reaction environment and thus illuminate the reactor from every direction. The illumination duration was 4h for HEMA/BIS and 16h for DAU/BIS. Here following the recipes:

Table 4. *Recipes of the synthesized bulk polymers.*

	Monomer (mg / µmol)	Crosslinker (mg / µmol)	Fmoc-pTyr (mg / µmol)
HEMA/BIS (NIP)	87 / 668	413 / 2679	
HEMA/BIS + pTyr (MIP)	87 / 668	413 / 2679	161 / 334
DAU/BIS (NIP)	93 / 663	407 /2641	
DAU/BIS + pTyr (MIP)	93 / 663	407 / 2641	160 / 331

5.5.13 Polymer cleaning and drying

After the synthesis the polymer samples were cleaned through a series of washing steps to remove the unreacted monomers, initiators and Fmoc-pTyr. The solvent used were in order: acetonitrile/water 1:1 v/v, acetonitrile, methanol/HCl 0.1M 1:1 v/v.
The synthesized HEMA/BIS NIP and MIP were put in 50 mL Falcon tubes and added of a volume of solvent 4 times the amount of polymer, mixed on an orbital rotor and centrifuged at 3000xgx20', at 25°C. The synthesized DAU/BIS NIP and MIP, after the solvent addition, were divided in aliquots in 2 mL eppendorf tubes, mixed on the orbital rotor for and centrifuged at 10000xgx20', at 25°C. This different treatment was needed because DAU/BIS MIP could not sedimentate at low speed. The supernatants were

then drained, analysed with UV-VIS spectrometry and replaced with fresh solvent. The graphs of the cleaning steps are reported in figure 22 and 23. Absorbance was measured with an Unicam UV2 UV-VIS spectrometer, at wavelength λ=214nm in quartz cuvettes, to evaluate the presence of double bonds (not reacted monomers).

After the cleaning samples were spread on a cellulose paper and left at ambient temperature (25°C) for 72h until dryness. The weights of the dry polymers are reported in table 10. Yields were calculated respect to the initial amount of monomers.

5.5.14 pTyr calibration curve

In order to evaluate pTyr presence in rebinding experiments two calibration curves were made. Firstly pTyr (Sigma) was dissolved in PBS buffer + 0.02% Tween-20 at increasing concentrations. The first curve was produced with an Unicam UV2 UV-VIS spectrometer, at wavelength λ=272nm in quartz cuvettes. The second one was obtained with a Jasco FP8200 spectrofluorimeter, in quartz cuvettes, at λ_{exc}=265nm and λ_{em}=297nm. All the measurements were made in triplicate.

5.5.15 Rebinding experiments

After extensive cleaning the polymers were subdued to rebinding experiments to evaluate capacity (μg substrate bound by 1mg of polymer) and specificity (K_D). Due to the limited amount of DAU/BIS polymer, only HEMA/BIS polymer was subdued to these measurements.

Ten mg aliquots of HEMA/BIS NIP and MIP were put in contact with 2 ml of increasing concentrations of pTyr and gently shaken on an orbital rotor for 4 hours. Then the solutions were centrifuged at 10000 x g x 20’ at 25°C. The supernatant was drained and filtered on 0.22 microns cellulose membrane to eliminate material in suspension. The pTyr concentration was evaluated on the initial solutions and on the drained solutions with a Jasco FP8200 spectrofluorimeter, in quartz cuvettes, at λ_{exc}=272nm and λ_{em}=297nm. Absorbance data from the initial solutions were used to produce a calibration

curve, from which concentrations could be calculated. The difference between the concentration of the initial solutions and of the same solutions left in contact with the polymer gives the amount of pTyr bound to the polymer. Then the pTyr bound for mg of polymer was calculated and max capacity estimated.

5.5.16 Cleaning after rebinding

Polymers subdued to rebinding experiments were cleaned through a series of passages in Methanol/HCl 0.1M 1:1 solution in ratio 20:1 respect to the polymer amount. The presence of pTyr was evaluated through absorbance measurements at wavelength 272nm. Cleaning passages were repeated until an absorbance < 0.01 was detectable (table 11, figure 25).

5.6 Results and discussion

5.6.1 Recipes

Nanoparticles were synthesized modifying the following parameters: type of monomers and crosslinkers, polymerization time, initiators amount, stirring, molar crosslinker percentage (%C_m), presence of template.

The samples were synthesized in triplets. Thirty-five different conditions were explored, and they are listed in table 5:

Table 5. *List of polymerization nanoparticles recipes. W= TRIS buffer 100mM, pH8.2; A/W=Acetonitrile/Water 9:1 v/v.*

Recipe	Monomers	% T	$\%C_m$	µM MB	mM TSIA	µM DPI	Time Polym-	Stirring	Solvent	Fmoc-pTyr
A1	HEMA/BIS	1	46	100	1	50	5'	y	W	
A2	HEMA/BIS	1	46	100	1	50	10'	y	W	
A3	HEMA/BIS	1	46	100	1	50	30'	y	W	
A4	HEMA/BIS	1	46	100	1	50	60'	y	W	
C	HEMA/BIS	1	46	10	1	50	10'	y	W	
D	HEMA/BIS	1	46	10	0.1	5	10'	y	W	
B1	HEMA/BIS	1	46	100	1	50	5'	n	W	
B2	HEMA/BIS	1	46	100	1	50	10'	n	W	
G	HEMA/BAP	1	40	100	1	50	5'	y	W	
E1	HEMA/BIS	1	72	100	1	50	5'	y	W	
E2	HEMA/BIS	1	72	100	1	50	10'	y	W	
H1	HEMA/BAP	1	67	100	1	50	5'	y	W	
H2	HEMA/BAP	1	67	100	1	50	10'	y	W	
F	HEMA/BIS	1	80	100	1	50	5'	y	W	
P	HEMA/BIS	1	80	100	1	50	5'	y	W	y
L1	HEMA/BIS	0.2	80	100	1	50	10'	y	A/W	
L2	HEMA/BIS	0.2	80	100	1	50	60'	y	A/W	
L3	HEMA/BIS	0.2	80	100	1	50	18h	y	A/W	
M1	DAU/BIS	0.2	80	100	1	50	10'	y	A/W	
M2	DAU/BIS	0.2	80	100	1	50	60'	y	A/W	
M3	DAU/BIS	0.2	80	100	1	50	18h	y	A/W	
I1	HEMA/BIS	0.2	80	100	1	50	5'	y	W	
I2	HEMA/BIS	0.2	80	100	1	50	60'	y	W	
J	DAU/BIS	0.2	80	100	1	50	5'	y	W	
S	HEMA/BIS	0.2	80	100	1	50	60'	y	A/W	y
T	DAU/BIS	0.2	80	100	1	50	60'	y	A/W	y
Q	HEMA/BIS	0.2	80	100	1	50	5'	y	W	y
R	DAU/BIS	0.2	80	100	1	50	5'	y	W	y
N	HEMA/BIS	0.1	80	100	1	50	60'	y	A/W	
O	DAU/BIS	0.1	80	100	1	50	60'	y	A/W	
K	DAU/BIS	0.1	80	100	1	50	5'	y	W	
U	HEMA/BIS	0.1	80	100	1	50	60'	y	A/W	y
V	DAU/BIS	0.1	80	100	1	50	60'	y	A/W	y

5.6.2 Dynamic Light Scattering analysis

DLS analysis was performed on the synthesized samples.

Results are reported in table 6:

Table 6. *DLS results for size (Z average ± standard deviation) and Polydispersion Index (PdI).*

Recipe	Monomers	% T	%C m	Time polym	Solvent	Fmoc-pTyr	Zave nm	PdI
A1	HEMA/BIS	1	46	5'	W		72 ± 65	0.9
A2	HEMA/BIS	1	46	10'	W		167 ± 35	0.4
A3	HEMA/BIS	1	46	30'	W		684 ± 100	0.2
A4	HEMA/BIS	1	46	60'	W		313 ± 150	0.3
C	HEMA/BIS	1	46	10'	W		174 ± 14	0.4
D	HEMA/BIS	1	46	10'	W		105 ± 44	0.6
B1	HEMA/BIS	1	46	5'	W		194 ± 52	0.6
B2	HEMA/BIS	1	46	10'	W		145 ± 47	0.8
G	HEMA/BAP	1	40	5'	W		232 ± 43	0.6
E1	HEMA/BIS	1	72	5'	W		155 ± 10	0.7
E2	HEMA/BIS	1	72	10'	W		187 ± 54	0.7
H1	HEMA/BAP	1	67	5'	W		79 ± 29	0.7
H2	HEMA/BAP	1	67	10'	W		113 ± 19	0.4
F	HEMA/BIS	1	80	5'	W		163 ± 15	0.3
P	HEMA/BIS	1	80	5'	W	y	153 ± 12	0.2
L1	HEMA/BIS	0.2	80	10'	A/W		110 ± 7	0.2
L2	HEMA/BIS	0.2	80	60'	A/W		147 ± 2	0.2
L3	HEMA/BIS	0.2	80	18h	A/W		121 ± 2	0.2
M1	DAU/BIS	0.2	80	10'	A/W		211 ± 18	0.3
M2	DAU/BIS	0.2	80	60'	A/W		164 ± 15	0.2
M3	DAU/BIS	0.2	80	18h	A/W		129 ± 4	0.2
I1	HEMA/BIS	0.2	80	5'	W		172 ± 18	0.2
I2	HEMA/BIS	0.2	80	60'	W		192 ± 10	0.3
J	DAU/BIS	0.2	80	5'	W		180 ± 62	0.4
S	HEMA/BIS	0.2	80	60'	A/W	y	174 ± 3	0.1
T	DAU/BIS	0.2	80	60'	A/W	y	120 ± 10	0.4
Q	HEMA/BIS	0.2	80	5'	W	y	131 ± 11	0.4
R	DAU/BIS	0.2	80	5'	W	y	183 ± 17	0.3

Recipe	Monomers	% T	%C m	Time polym	Solvent	Fmoc-pTyr	Zave nm	PdI
N	HEMA/BIS	0.1	80	60'	A/W		208 ± 32	0.2
O	DAU/BIS	0.1	80	60'	A/W		239 ± 10	0.2
K	DAU/BIS	0.1	80	5'	W		219 ± 24	0.3
U	HEMA/BIS	0.1	80	60'	A/W	y	245 ± 18	0.2
V	DAU/BIS	0.1	80	60'	A/W	y	301 ± 10	0.2

Here following the systematic evaluation of the effect of the variation of conditions explored in nanoparticles production.

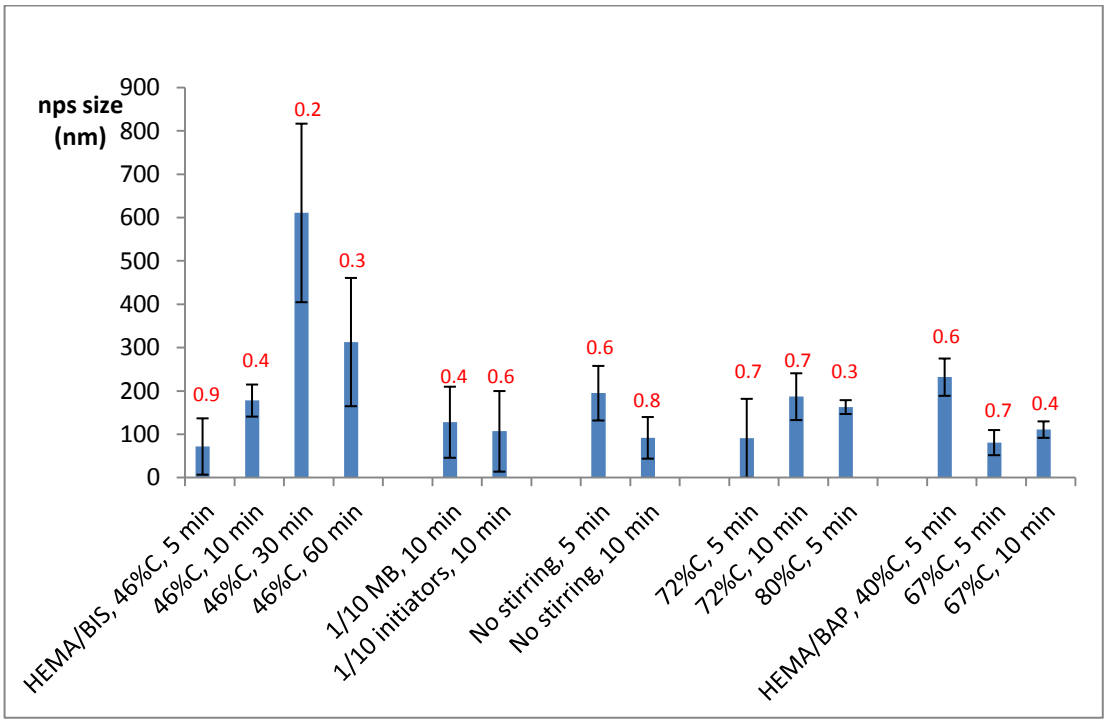

Figure 12. *nps size modification due to different experimental conditions in recipes containing 1% of total monomers (1%T). PdI values are the red numbers above the bars.*

In figure 12 emerges the tendency to the increase of nps size with a longer polymerization time in Tris buffer (first four bars).

The lowering of initiators content increases the standard deviation and the polydispersity of the sample.

Avoiding of stirring also has an effect on the standard deviation and on polydispersity; moreover, the turbidity of the reaction mixture appears earlier

when the sample is not stirred (20' instead of 25'). The inturbidation means a size increase above the micron, thus it can be seen with the naked eye.

The use of a higher crosslinker percentage does not induce size shrink or enlargement on HEMA/BIS nps, but it clearly shrinks HEMA/BAP ones, probably due to greater mechanical properties. Bis-acryloyl piperazine was also shown to provide slightly larger pores in gels (213). In general a higher crosslinker amount helps MIP cavities to retain their shape by making the structure more rigid and the use of a 80%C composition gave good results both for size and polydispersion.

HEMA/BAP particles, even though smaller than HEMA/BIS ones, have a high PdI and batch to batch synthesis is less reproducible.

Literature reports a controlled size increase through the "post dilution method", by which dilution of the reaction mixture is made just before the gelation point to reach a %T lower than critical concentration (194). This method could be mimed by using low %T from the beginning or a worse solvent, in which particles can precipitate when they reach a size big enough to not stay in suspension.

The initial recipe modified for crosslinker percentage (80%C instead of 46%C) was thus subjected to the following experimental variations: lower %T, solvent change and functional monomer change.

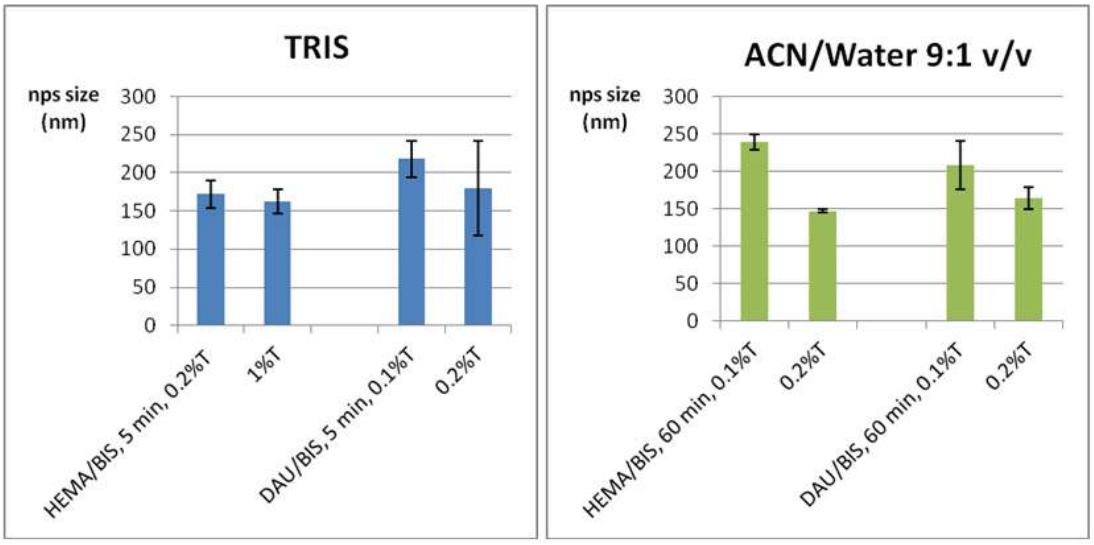

Figure 13. *nps size modification due to the variation of total monomers content %T.*

In figure 13 it is shown the effect of total monomers content on nps size. The first part of the figure (blue bars) reports results obtained in Tris buffer at low polymerization time, while the second part (green bars) concerns experiments made in ACN/W at higher polymerization time. No high polymerization time is available for synthesis in Tris buffer because solutions get turbid for the same monomer composition, indicating the presence of micron-size particles.

Raising the monomers amount has a slightly shrinking effect on the nps. The most interesting fact in using a lower monomer content is however the low PdI of the samples, resulting above 0.3 only in 3 recipes on 18 with %T≤0.2 (table 6). This fact was already observed by Wulff et al., that reported a higher molecular weight and polydispersity for hydrogels produced with high crosslinking and monomers amount (194). This significant improvement suggests the use of a low monomer amount in the progress of the analysis, and polydispersity issues will be no further considered.

The effect of the solvent was subsequently explored (figure 14). ACN/Water 9:1 v/v was chosen as dispersing media. In order to facilitate the dissolution of the reagents, these were firstly added of 1 volume of water, then diluted with 9 volumes of acetonitrile.

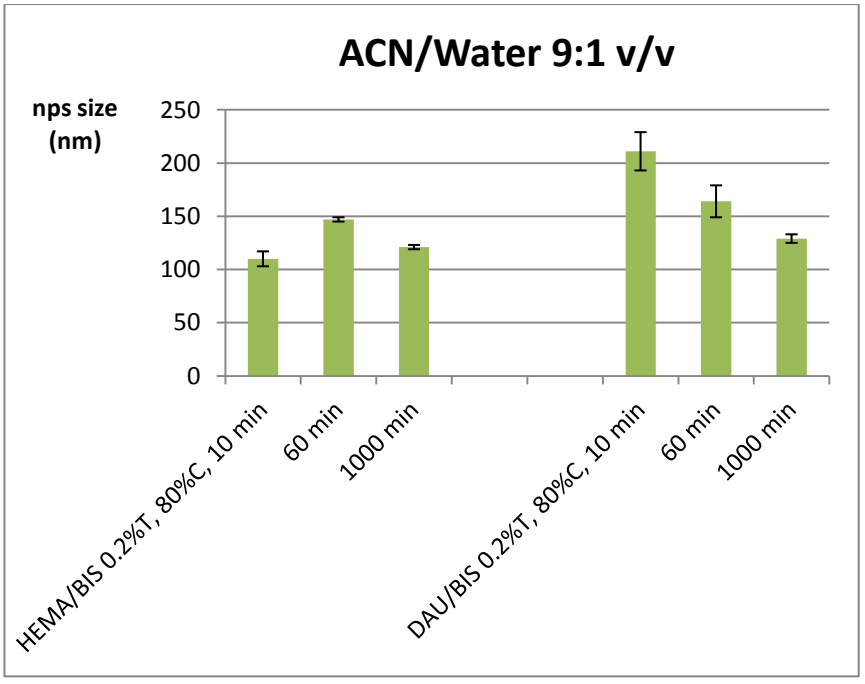

Figure 14. *Effect of the solvent on nps size.*

The most interesting effect of the use of ACN/Water 9:1 v/v is its property of keeping the size of the particles in the nano range, without generating turbidity (thus letting particles to grow to the micro range) as happens in Tris buffer, at least at low total monomer amount (less than 1%T). This can be possible in virtue of its worse solubilizing properties respect to the growing particle, that cannot grow too much in solution before to precipitate (194). This is evidenced by the clear aspect of the solutions after 18h (1000 min) of reaction and by the stopped nps growth in 10 min, 60 min and 18h of reaction (figure 14). A decrease in nps size for longer polymerization time was also observed with the use of DAU monomer. This fact can be explained with the faster kinetics of DAU in being incorporated in the growing particles: an initial fast production of particles consumes the monomers, that remain in lower concentration in solution but still in presence of an excess of initiators. The next step was thus the exploration of the effect of monomer substitution from HEMA to DAU.

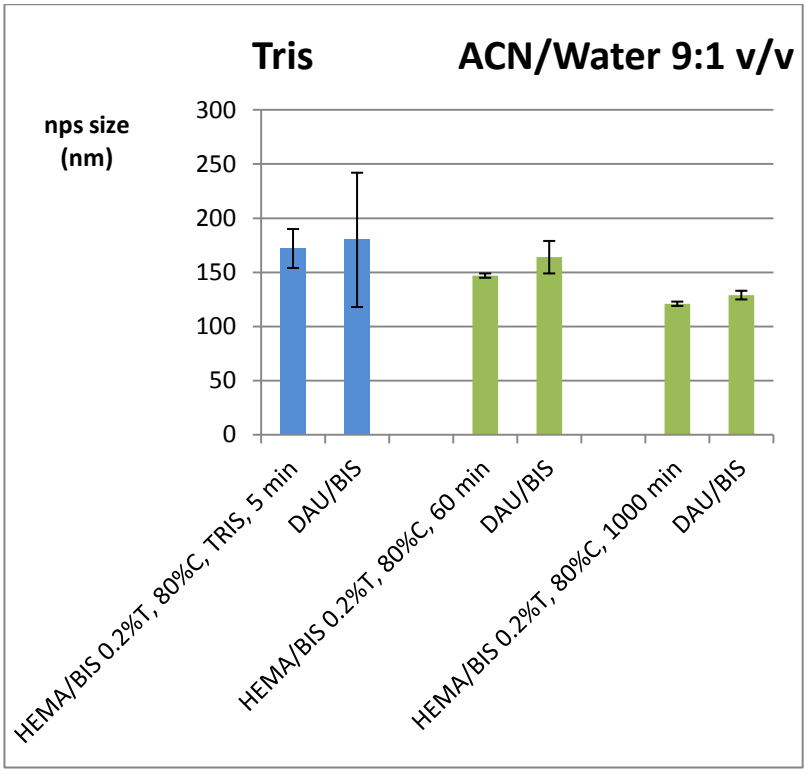

Figure 15. *Comparison of different functional monomers.*

There is not a high nanoparticle size variation in the use of HEMA and DAU, both in Tris buffer and ACN/W for short and long polymerization time. Anyway DAU shows a faster polymerization kinetics than HEMA, showing a turbidity point (visible particles in the reaction mixture) of 3' at 1%T and 15' at 0.2% in TRIS buffer (HEMA gives turbidity in 20' with the first recipe and remains transparent for longer than 60' with the second one). Literature reports a generally different kinetics of the different monomers in being included in the growing polymer, as well as a different solubility of the nanoparticles made with different monomers (214).

The following step was the study of the effect of the template in the polymerizing mixture. The tested recipes are reported in table 7 and the results in figure 16.

Table 7. *Evaluation of template effect on the size of the nanoparticles. Samples F-O (left side of the table) were produced without the template, while samples P-Q (right side of the table) were produced by following the same recipes plus the addition of template.*

Recipe	Monomers	% T	% Cm	Time polymerization	µmol crosslinker	µmol monomer	Solvent	Zave nm	PdI	Recipe	µmol pTyr	Zave nm	PdI
F	HEMA/BIS	1	80	5'	630	160	W	163 ± 15	0.3	P	80	153 ± 12	0.2
I1	HEMA/BIS	0.2	80	5'	126	32	W	172 ± 18	0.2	Q	16	131 ± 11	0.4
J	DAU/BIS	0.2	80	5'	126	32	W	180 ± 62	0.4	R	16	183 ± 17	0.3
L2	HEMA/BIS	0.2	80	60'	126	32	ACN/W	147 ± 2	0.2	S	16	174 ± 3	0.1
M2	DAU/BIS	0.2	80	60'	126	32	ACN/W	164 ± 15	0.2	T	16	120 ± 10	0.4
N	HEMA/BIS	0.1	80	60'	63	16	ACN/W	208 ± 32	0.2	U	8	245 ± 18	0.2
O	DAU/BIS	0.1	80	60'	63	16	ACN/W	239 ± 10	0.2	V	8	301 ± 10	0.2

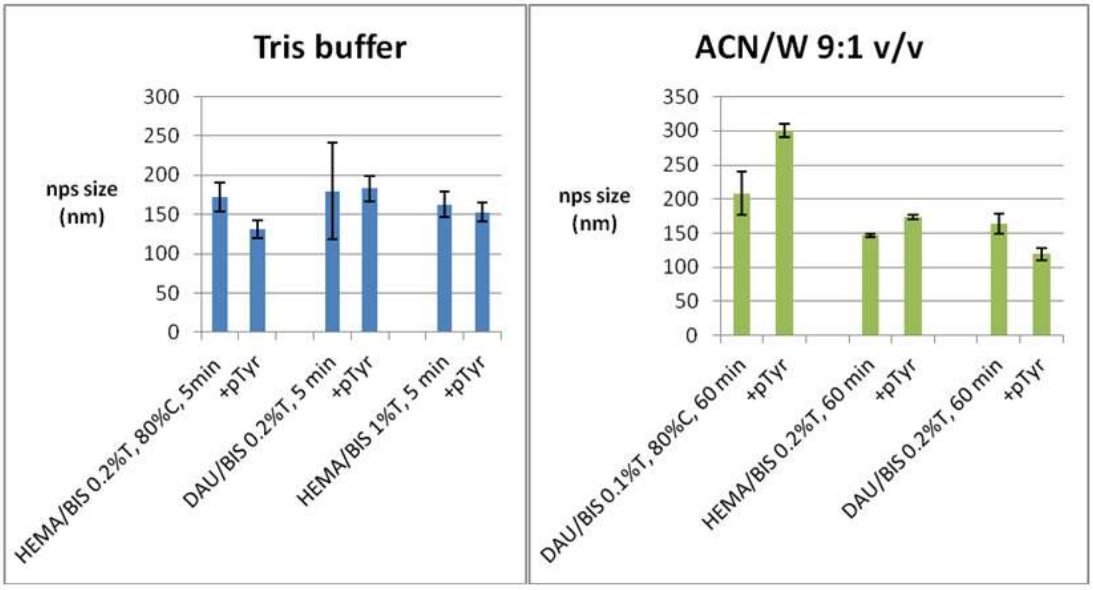

Figure 16. *nps size modification due to the addition of Fmoc-pTyr in molar ratio 1:2 respect to the functional monomer.*

The presence of pTyr in the polymerizing mixture does not change significantly the dimensions of the nanoparticles. This “template effect” is instead reported in some other literature examples (215).

5.6.3 Yield evaluation of small-scale synthesized nanoparticles

Reaction yield was measured for some recipes (Tab. 8). Their choice was made in dependence of the size of the nanoparticles and the Polydispersion Index.

Table 8. *Yield of reaction for some chosen recipes. The lyophilized volume corresponds to 10ml of the initial solution.*

Recipe	Monomers	% T	$\%C_m$	Time polymerization	Solvent	Amount (mg)	Yield %
H1	HEMA/BAP	1	67	5'	W	2.8	2.8
F	HEMA/BIS	1	80	5'	W	2.3	2.3
L1	HEMA/BIS	0.2	80	10'	A/W	0.1	0.5
L2	HEMA/BIS	0.2	80	60'	A/W	0.5	2.5
L3	HEMA/BIS	0.2	80	18h	A/W	1	5
M1	DAU/BIS	0.2	80	10'	A/W	0.9	4.5
M2	DAU/BIS	0.2	80	60'	A/W	0.6	3
M3	DAU/BIS	0.2	80	18h	A/W	1.1	5.5
I1	HEMA/BIS	0.2	80	5'	W	4.1	20.5
I2	HEMA/BIS	0.2	80	60'	W	0.5	2.5
J	DAU/BIS	0.2	80	5'	W	0.4	2
N	HEMA/BIS	0.1	80	60'	A/W	0.1	0.5
O	DAU/BIS	0.1	80	60'	A/W	0.1	1
K	DAU/BIS	0.1	80	5'	W	0.1	1

The yield evaluation evidenced a percentage ranging between 0.5% and 5.5%, with not significant difference between the use of different monomers (table 3). The evaluation of the variation in the product amount gave a ± 1.0mg of uncertainty.

Recipes H1, F, L3 and M3, evidenced in tab.4, seemed to be the most promising to proceed with a large-scale synthesis, with the intention of not excluding the use of any monomer or solvent. Recipes I2 and J, even though seemly promising, would have required a huge amount of starting material to produce enough polymer. Recipe I1 seems to be an experimental deviation (error in the synthesis step, because weight measurement on another part of the solution gave the same result), in fact a longer polymerization time gave a lower amount of product.

5.6.4 AFM images

The four samples chosen to be produced on a larger scale and thus subdued to rebinding experiments were analysed by AFM. Images were taken for not dialysed samples. Dialysed samples showed no presence of particles on the mica surface both with the same immobilization method used for not dialysed samples and by doubling the contact time from 5 to 10 min.

Figure 16. *AFM images of a sample prepared with the recipe "F" through the procedure explained in the section "materials and methods". The bar on the right side of the pictures is the height of the objects expressed in nanometers.*

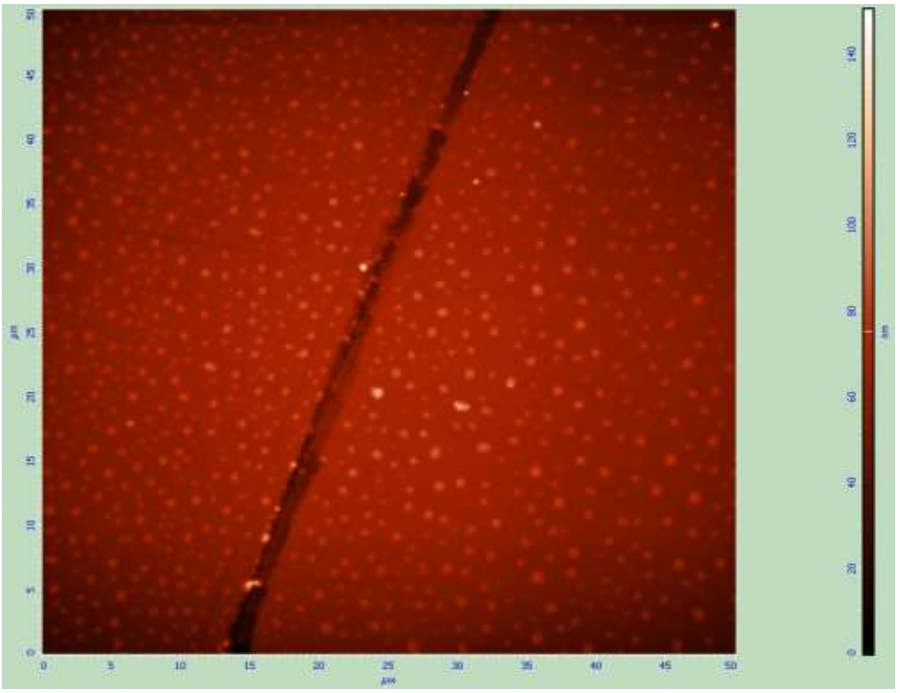

Figure 16.1. *50x50µm.*

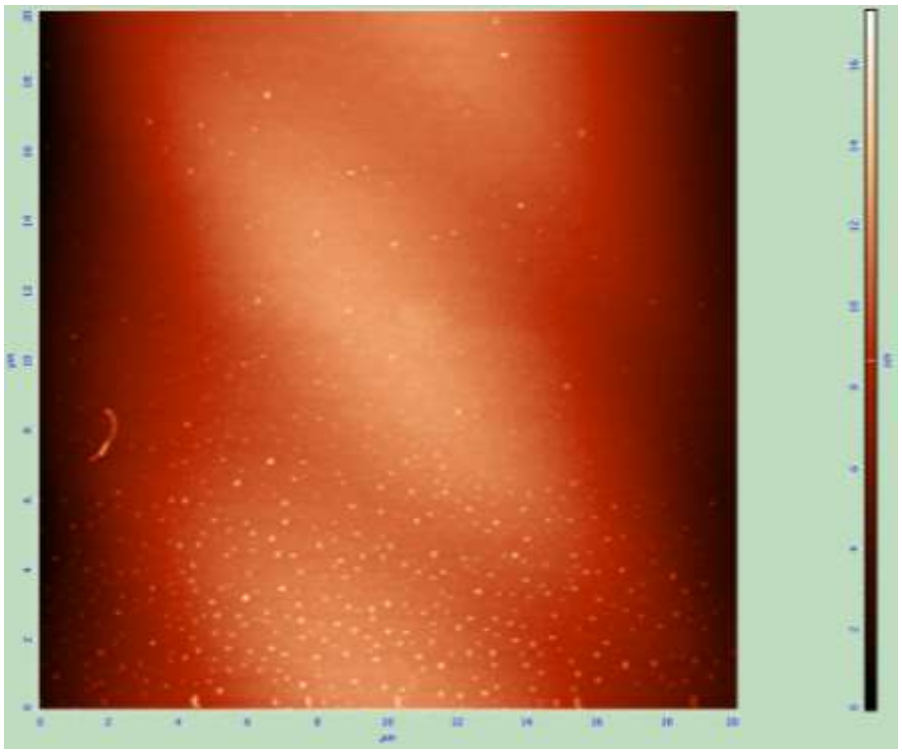

***Figure 16.2**. 20x20µm.*

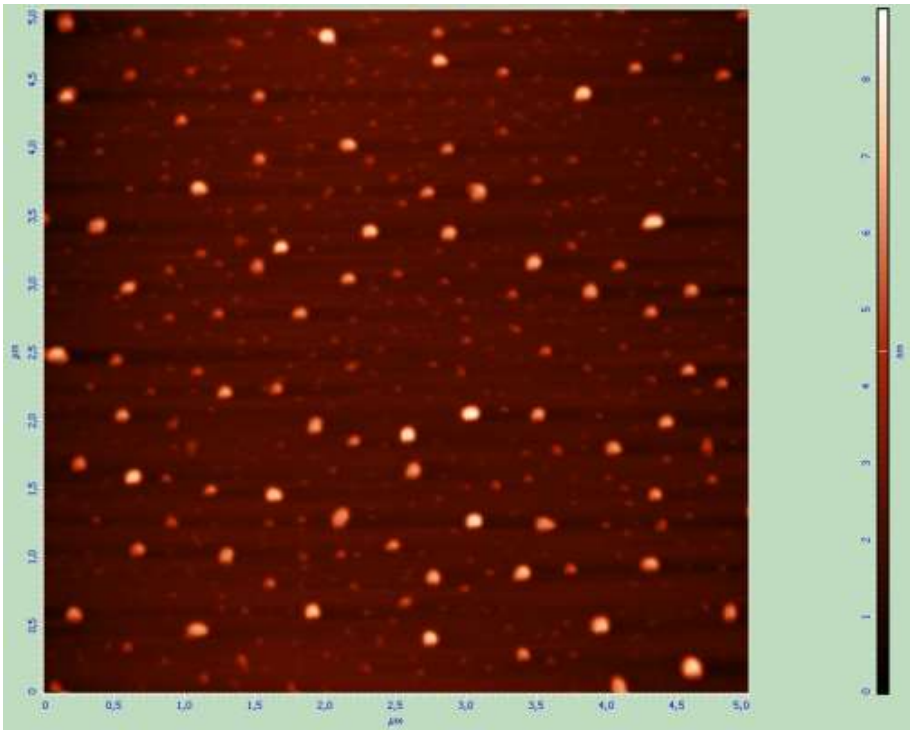

***Figure 16.3.** 5x5µm.*

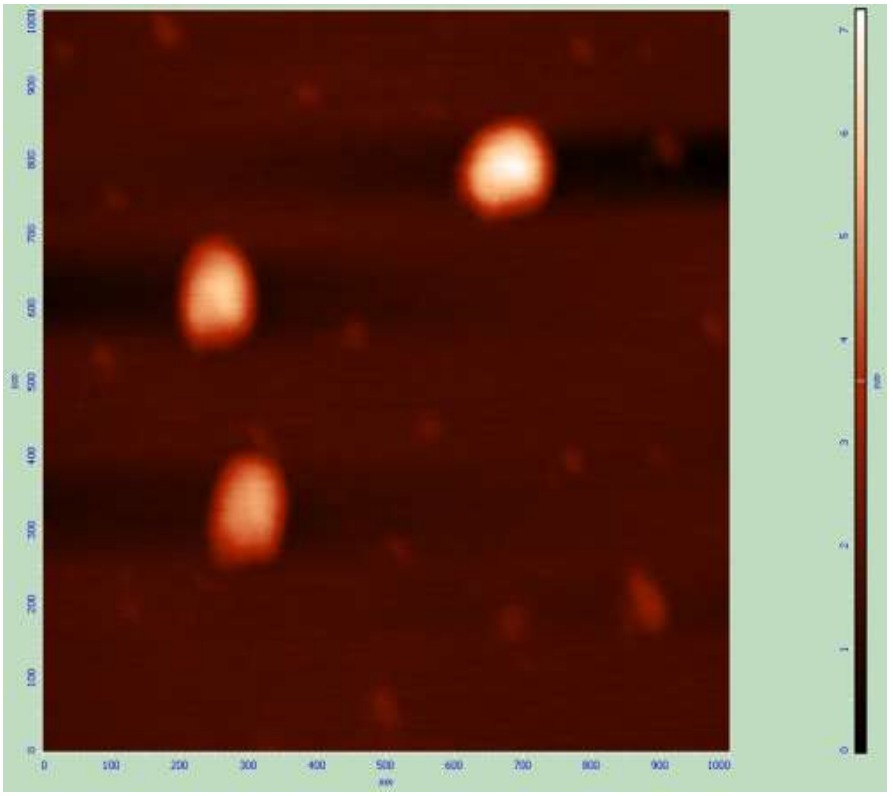

Figure 16.4. *1x1µm.*

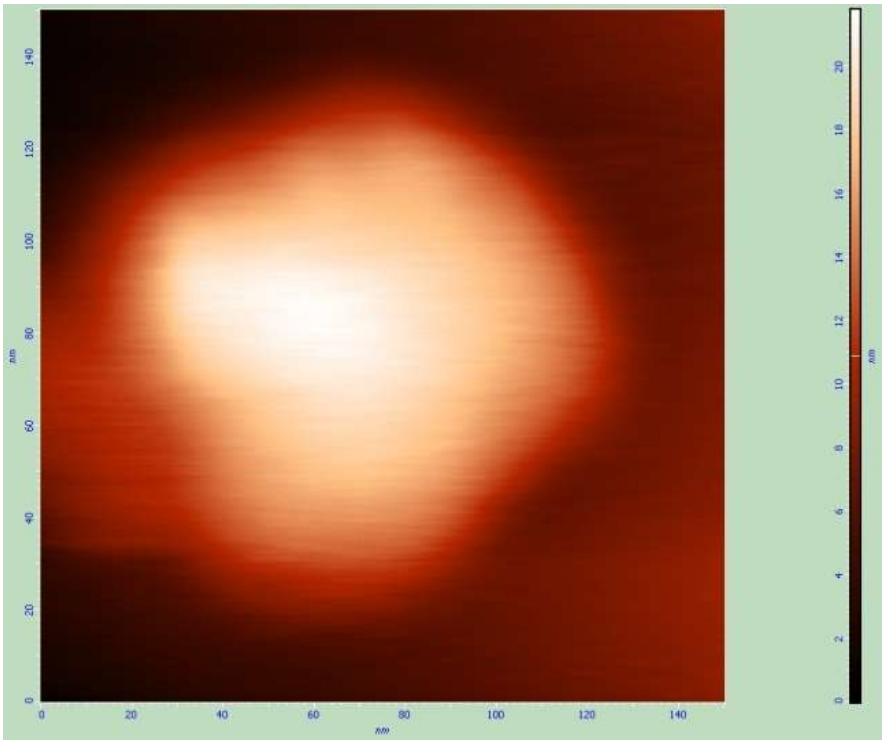

Figure 16.5*. 150x150nm.*

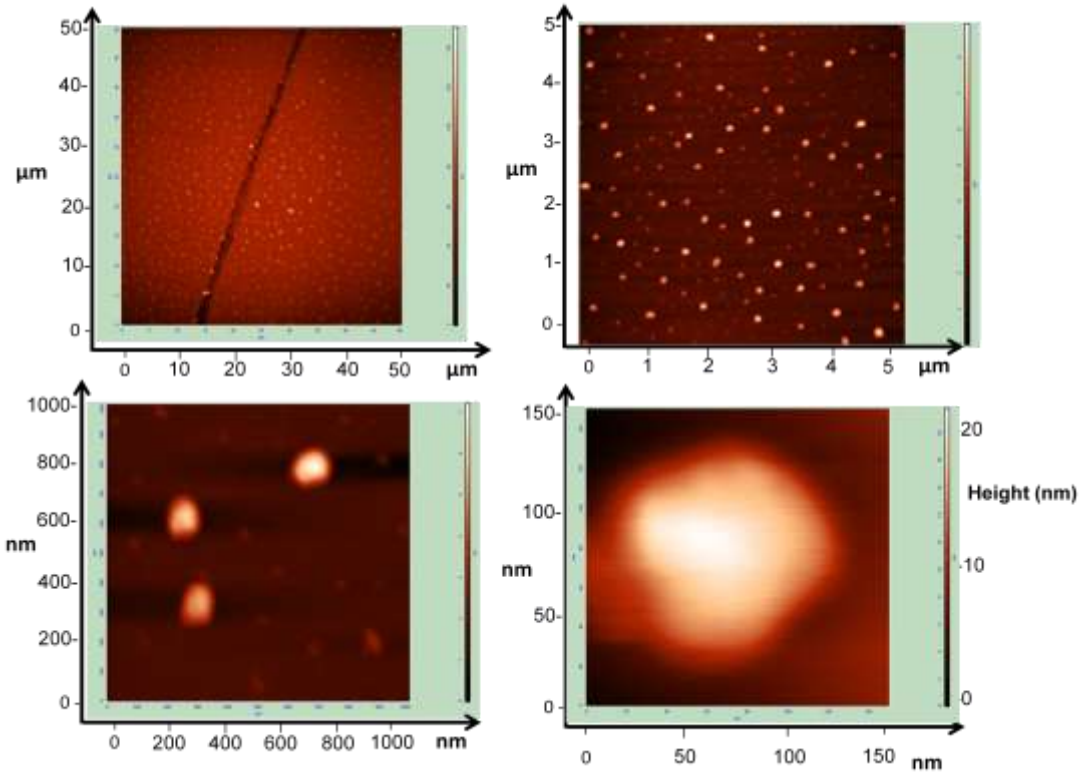

Figure 16.6. *Increasing magnification of the same sample.*

The particles show a flat, irregular shape, with few aggregates present. The size range is approximately from 20nm x 2nm (width x height) to 200nm x 20nm.

Another immobilization method was tried on the same sample, employing $NaHCO_3$ buffer (200mM pH 9.0) 1:1 v/v instead of ethanol. The results are visualized in the next pictures.

Figure 17. *AFM images the same sample (recipe "F") immobilized on mica dish through previous dilution with $NaHCO_3$ buffer (200mM pH 9.0) 1:1 v/v instead of ethanol.*

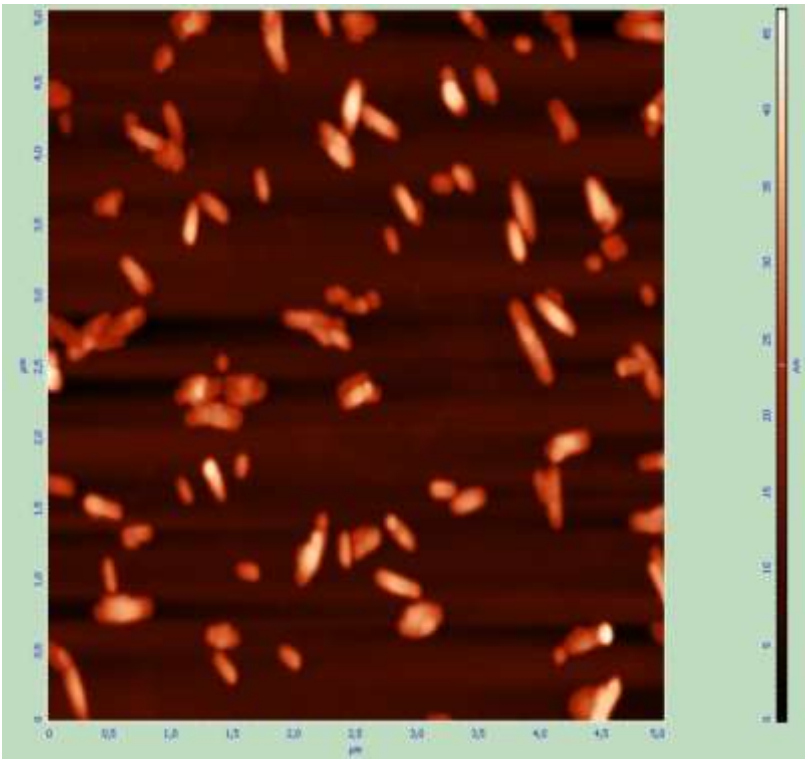

Figure 17.1*. 5x5µm.*

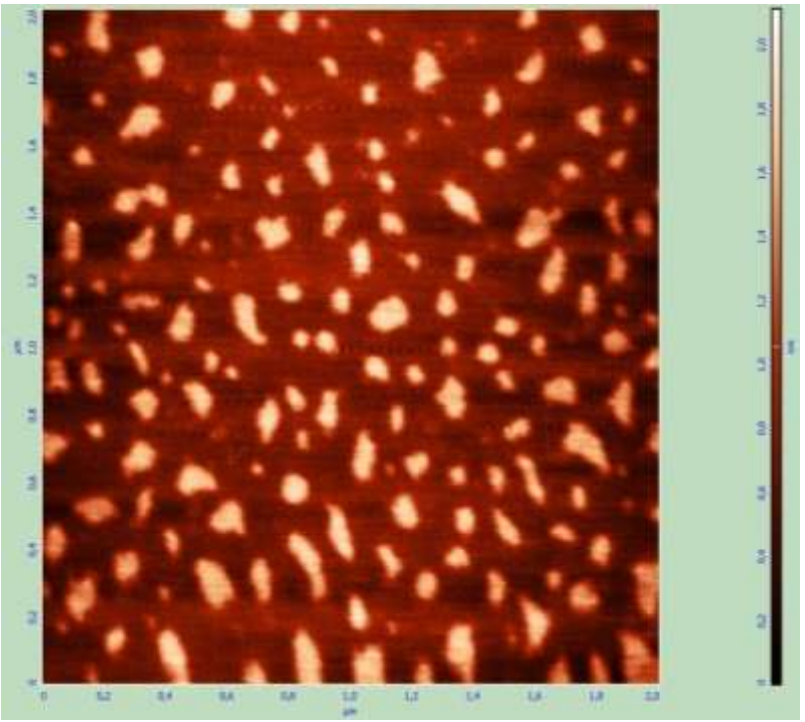

Figure 17.2*. 2x2µm.*

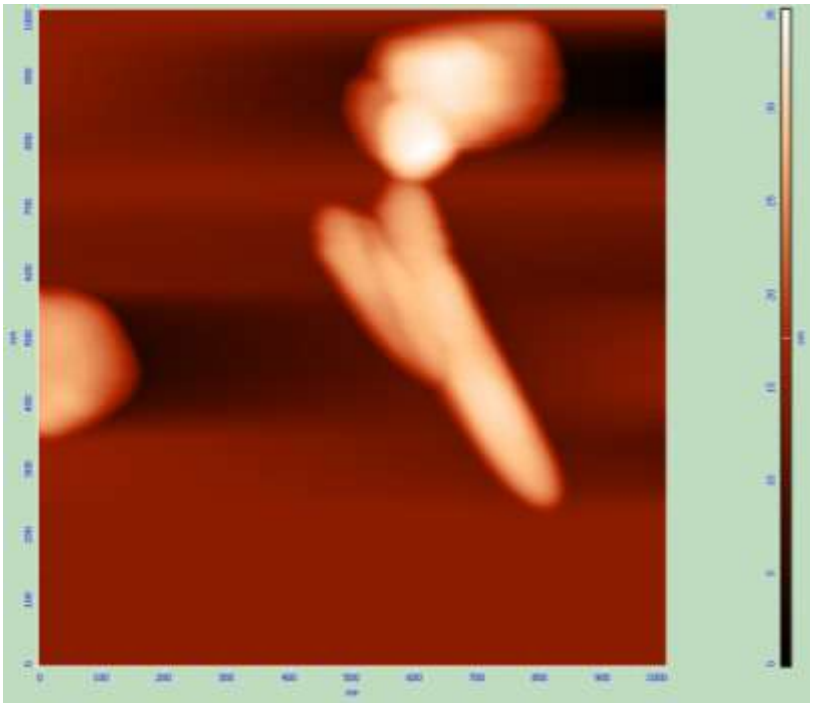

Figure 17.3. *1x1µm.*

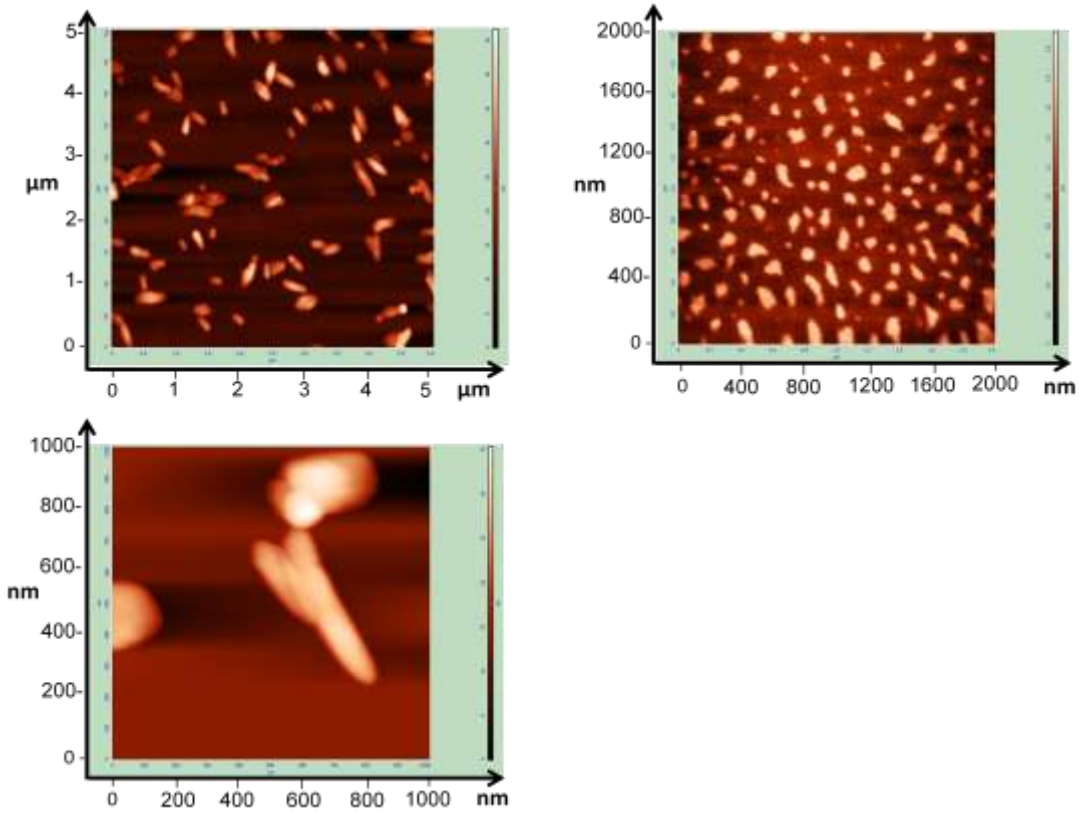

Figure 17.4. *Increasing magnification.*

The comparison of the two immobilization methods evidences a tendency to aggregation with the use of the basic buffer instead of ethanol. The other samples were therefore analysed through immobilization after a 1:1 v/v dilution with ethanol.

Figure 18. *AFM images of a sample prepared with the recipe "H1" through the procedure explained in the section "materials and methods".*

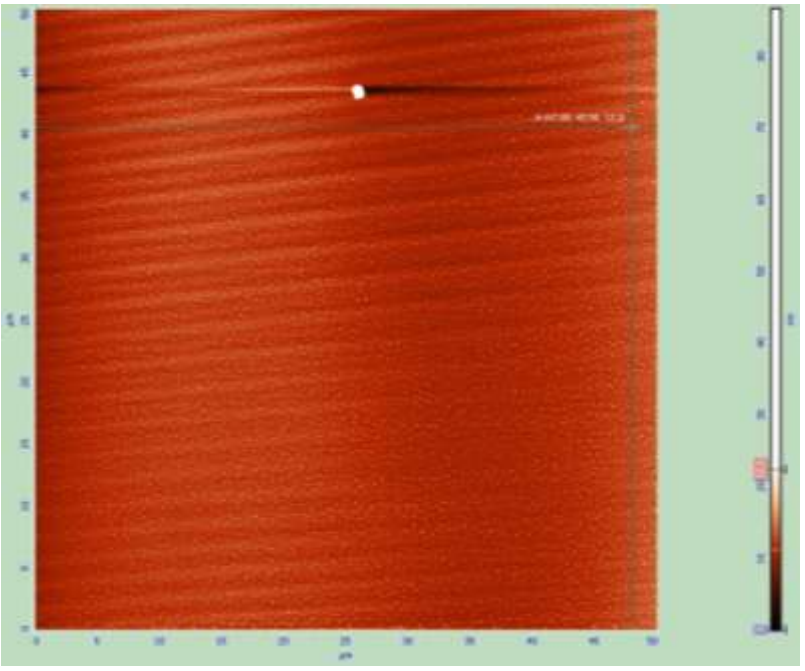

Figure 18.1*. 50x50µm.*

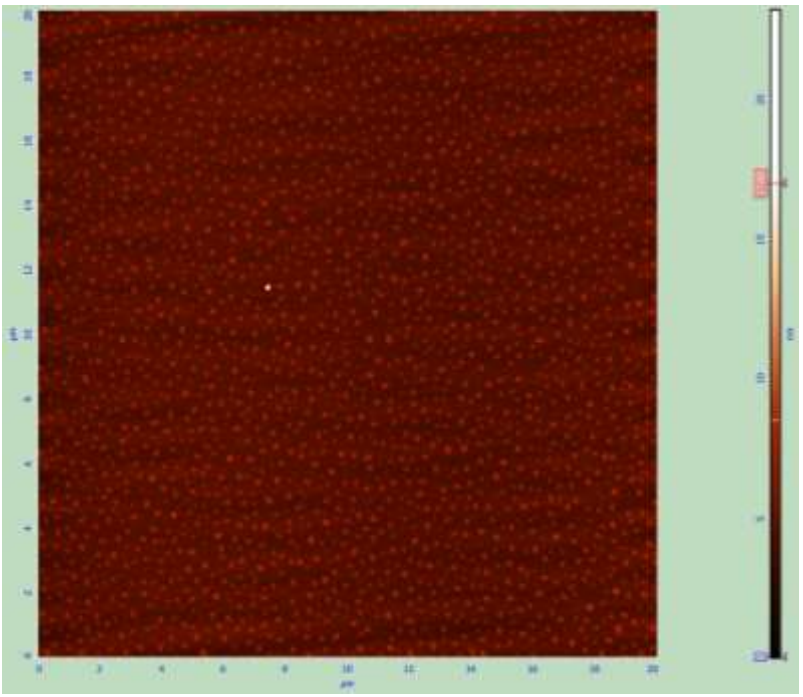

Figure 18.2. *20x20µm.*

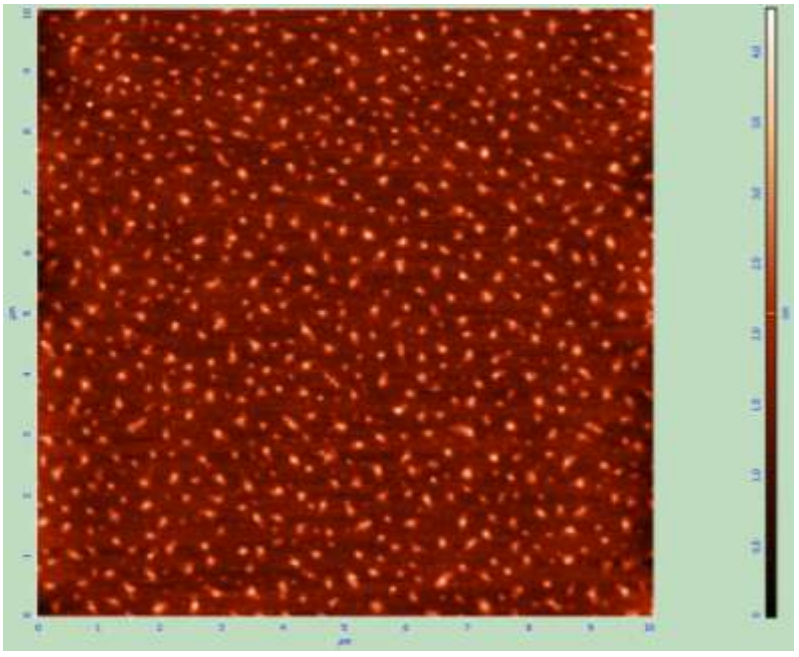

Figure 18.3. *10x10µm.*

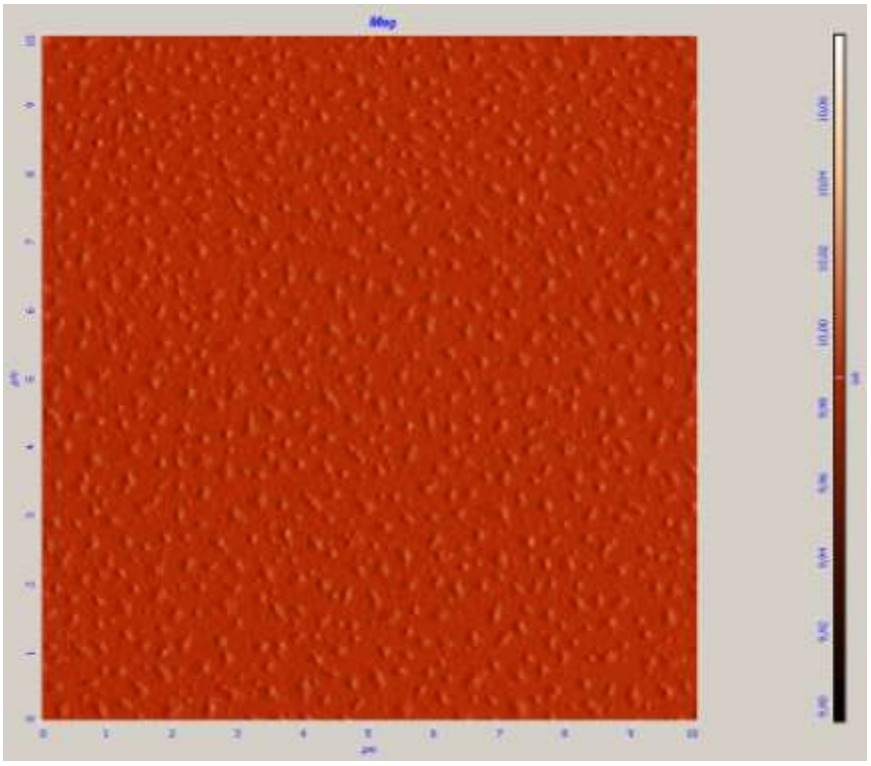

Figure 18.4. *10x10µm with semi-contact error mode acquisition, to put in evidence changes in altitude.*

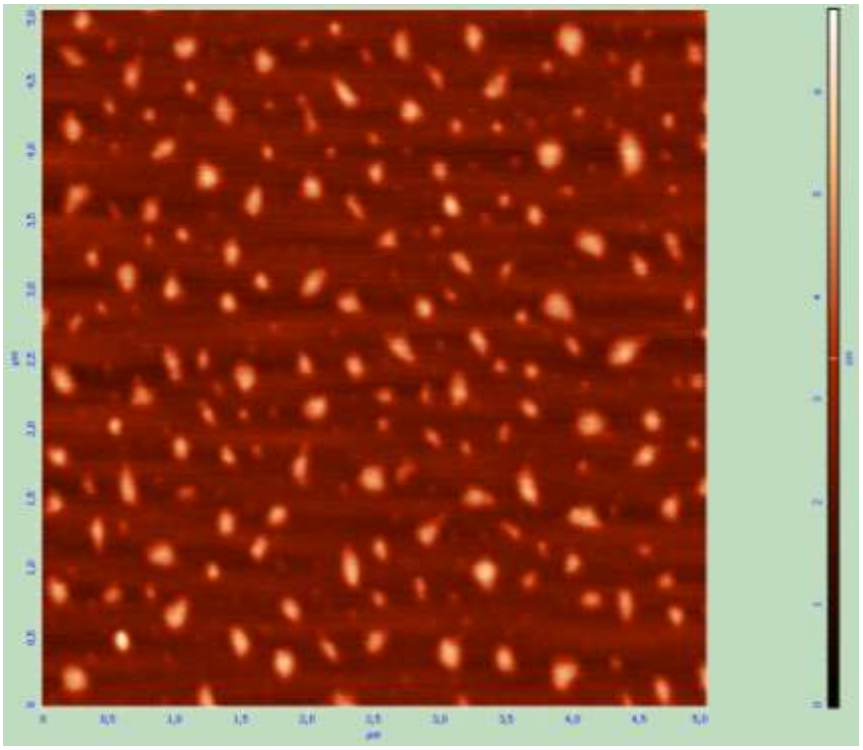

Figure 18.5. *5x5µm.*

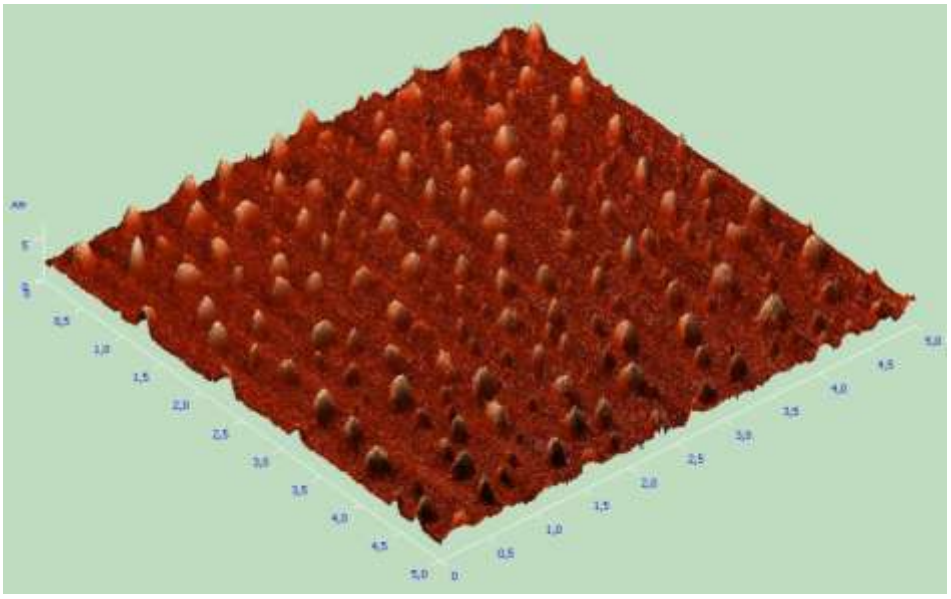

Figure 18.6. *5x5µm with 3D image elaboration.*

The particles show a flat shape, with regular distribution on the surface.

Figure 19. *AFM images of a sample prepared with the recipe "L3" through the procedure explained in the section "materials and methods".*

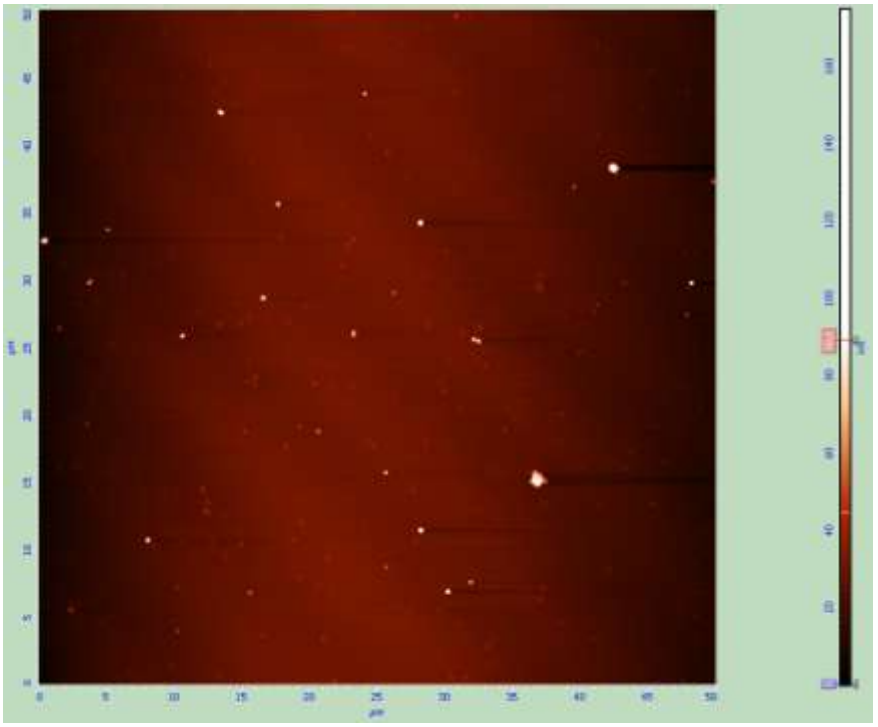

Figure 19.1. *50x50µm.*

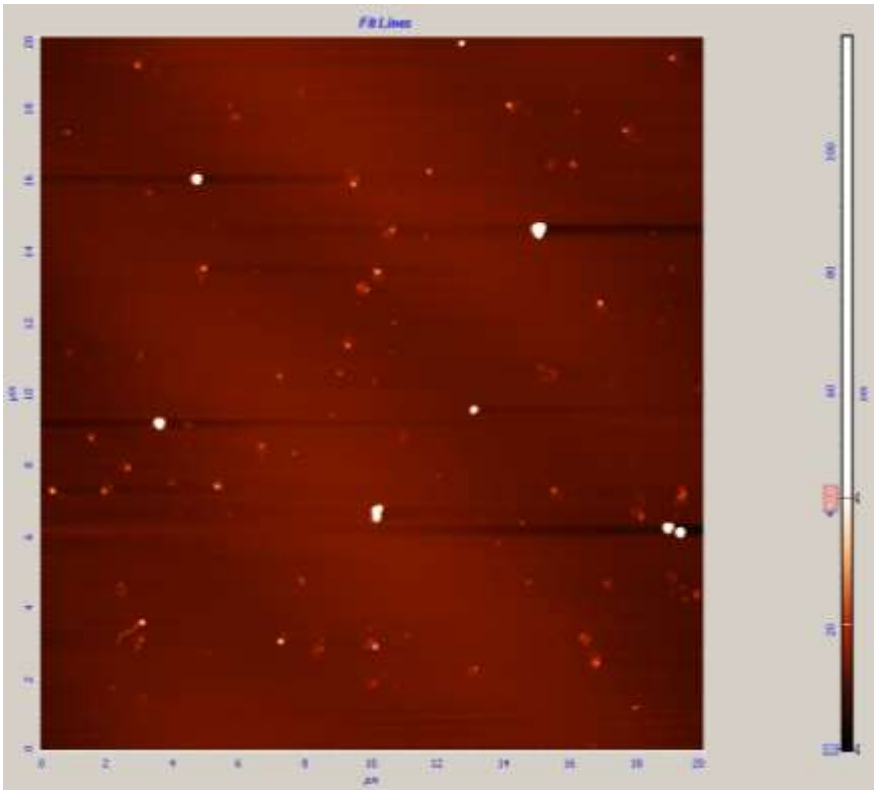

***Figure 19.2**. 20x20µm.*

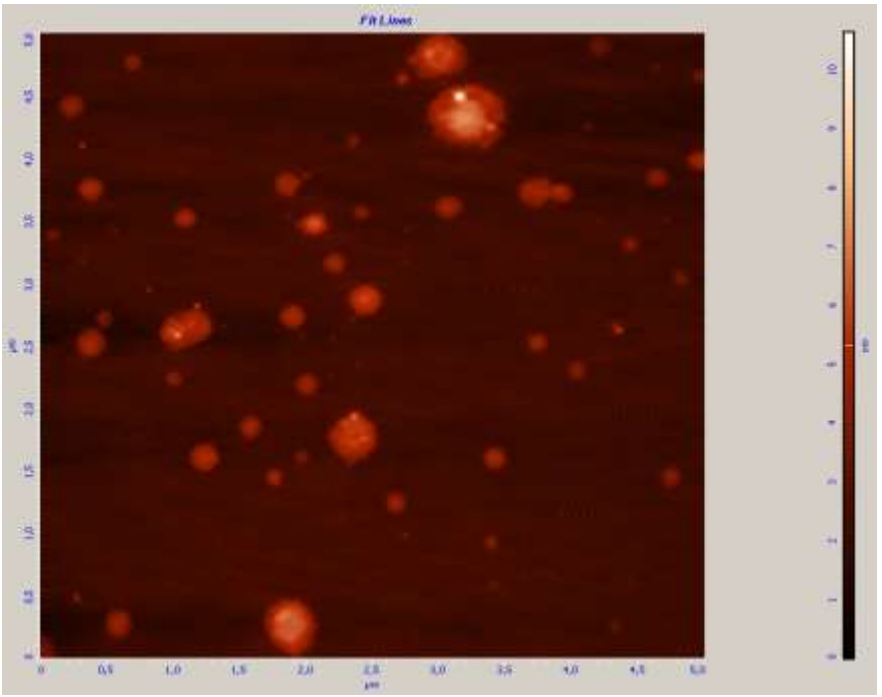

***Figure 19.3.** 5x5µm.*

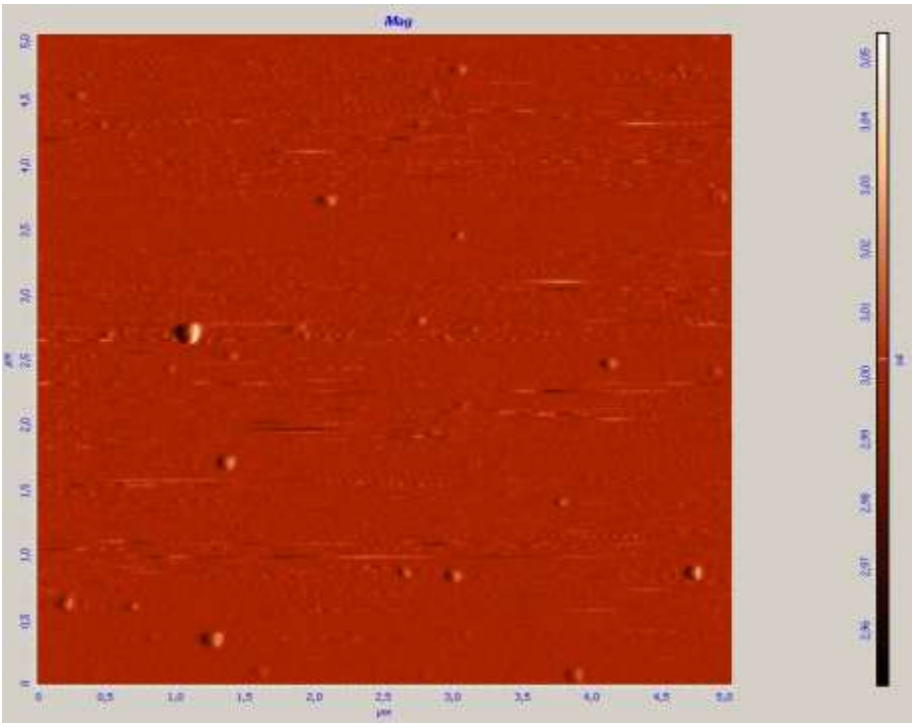

Figure 19.4. *5x5µm with semicontact error acquisition, to put in evidence changes in altitude.*

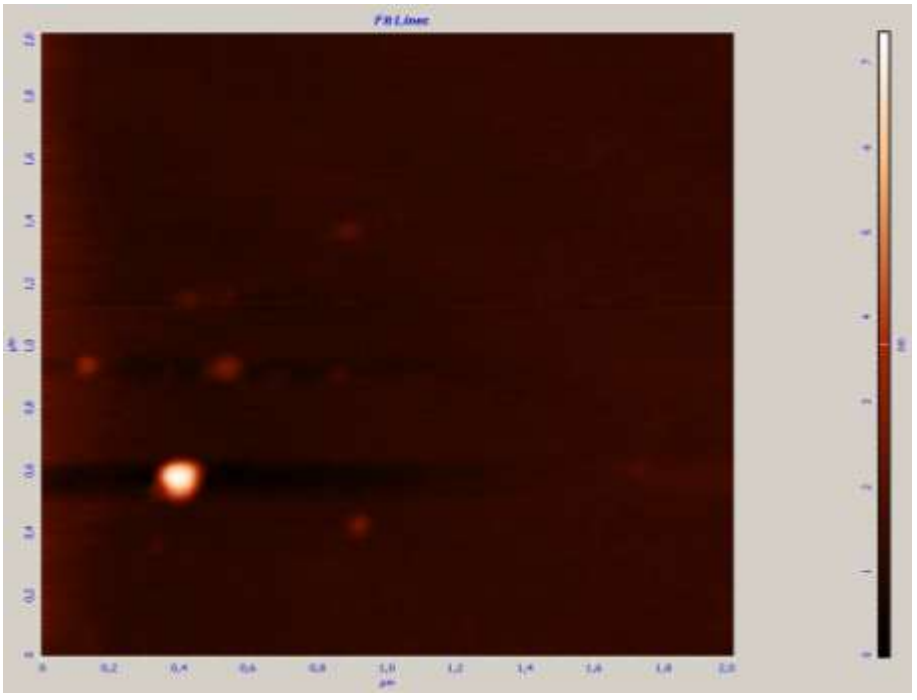

Figure 19.5*. 2x2µm.*

The particles show a flat shape, with more aggregates than the samples prepared in Tris buffer. Moreover less particles are present, probably due to the fact that the particles were initially immersed in ACN/W instead of Tris

buffer. This could have hampered the adsorbtion of the particles to the mica surface.

Figure 20. *AFM images of a sample prepared with the recipe "M3" through the procedure explained in the section "materials and methods".*

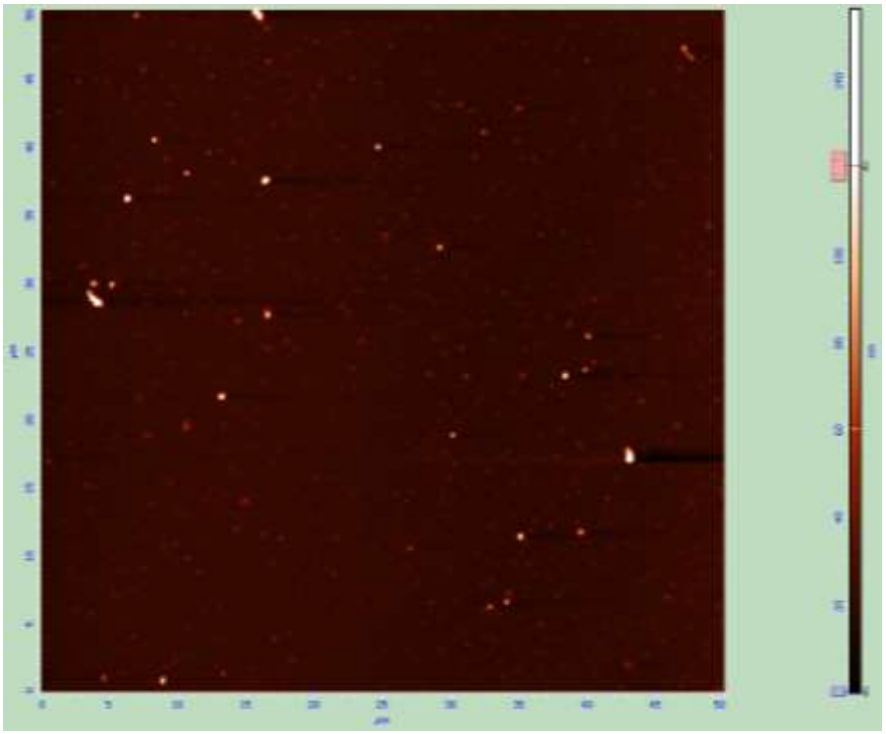

Figure 20.1*. 50x50µm.*

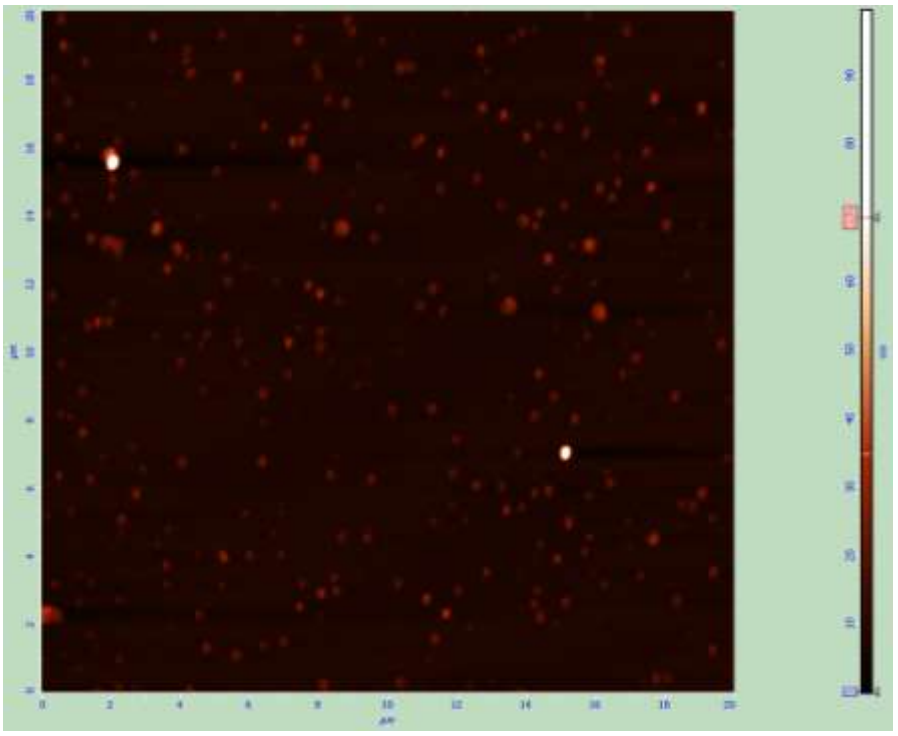

Figure 20.2. *20x20µm.*

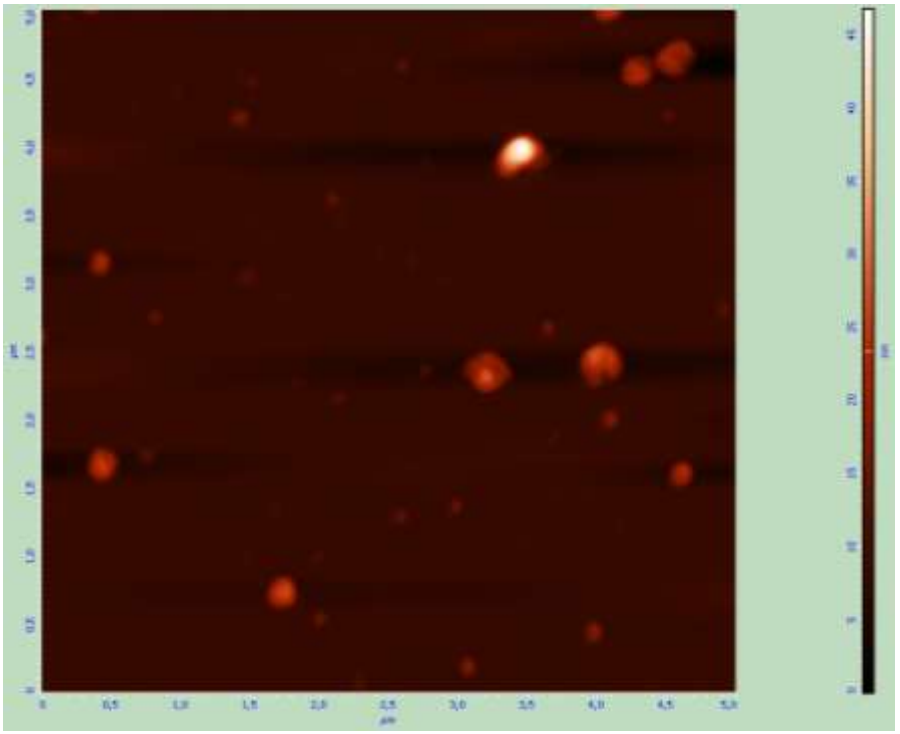

Figure 20.3. *5x5µm.*

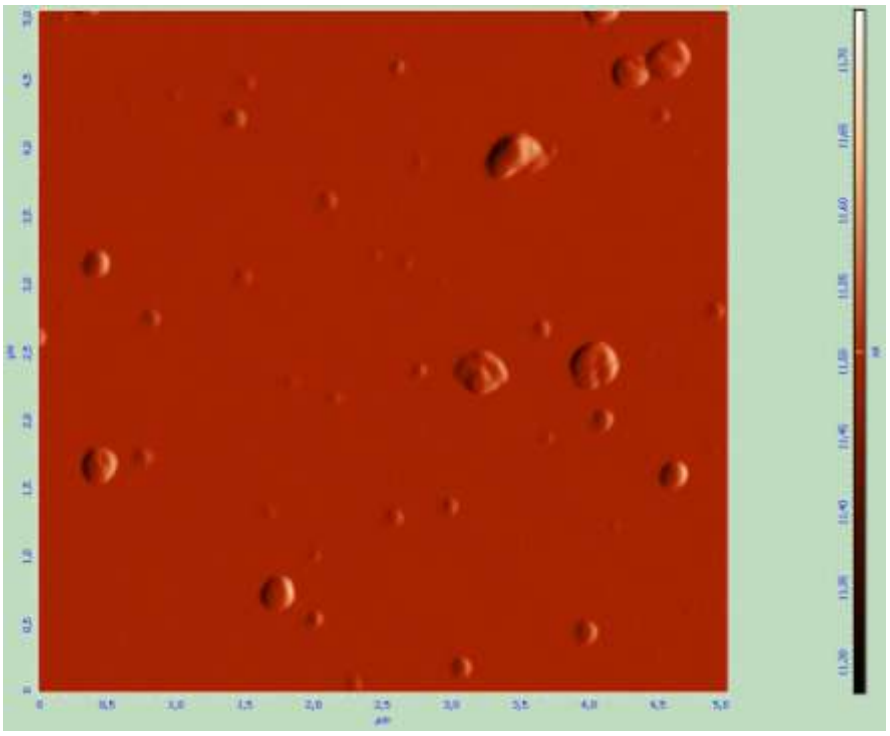

Figure 20.4. *5x5µm with semicontact error-mode acquisition.*

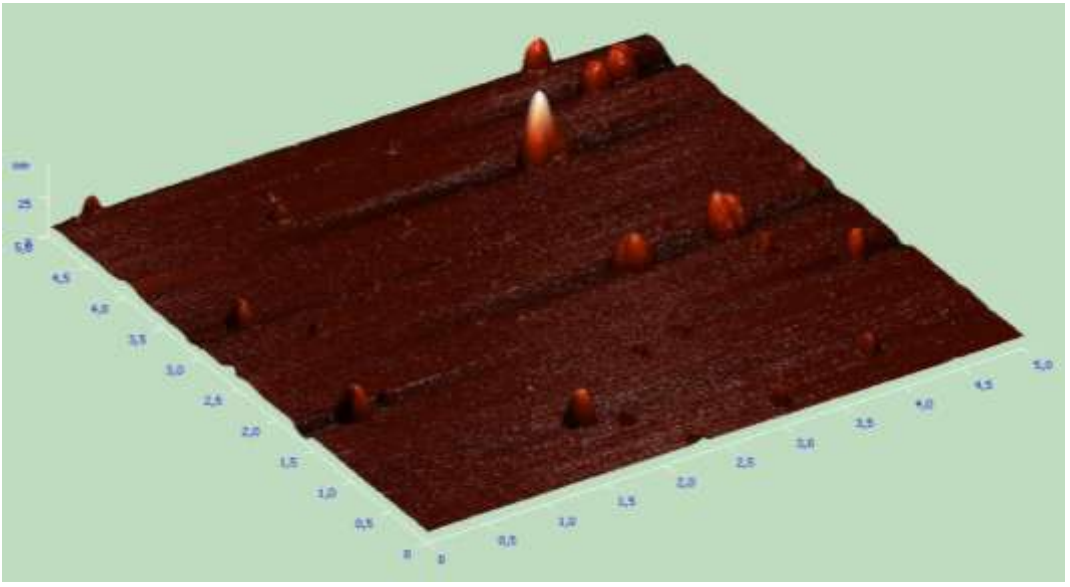

Figure 20.5. *5x5µm with 3D image elaboration.*

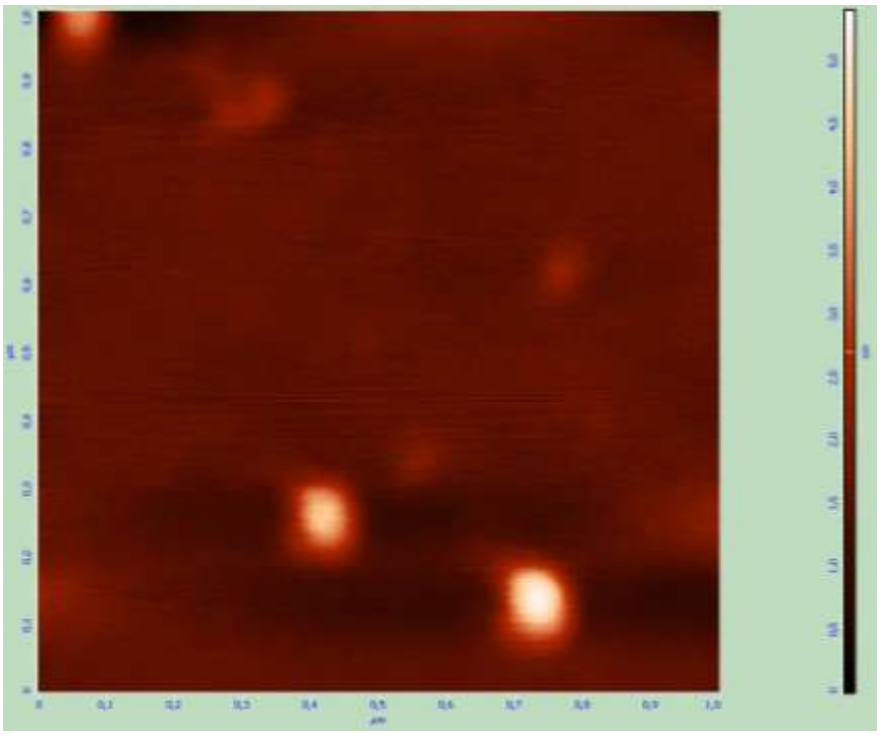

Figure 20.6. *1x1µm.*

The particles show a flat shape, similar to what can be observed in the sample prepared with recipe “L3”. Few particles are actually present, probably due to the fact that the particles were initially immersed in ACN/W instead of Tris buffer. This could have hampered the adsorption of the particles to the mica surface.

Figure 21. Comparison of images from the four samples for different magnifications.

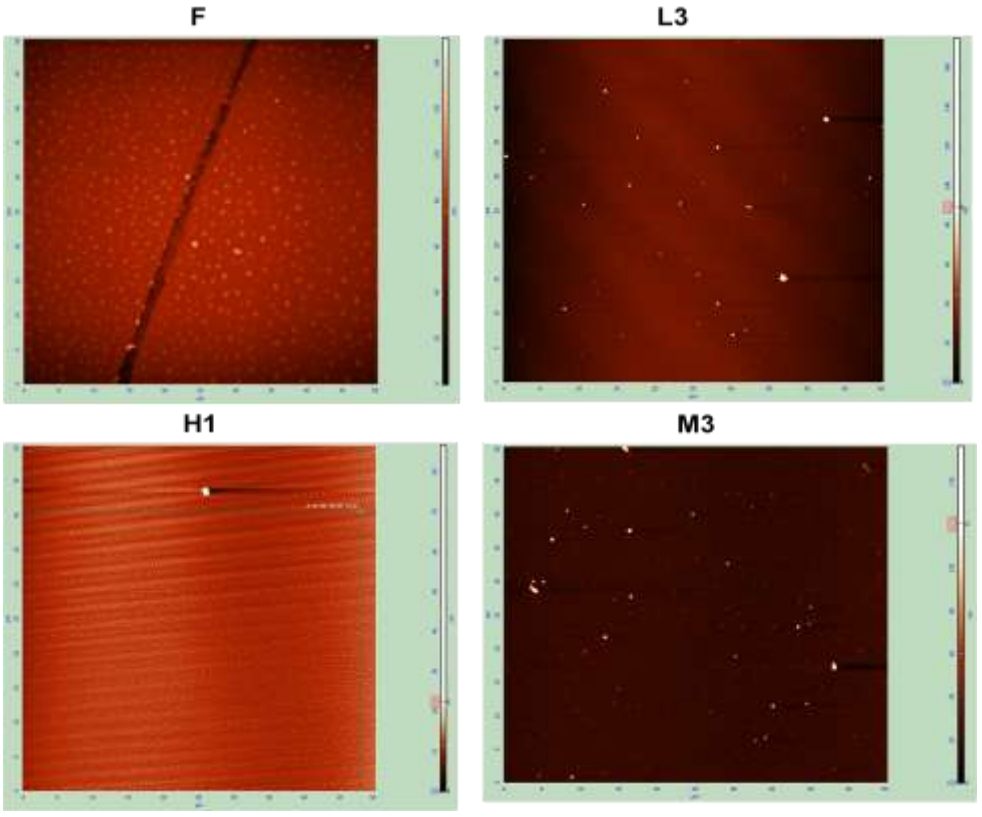

Figure 21.1. *50 x 50 µm magnification.*

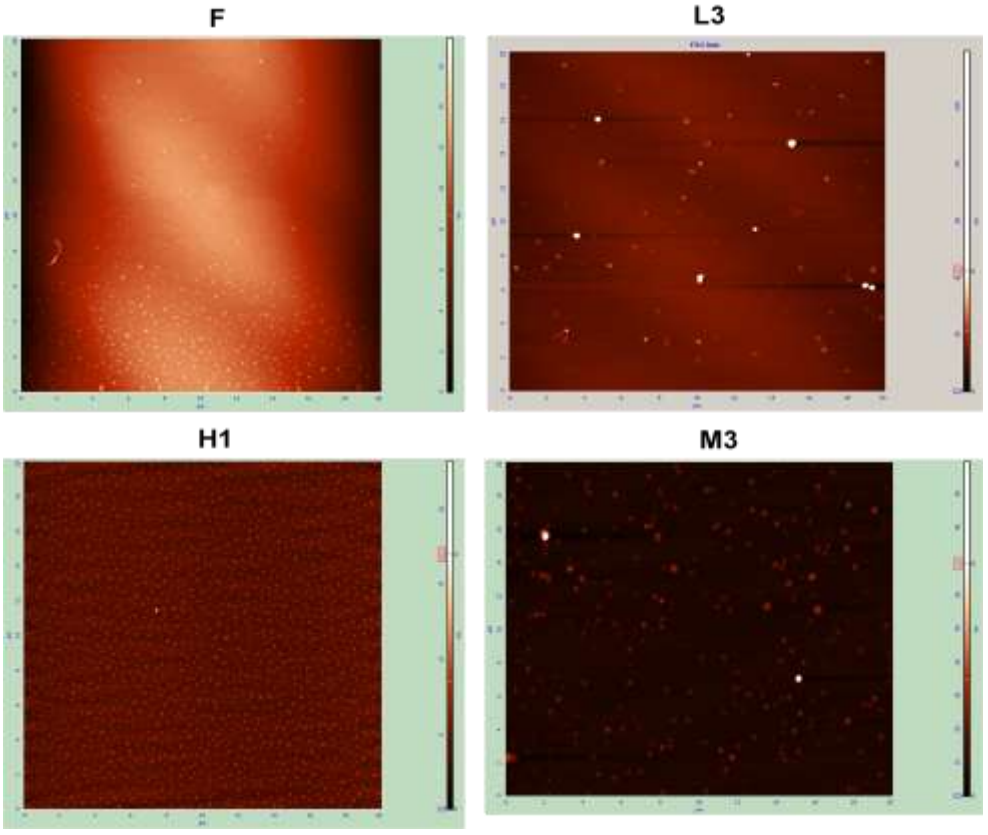

Figure 21.2. *20 x 20 µm magnification.*

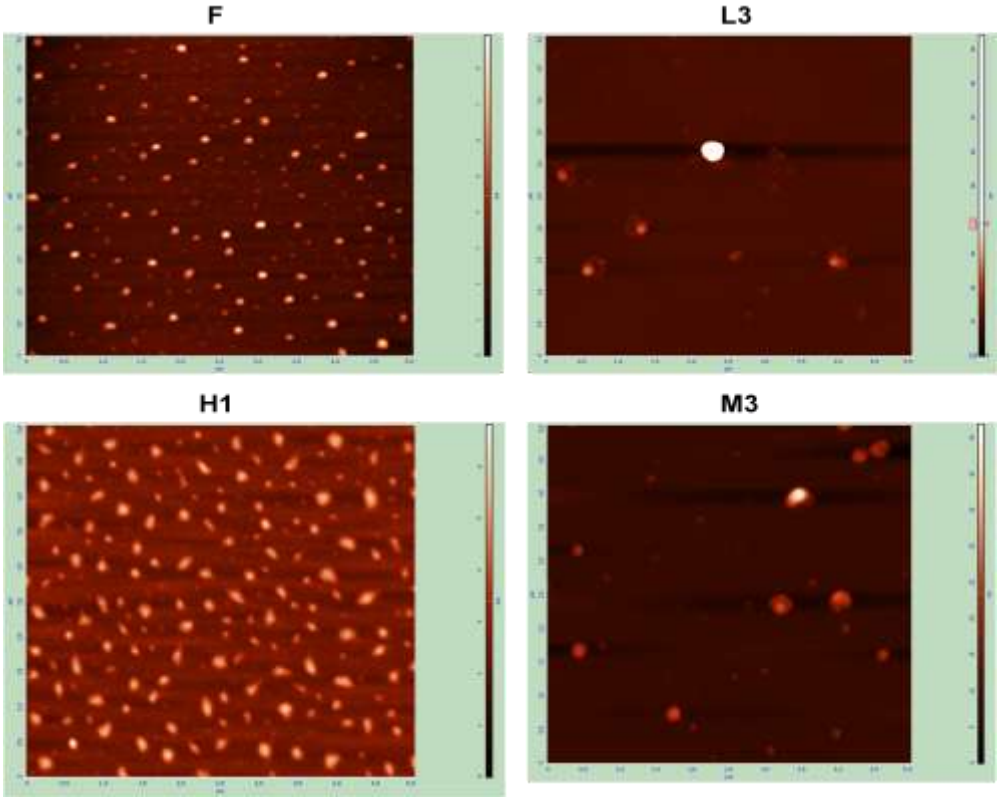

Figure 21.3. *5 x 5 µm magnification.*

The general appearance of the nanoparticles is flat, with height 1/10 of the width. The size range is approximately from 20nm x 2nm (width x height) to 200nm x 20nm.

There is a higher density of particles for samples produced with recipes “F” and “H1”. One possible explanation can be the solvent: they are dissolved in Tris buffer, while samples “L3” and “M3” in ACN/Water 9:1 v/v. This fact could hamper the attachment of the particles to the mica surface. More aggregates are present in samples prepared in ACN/W.

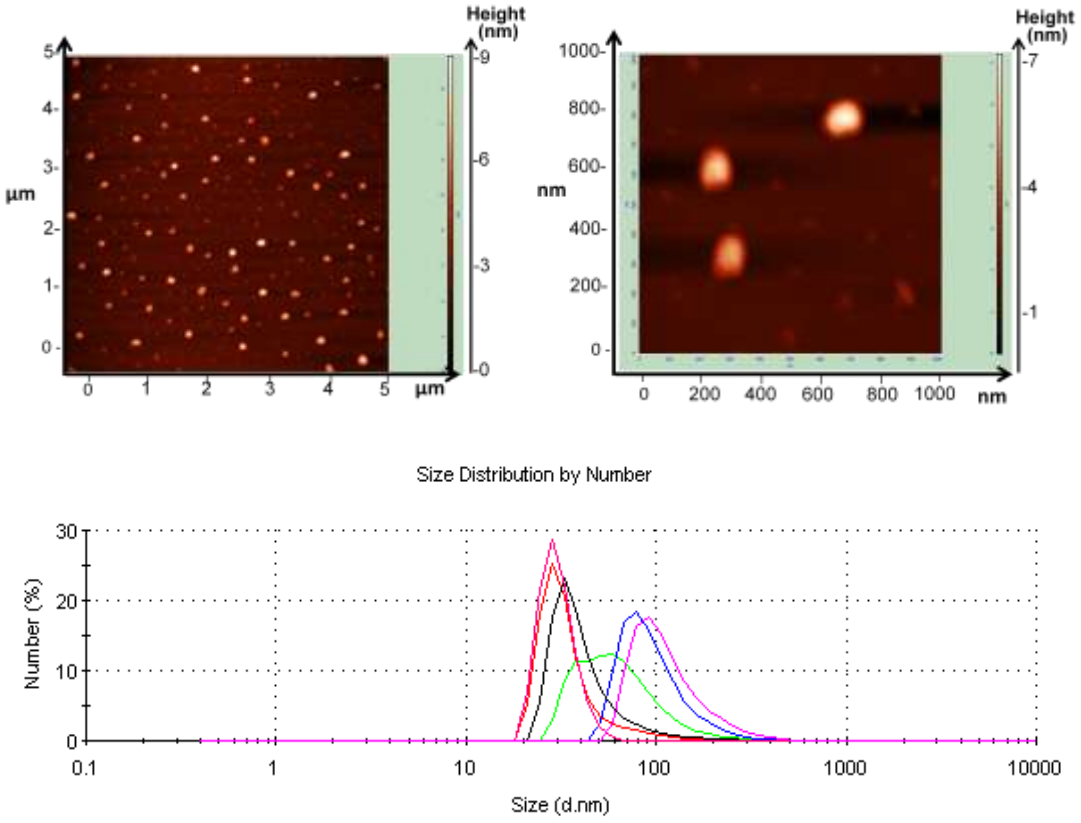

Figure 22: *Comparison of AFM and DLS data on a sample prepared with recipe "F".*

There is a seemingly comparable size pattern between AFM and DLS data: AFM pictures show a general pattern of bigger, evident nanoparticles with dimension around 100nm x 7nm (width x height) on a layer of smaller particles with dimension around 20nm x 5nm. A similar pattern seems to emerge from DLS data, with a detected population apparently splitted in two parts: a first one having hydrodynamic diameter of approximately 20nm and a second one 80nm.

5.6.5 Yield evaluation of large-scale synthesized nanoparticles

Here following the assessment of particles presence in concentrated samples. The amount of monomer, crosslinker and pTyr indicated in the table are the theoretically present in 1mL of sample if all the starting material was converted to nanoparticles. The crosslinker content was 80%C (mol/mol) for all the recipes.

Table 9. *Weight of particles in large-scale synthesized samples.*

Recipe	Monomers	% T	mg crosslinker	mg monomer	mg Fmoc-pTyr	Solvent	Amount (mg)
F	HEMA/BIS	1	97.4	20.6		W	1.0
F + Fmoc-pTyr	HEMA/BIS	1	97.4	20.6	38.2	W	0.0
H1	HEMA/BAP	1	88.4	29.6		W	0.3
H1+ Fmoc-pTyr	HEMA/BAP	1	88.4	29.6	53.2	W	0.5
L3	HEMA/BIS	0.2	19.5	4.1		A/W	0.0
L3+ Fmoc-pTyr	HEMA/BIS	0.2	19.5	4.1	7.7	A/W	0.9
M3	DAU/BIS	0.2	19.5	4.5		A/W	0.2
M3+ Fmoc-pTyr	DAU/BIS	0.2	19.5	4.5	7.7	A/W	0.3

The results show a proportionally lower amount of material produced on a large scale respect to the amount prepared in small scale (from 2 to 10 times less). This reduced efficiency could be due to the reduced amount of light that reaches the reagents. The glass of a bottle is in fact thicker than the glass of a vial and the reagents are in media less exposed to the light due to the bigger volume of liquid.

5.6.6 Cleaning of polymers prepared with standard bulk synthesis

Only HEMA/BIS and DAU/BIS in Tris buffer were prepared with a standard synthesis method to evaluate binding properties. Here following the graphs of the cleaning of the polymers. The cleaning proceeded until there was no further decrease of the signal (Abs< 0.05).

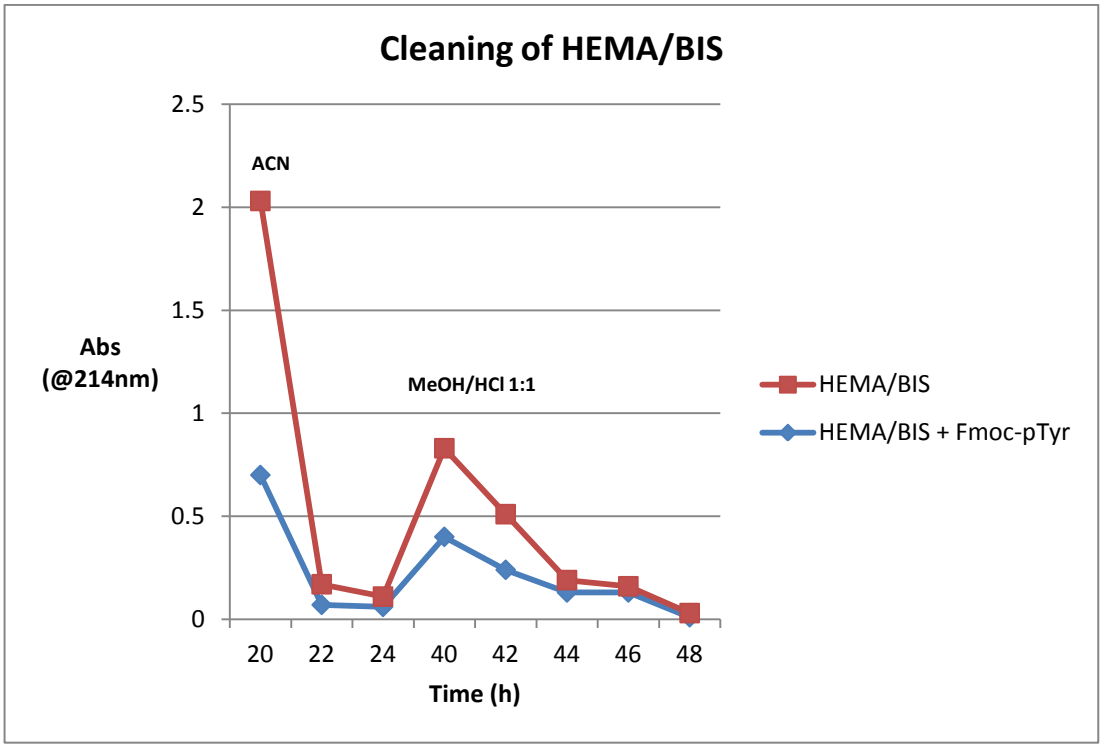

Figure 22. *Cleaning of HEMA/BIS NIP and MIP.*

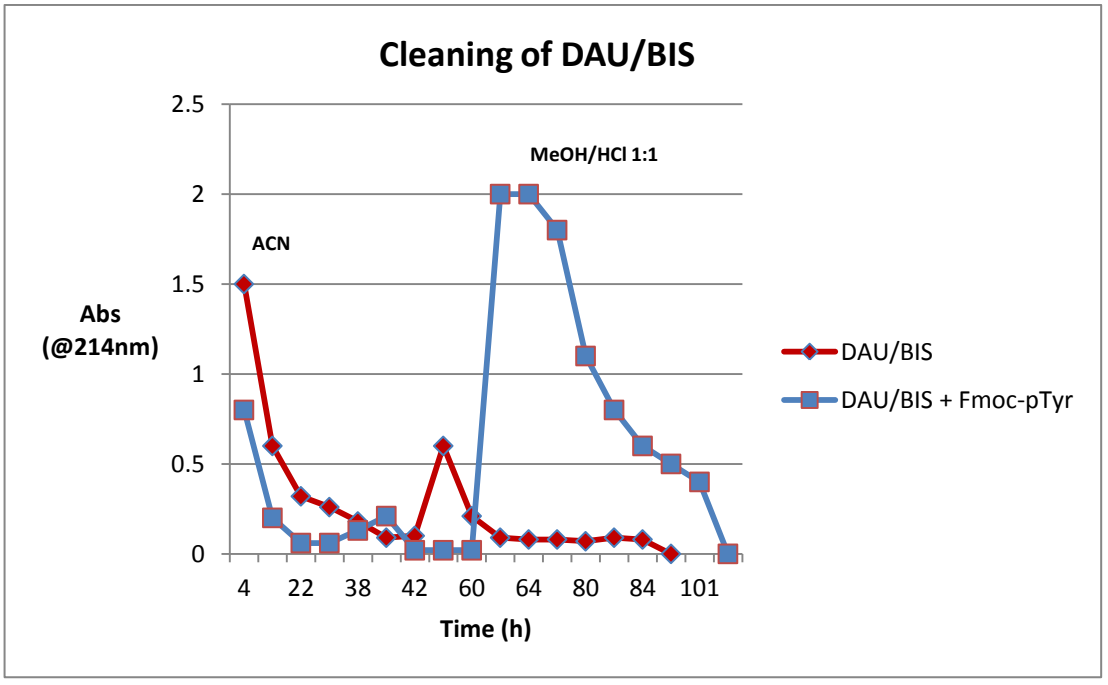

Figure 23. *Cleaning of DAU/BIS NIP and MIP.*

After the cleaning samples were dried on a cellulose filter paper for 72h. The amount of polymer is reported in table 10 with the corresponding yields:

Table 10. *Amount and yield of the polymers prepared with standard bulk synthesis.*

	HEMA/BIS MIP	HEMA/BIS NIP	DAU/BIS MIP	DAU/BIS NIP
Amount (mg)	216	143	43	118
Yield %	43	29	9	24

The amount of DAU/BIS MIP was not sufficient to perform rebinding experiments, that were thus carried out only on HEMA/BIS polymers.

5.6.7 Rebinding experiments

Here following the calibration curve for pTyr and the graph showing the evaluation of pTyr binding properties of HEMA/BIS NIP and MIP. The measurements were made in triplicate.

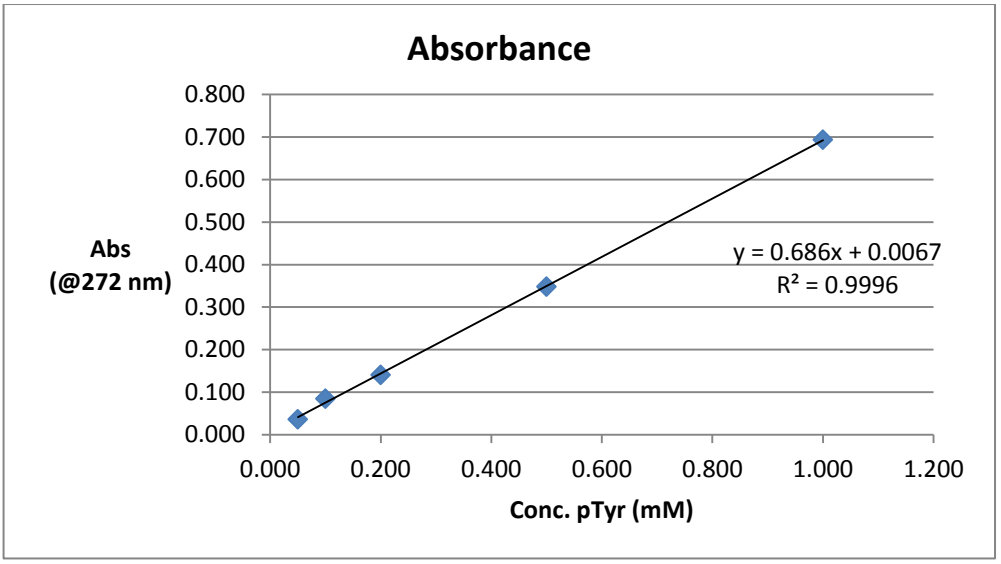

Figure 24. *Calibration curve for increasing concentration of pTyr.*

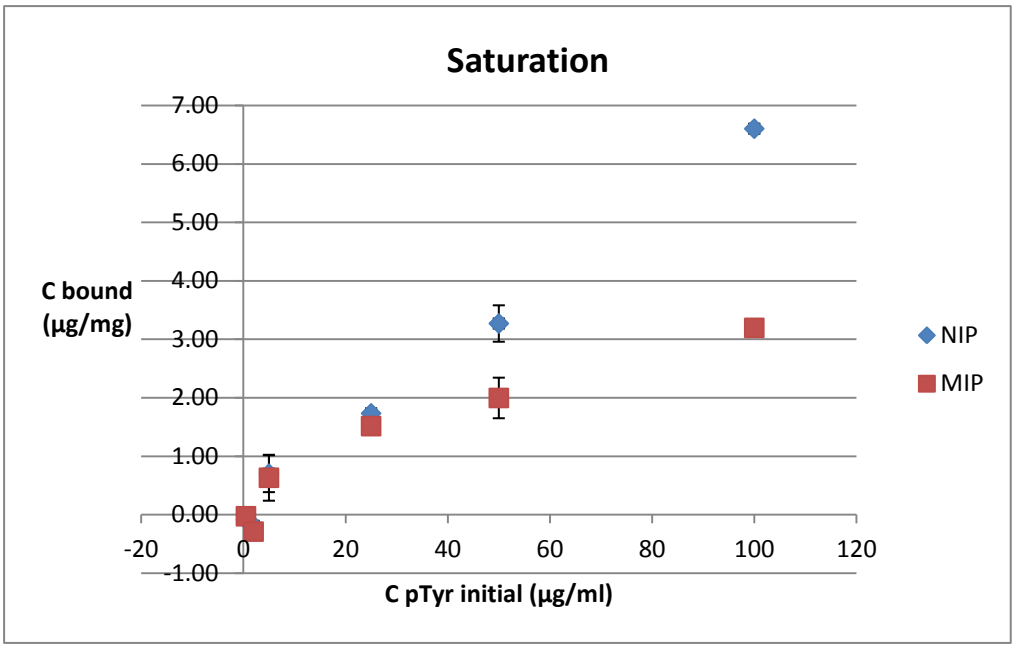

Figure 25. *Saturation curve for increasing concentration of pTyr.*

From the graphs it emerges that the MIP polymer has the tendency to have a saturation behaviour, while NIP definitely increases the substrate incorporation at increasing concentrations. The capacity of the MIP resin tends to settle around 3 µg/mg resin.

5.6.8 Cleaning of polymers after rebinding

Here following the absorbance data and the graph reporting the cleaning passages. Absorbance data of NIP and MIP were put together given their identical behaviour in pTyr release.

Table 11. *Absorbance data at 272nm for the cleaning solutions.*

	HEMA/BIS and HEMA/BIS + pTyr	time (h)	total time (h)
MeOH/HCl 1:1	0.33	2	2
MeOH/HCl 1:1	0.31	1	3
MeOH/HCl 1:1	0.24	15	18
MeOH/HCl 1:1	0.16	1	19
MeOH/HCl 1:1	0.12	1	20
MeOH/HCl 1:1	0.06	1	21
MeOH/HCl 1:1	0.04	1	22
MeOH/HCl 1:1	0.18	15	37
MeOH/HCl 1:1	0.05	1	38
MeOH/HCl 1:1	0.003	2	40
Tris	0.001	2	42
Tris		final	final

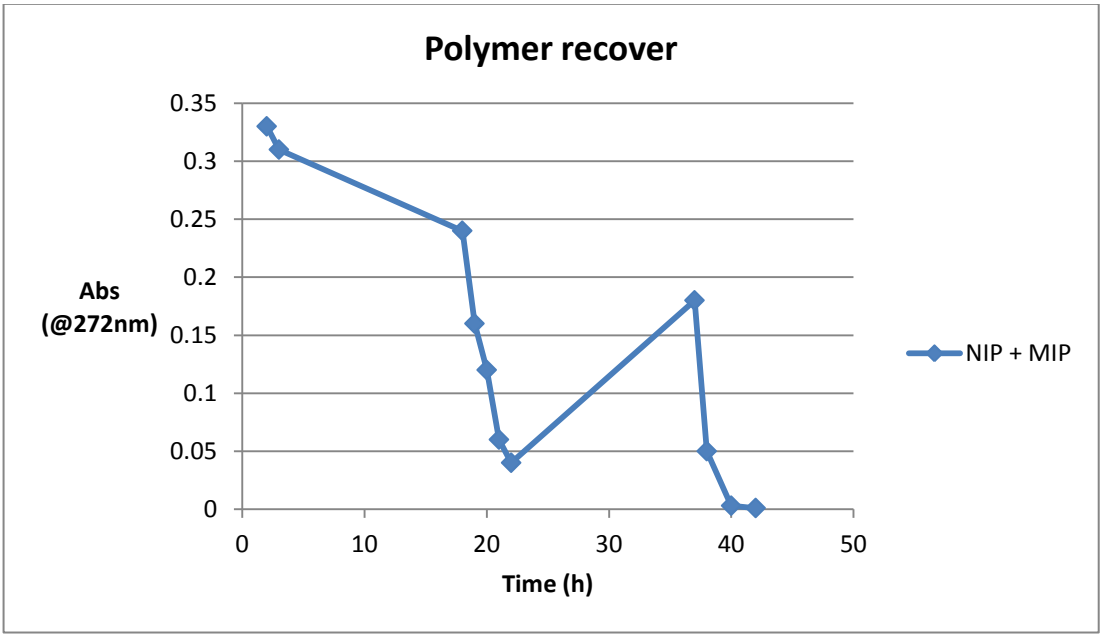

Figure 26. *Trend of pTyr amount extracted from the polymers.*

Two days were necessary for the complete cleaning of the polymers from the substrate pTyr (Abs <0.01).

5.6.9 Rebinding after cleaning

Here following the data and the related graph obtained in the rebinding experiments after polymer cleaning.

Table 12. *Absorbance data obtained in rebinding experiments.*

H/B (NIP) µg/ml	Abs	Conc (µg/ml)	C Bound (µg/ml)	C Bound (µg/mg)
13	0.039	12	0.71	0.14
26	0.070	24	1.92	0.38
52	0.136	49	2.81	0.56
130	0.337	126	4.33	0.87
260	0.667	251	8.78	1.76

H/B pTyr (MIP) µg/ml	Abs	Conc (µg/ml)	C Bound (µg/ml)	C Bound (µg/mg)
13	0.038	12	1.09	0.22
26	0.076	26	-0.37	-0.07
52	0.138	50	2.04	0.41
130	0.344	128	1.67	0.33
260	0.676	255	5.35	1.07

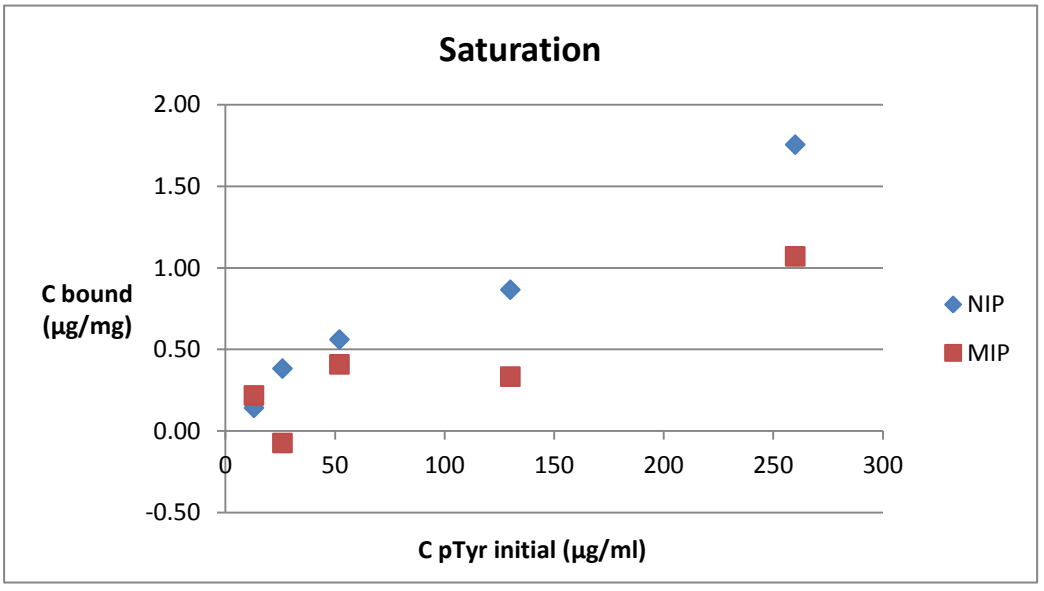

Figure 27. *Graph reporting the saturation of NIP and MIP polymers.*

From the graph it can be noted that MIP tends to bind less substrate than NIP. The binding capacity after cleaning showed to be much lower than before the cleaning, being 6 times less.

The complete saturation of the polymers could not be reached, anyway higher concentrations of substrate would give absorbance values out of the range of confidence of the instrument (0.001<Abs<1.0).

6 Conclusion

A photopolymerization method for the production of MIP nanoparticles was here evaluated.

The method was tested in different conditions, included the use of different monomers, crosslinkers and solvents.

A remarkable result, already reported by Wulff et al. (194), regards the effect of a “bad” solvent, that keeps the size of the particles small avoiding their continuous growth in solution through precipitation.

Good results both for size and polydispersity were obtained with the following recipe (“F”): HEMA/BIS 1%T, 80%C, MB 100µM, TSIA 1mM, DPI 50µM, agitation, 5’ polymerization. Zave was 163±16nm and PdI 0.332±0.101, with good reproducibility.

Good size results were obtained also with the use of BAP as crosslinker (“G” recipe: Zave 81±29nm), but paying the price of a higher polydispersity (PdI 0.756±0.219).

Lowering the monomers content from 1% to 0.2% brings a not expected nanoparticles enlargement both in TRIS buffer and acetonitrile/water 9:1 v/v (recipes F-I, P-Q, fig.12).

DAU shows a quicker polymerization kinetics than HEMA in TRIS buffer, having a turbidity point of 3’ at 1%T and 15’ at 0.2%T (HEMA does not give turbidity for both recipes after 60’). Moreover DAU nanoparticles are in general bigger than HEMA ones (fig.13).

The addition of Fmoc-pTyr does not bring a significant size and polydispersion change (recipes F-P, L-S and M-T, fig.15).

The yield evaluation evidenced a percentage ranging between 0.5% and 5.5%, with not significant difference between the use of different monomers (table 8).

HEMA/BIS recipe was produced with a standard bulk synthesis and subdued to rebinding experiments. The results show a saturation behavior for the MIP and a tendence to accumulate the substrate for the NIP. The binding capacity for the MIP was 3µg/mg resin.

The results can be considered as still preliminary, with the perspective to evaluate binding characteristics for other recipes.

Nevertheless the DLS analysis showed that our method of synthesis is effective in the production of particles with size around 100nm, confirmed through AFM microscopy. Moreover an interesting result was the low polydispersity of the particles, that in many cases was under 0.2.

AFM showed particles with flattened shape, probably due to the fact that a hydrogel is soft and the combined effect of gravity, surface attraction and pressure of the tip of the probe lower their height (216). The future perspectives of this research line consist in extending the evaluation of the binding properties to other recipes. In particular, testing the properties of the nanometric format (the four recipes produced on large scale) would give us an indication of the possibility of production of a valid alternative material to phosphospecific antibodies.

Chapter 3

DEVELOPMENT OF AN SPR BIOSENSOR FOR HEPCIDIN HORMONE

1 Introduction

Iron homeostasis related disorders have a high incidence in the population. Both anemias, in which iron is deficient, affecting at least 500,000,000 people in the world, including at least 2-5% of adolescent at every latitude (225), and iron overload disorders, as Hereditary Haemocromatosis (HH) are widespread. The C282Y allele on the HFE gene, which is mainly linked to HH, occurs in the 5-10% of European population (225). It was demonstrated that iron homeostasis is regulated by the 25 aminoacid peptide hormone Hepcidin (Hepc) and that urinary and blood levels of Hepc are associated with dis-regulation of martial metabolism (226).

Hepcidin regulates iron export from enterocytes and macrophages by binding the only known iron export protein, ferroportin (227). It is synthesized in the liver as an 84-aminoacid pre-pro-hormone and matured by proteolysis through a furin cleavage to generate the biologically active 25-aa peptide (Hepc-25) that is secreted into circulation (228). Hepc-25 leaves the body via secretion through the kidneys (229).

In contrast to the serum, where almost exclusively Hepc-25 (2789.4 Da) is detectable, urine also contains N-terminally truncated peptides of 22 aminoacids (Hepc-22; 2436 Da) and 20 aminoacids (Hepc-20; 2191.7 Da) (229), (230).

Structurally, hepcidin shows a secondary amphipathic structure and is particularly rich in basic aminoacids that confer a positive charge with an isoelectric point of 8.2 (230). The eight cysteine residues contained within hepcidin form four disulfide bridges (figure 1) (229).

Figure 1. *NMR structure of the major form of human hepcidin The amino and carboxy termini are labeled as N and C respectively Disulfide bridges are in yellow (This research was originally published in Journal of Biological Chemistry Jordan JB, Poppe L, Haniu M, Arvedson T, Syed R, Li V, Kohno H, Kim H, Schnier PD, Kim H, Schnier PD, Harvey TS, Miranda LP, Cheetham J, Sasu BJ, Journal of Biological Chemistry 2009, 284, 24155, 24167 © The American Society for Biochemistry and Molecular Biology].*

Because hepcidin levels reveal important clinical information about pathological states, measurement of hepcidin in urine or plasma as a biomarker may be interesting to apply in clinical practice.

Despite significant efforts, the development of a robust assay to detect hepcidin proved to be problematic. Initially, hepatic hepcidin mRNA expression in the liver was successfully used as a marker, but liver biopsies are rarely clinically indicated (231). Immunoassays are commercially available for prohepcidin (DRG Diagnostics,Marburg, Germany), however, the assay does not recognize the biologically active Hepc-25 (232). By contrast, the only available immunoassay against Hepc-25 is not widely available yet as a commercial product (233), (234), (235). Therefore, several groups have developed assays to detect Hepc-25 based on mass spectroscopy (236), (230), (238), (239), (240), (241).

These last techniques have the disadvantage to be quite expensive and demanding in terms of sophisticated instrumentations and dedicated staff. Moreover, MS methods revealed the presence, in biological fluids, of non-functional truncated isoforms of Hepc (e.g. Hepc-22 and Hepc-20), which complicated even more the interpretation of the most advanced

immunological assays. These forms, in fact, are revealed by the immunoassays but do not intervene in iron balance regulation (116).

It can be concluded that, notwithstanding the very last progresses, it is not still available a method for blood and urine Hepc measurement having characteristics of accuracy, ease of implementation, and large scale distribution at fairly low cost.

De Domenico et al. (242) identified the hepcidin-binding domain (HBD, figure 2) on ferroportin and showed that a synthetic 20 aminoacid peptide corresponding to the HBD recapitulates the characteristics and specificity of hepcidin binding to cell-surface ferroportin. They subsequently developed a competitive assay to measure hepcidin concentrations in small volumes of biological fluids.

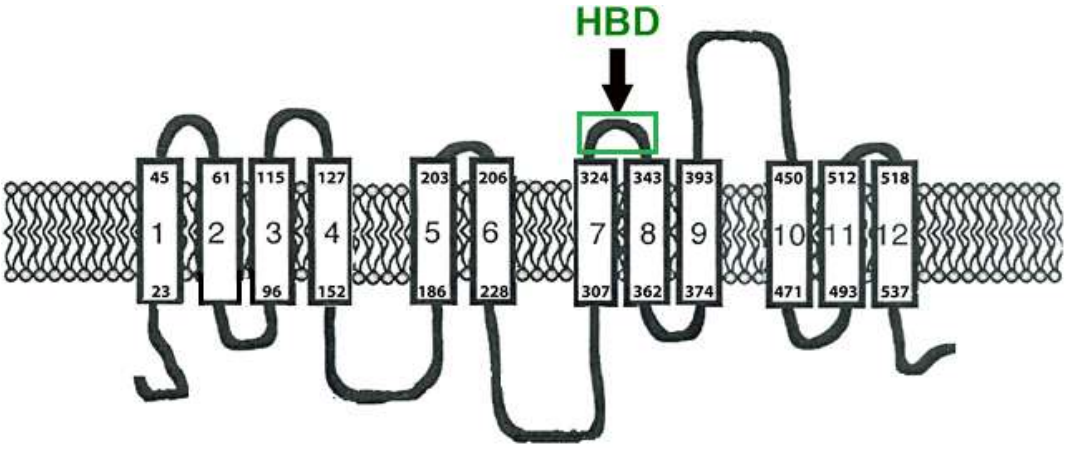

Figure 2. *Predicted topology of ferroportin (Fpn) The structure of Fpn is based on the study of Liu et al, 2005 [adapted from ref.108]. We can note the HBD synthetically mimed.*

Our attempt is to improve the measurement of the hepcidin levels in body fluids developing a point-of-care and label-free assay based on the affinity between hepcidin and this synthetic peptide. For the purpose we exploited the Surface Plasmon Resonance (SPR) technique (see next paragraph) and the immobilization of the synthetic ligand on CM5 Biacore chips. These chips present a carboxymethyl dextrane matrix on the surface, to which the N-terminal of HBD can be bound through the use of EDC/NHS chemistry.

The sequence of the wild-type HBD is FDCITTGYAYTQGLSGSILS (pI=3.8). To increase solubility, the peptide was synthesized with two arginines added at the amino and carboxyl termini (pI=10.0). The arginines did not affect the specificity, temperature dependence, or affinity of HBD for hepcidin (243). The presence of these extremities could favor the binding of hepcidin, freeing aminoacids able to link the hormone. We tested the effectiveness of the peptide bait linking it to the chip and evaluating the instrumental response to different concentrations of hepcidin-25.

2 Surface Plasmon Resonance

Surface Plasmon Resonance is a biosensing technique widely employed in testing the affinity between ligands and analytes. Biosensors can be defined as "…devices comprising a biologically sensitive material immobilized in intimate contact with a suitable transducing system to convert the biochemical signal into a quantifiable and processible electric signal" (244). The physical phenomenum at the core of the system is the variation of refractive index of a dielectric medium in contact with a metal (245). Usually gold is chosen for its better performance and inertness.

When a linearly polarized beam of light (polarization parallel to the plane of incidence) hits the surface of the metal, the radiation is totally reflected if the angle of incidence is higher than the critical angle. At a certain angle of incidence, called SPR angle (Θ_{SPR}), the component of the wave of light parallel to the surface excites the polaritons, waves of electrons along the surface of the metal, if their wavelength corresponds to the wavelength of the incident light (i.e. there is resonance). In this case an evanescent field is generated at the interface between metal and medium. The amplitude of this field decays exponentially from the surface and is sensed usually at a maximum distance of 100nm from the surface. The SPR angle depends on the wavelength, on the metal, on the temperature and on the polarizability of the medium at the interface of the metal, strictly connected to its refractive index (*n*) by the Eq 1:

1) $$n = \sqrt{\epsilon_r \mu_r}$$

where ε_r is the relative permittivity of the material and μ_r is its relative permeability.

This absorption is evidenced by a minimum of reflected light that arrives to a detector (usually a photodiode array) at the SPR angle (Θ_{SPR}). The dependence of Θ_{SPR} from the refractive index of the medium in contact with the metal is the principle at the basis of the system. By immobilizing a ligand on the surface, for example, the binding events of analytes to the ligand can be monitored through the variation of the refractive index, proportional to the mass of analyte in proximity to the interface metal/dielectric (Fig.3).

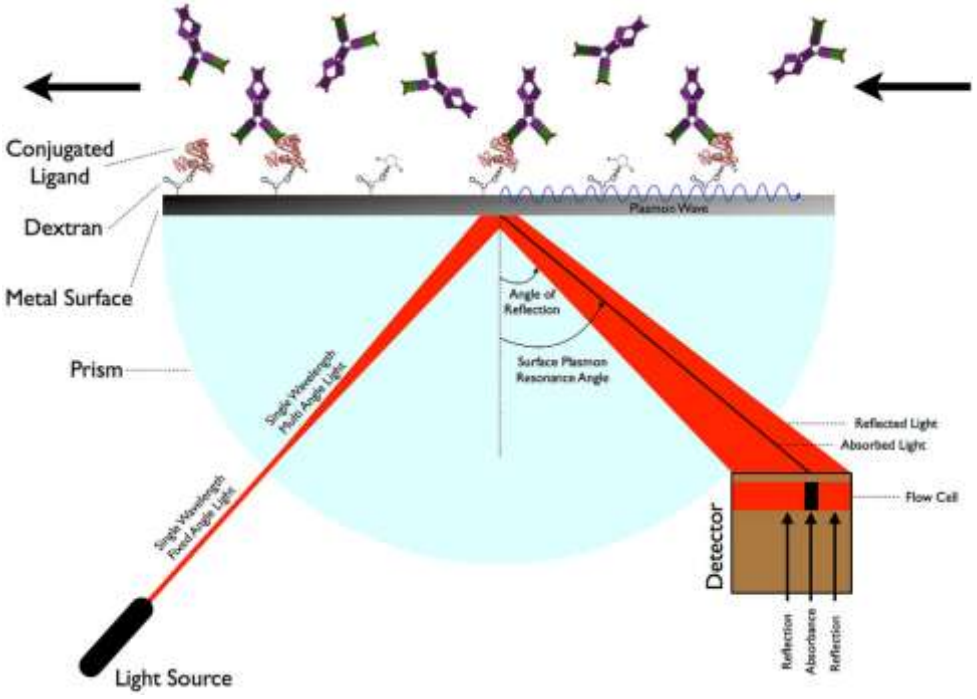

Figure 3. *Representation of the SPR principle. The SPR angle (angle at which the incident light is absorbed and not totally reflected) depends on the refractive index of the medium in contact with the metal layer on which the light impinges. This refractive index is directly proportional to the mass of analyte bound to the metal surface (Picture taken from: Wikipedia).*

The variation of *n* is converted in Responsive Units (RU), proportional to the mass of analyte. In the case of proteins, these molecules all have a similar *n*, thus a binding event or simply the presence of any protein in proximity of the

surface generates a signal proportional to the mass: 1RU corresponds to 1pg/mm^2 of protein. The binding event is actually a dynamic process that is expressed by a profile of RU variation, called sensorgram (Fig.4).

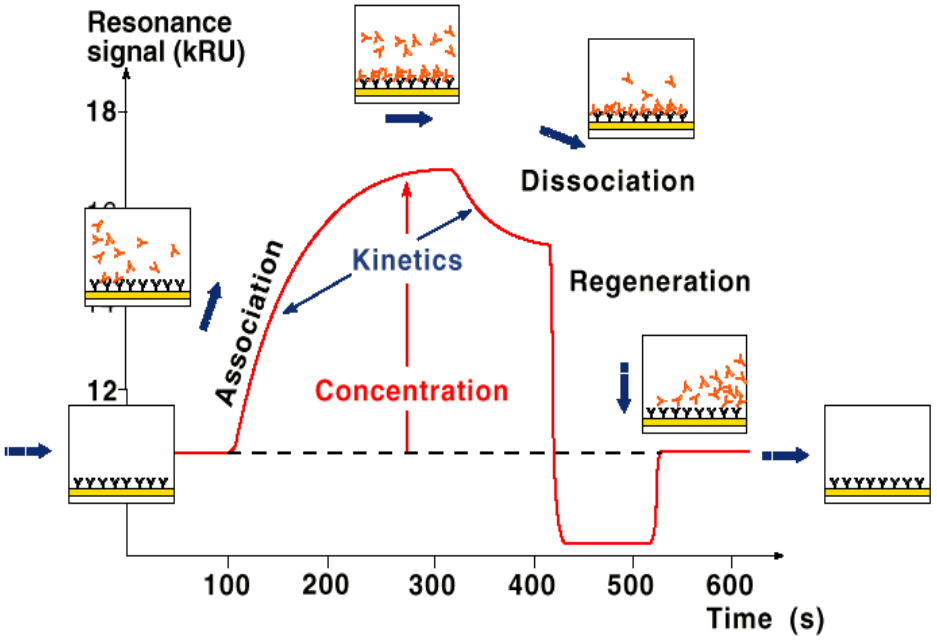

Figure 4. *Typical SPR sensorgram depicting a binding event (picture taken from: Biacore website).*

When a solution of analyte is injected in the system and arrives to the detecting zone, firstly a variation of RU due to the different refractive index of the media is sensed: this is called “bulk effect”.

The binding of the analyte to the surface is subsequently detected, generating an increase of the signal that finally reaches a plateau, when a dynamic equilibrium occurs. By stopping the injection of analyte a decrease of the signal is detected, and this decrease depends on the affinity between analyte and ligand. With SPR the strength of interaction between partners, one of which is immobilized on the surface, can be evaluated, as explained in par.3.4. Kinetic constants can also be measured by fitting the profile of binding and detachment (Fig.4).

Biacore furnishes chips with different matrixes on a golden layer, to meet the need of the researchers. For example a carboxymethylated matrix gives good performance with proteins by furnishing sites of attachment through

EDC/NHS chemistry and by minimizing aspecific binding, a relevant problem when SPR technique is used with complex matrixes.

A commonly used Biacore chip is CM5, with a carboxymethylated highly branched matrix able to furnish multiple points of attachment to the ligand molecules.

3 Materials and methods

3.1 Reagents

CM5 chips were purchased from Biacore (Sweden). Ethanolamine (Eth), 1-ethyl-3-(3-dimethylaminopropyl)carbodiimide (EDC), N-hydroxysuccinimide (NHS) were from Sigma Aldrich (UK). Synthetic Hepc-20 and Hepc-25 were purchased from AbCam (UK); peptide ligands (HBD 20-mer and RR-HBD-RR 24-mer) are custom made at Peptide 2.0 (USA). All reagents and solvents were used at analytical grade.

3.2 Peptide immobilisation on CM5 chips

The CM5 chips were activated with the coupling mixture EDC/NHS (200mM/50mM) for 75 min (75µl at 10µl/min). The peptide RR-HBD-RR was dissolved at concentration of 50µg/mL in 10mM phosphate buffer at pH 7.0 and flushed for 12 sec at 10 µL/min flow rate. Quenching of reaction was performed with 1M Eth at flow rate 10µl/min for 25 min (total volume: 25 µl) One channel was kept as reference by injecting only Eth after EDC/NHS activation.

3.3 Hepcidin measurements

Hepcidin-25 was injected simultaneously in three flow channels of the IFC (Integrated Microfluidic Cartridge). A fourth channel was kept as reference. The signal from this reference channel was subtracted from the RU response of the three channels to give the final value of RU. The chosen concentrations were: 1, 5, 10, 25, 50, 100 ng/mL. Running buffer was PBS, whose flow was kept at 2µl/min.

3.4 K_D estimation

An estimation of the affinity between the ligand RR-HBD-RR and hepcidin-25 was attempted through the use of Biacore Biasimulation software.

Curve-fitting of the experimental data enables the association and dissociation rate constants and the equilibrium dissociation constant to be determined. Of the models proposed by Biacore®, the “1:1 binding” model was the one that gave the best fit (the lowest χ2). It is the simplest model and describes the interaction between an analyte A and a ligand B as:

(1) $A + B \rightleftharpoons AB$

The association rate ka (in L/(mol s)) corresponding to the number of complexes formed per second in a molar solution of HBD and Hepc-25, is defined by the formula:

(2) $\frac{d[AB]}{dt} = k_a[A][B].$

Where [A], [B] and [AB] are the concentrations of A, B and the AB complex The dissociation rate constant kd (in s^{-1}), corresponding to the portion of the complex that dissociates in 1 s, is given by the formula:

(3) $-\frac{d[AB]}{dt} = k_d[AB]$

Association and dissociation actually occur at the same time. Furthermore, association is equal to dissociation at equilibrium, resulting in an equilibrium dissociation constant of:

(4) $K_D = \frac{[A][B]}{[AB]} = \frac{k_d}{k_a}.$

A high K_D therefore means that there is low affinity between the analyte and the ligand. By fitting the analytical expressions of the response R(t) to the R(t) curves in RU obtained in real time by the Biacore® system, it is possible to deduce these various constants, ka, kd and K_D, that characterise the binding of the analyte (Hepc-25 or Hepc-20) to the ligand (RR-HBD-RR).

4 Results and discussion

4.1 Immobilization

The maximum amount of ligand to be bound to a CM5 chips was assessed to be 5500 ± 500 RU (1000RU=1ng/mm^2). The choice was therefore to keep the ligand level around 3000 RU, to permit the analyte to sneak between the immobilized ligands avoiding the crowding of them on the chip surface.
This result was obtained with a 12µl injection at 10µl/min flow (table 1).

Table 1. *Immobilized peptide amount in three channels, expressed in RU (1000RU=1ng/mm^2).*

	Flow channel 1	Flow channel 2	Flow channel 3
Peptide (RU)	2800	3700	2250

4.2 Detection

Increasing amounts of hepcidin-25 and hepcidin-20 were injected, starting from 1 ng/mL rising up until 100 ng/mL. The response for the three channels is reported in Table 2. In this case a regenerating solution was not used during the experiment between the different injections, because the level of saturation of the surface was minimal compared to the total amount of binding sites available (<5% considering the mass of analyte compared to the mass of ligand bound).

4.3 Regeneration

Different regenerating solutions were tried with the purpose of removing bound hepcidin while not spoil or remove the ligand bound on the chip surface. Salt solutions were initially considered, with the idea of a “soft” regeneration. Increasing concentrations of NaCl were injected, and finally NaCl 500mM proved to be effective for the purpose. Other regenerating solutions (NaOH 1mM, 10mM glycine pH 2.5) had the drawback of reducing significatively the binding capacity of the ligand upon their use.

Table 2. *Hepcidin concentrations and relative instrumental response.*

Hepcidins concentration (ng/mL)	Hepc-25 media (RU)	Hepc-20 media (RU)
1	10 ± 4	5 ± 2
5	15 ± 3	10 ± 2
10	21 ± 6	14 ± 3
25	26 ± 8	16 ± 3
50	36 ± 9	14 ± 3
100	67 ± 21	5 ± 2

Graph 1 shows a sensorgram depicting the instrumental response due to different concentrations of analyte in a single flow channel. It can be noticed the proportionality of slope due to increasing concentrations of analyte. Stabilization of baseline was waited after every injection.

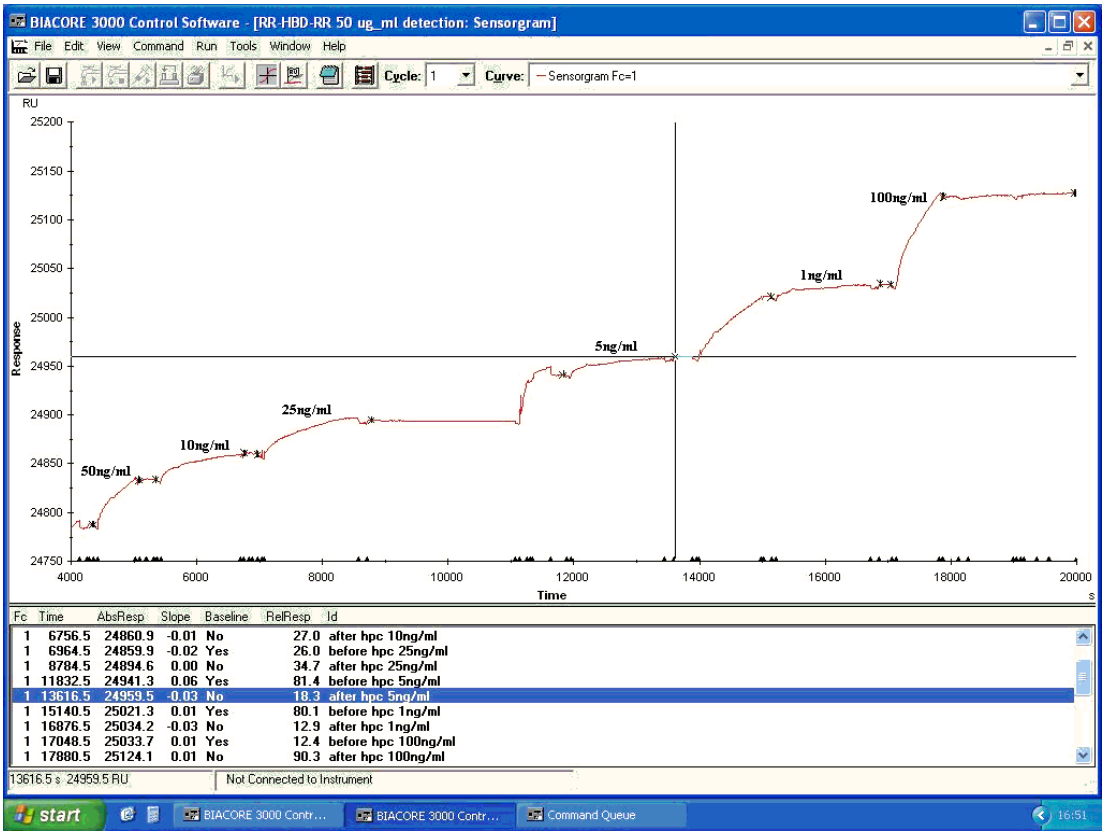

Graph 1. *Instrumental response following sequential injections of hepcidin in one of the available channels.*

The binding curves following the sequential injections of increasing concentrations of hepcidin were then superimposed to highlight the proportionality of the signal to hepcidin presence (Graph 2).

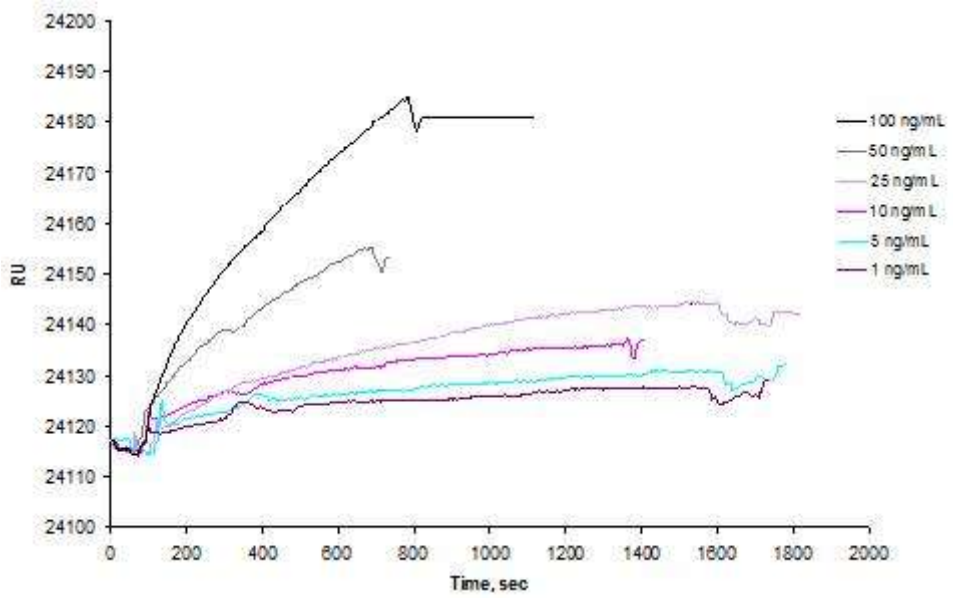

Graph 2. *Superimposition of instrumental responses due to increasing concentrations of hepcidin-25.*

The response of the system to the increasing hepcidin concentration was used to produce a calibration curve (Fig.3).

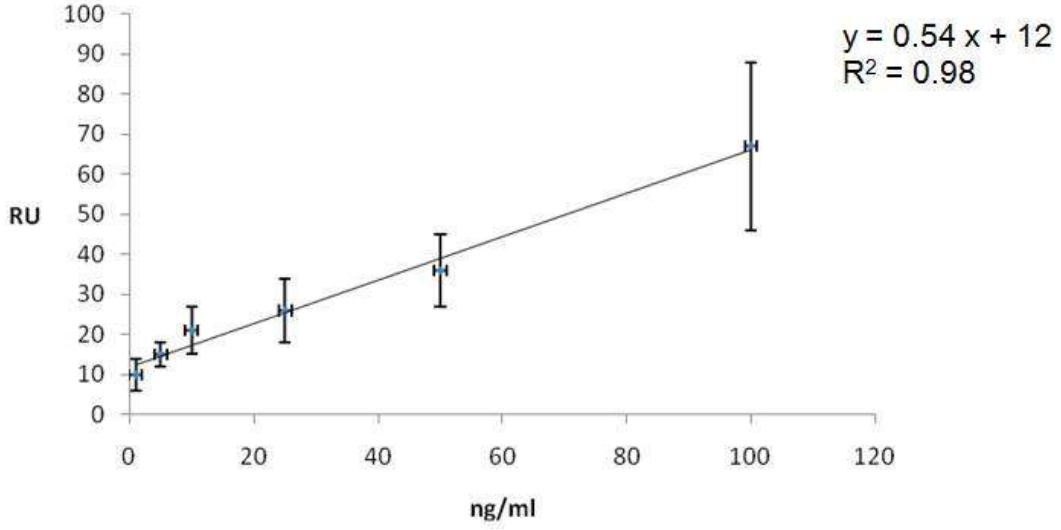

Figure 3. *Calibration curve related to increasing hepcidin-25 concentrations.*

The response of the system was linear in the range of concentrations evaluated (R^2= 0.98). Sensitivity was not excellent (slope=0.54), as it was the intermediate precision (average intra-assay CV%=29). The specificity against the competitor hepcidin-20 is however good, even though not quantified for not having reached a saturation value of concentration. Anyway the response for hepcidin-20 at the highest concentration measured (100ng/mL) was 7% than the response of hepcidin-25 (Tab.2), and this result is therefore encouraging.

4.4 K_D estimation

The evaluation of K_D with our data gave us an attempted value of K_D of $50*10^{-9}$M, consistent with previously reported data in solution. De Domenico et al, in fact, estimated the interaction of RR-HBD-RR with hepcidin to be 200nM (242). The discrepancy could be explained with the different interaction between partners in solution and when a ligand is immobilized on a surface (246).

4.5 LLOD estimation

The Lower Limit Of Detection (LLOD), considered as a signal 3 times the standard deviation of the blank (injection of simple buffer), was assessed to be 5ng/mL.

5 Conclusion

The clinical relevance of hepcidin quantification is elevated. Therefore, the measure of hepcidin in serum and urine has been standing as a valuable parameter for the differential diagnosis of physiopatological states. In iron overload syndromes the hepcidin level allowed to draw a diagnostic pre-genetic scheme for grouping patients (247). Whereas in anaemic patients, a hepcidin level threshold was proposed at 129.5 µg/L to distinguish iron deficiency in critically ill patients thus targeting to them an appropriate therapy (248). After myocardial infarction the levels of hepcidin have been observed to increase both in the ischemic and in the remote myocardium;

such up-regulation seems specifically associate with hepcidin, as other iron-regulatory molecules did not show changes, and it was hypothesized to correlate with a defense mechanism to reduce iron toxicity and thus to reduce the expansion of the infarction (249). Hepcidin expression does correlate with inflammation and increase with increased interleukin-6 (IL6) (250) and is negatively correlated with erythropoietin as shown in kidney impairment patients (251).

Our results show the ability of the HBD ligand to bind hepcidin-25, indicating the possibility of the measurement of the analyte by the use of the SPR technique.

The system showed poor binding for the competitor hepcidin-20, that is considered to be an interferent in the measurement of hepcidin-25 with ELISA (252). Regarding this aspect our system could therefore have a significative advantage.

SPR is also a rather straightforward technique: once optimized the protocol of analysis the measurement could be made from not specialized personnel. The system permitted to measure hepcidin in the pato-physiological concentration range of 5-100ng/L (1.5-35nM), with LLOD of 5ng/mL (1.5nM). This limit is higher compared to c-ELISA (0.01nM) (252) and similar to MS approaches (0.55-1-55nM for SELDI-TOF (116), 0.5nM for WCX-TOF (252), 0.75nM for MALDI-TOF (253)) but nevertheless can reveal an hepcidin deficit, that starts to be pathological at 5nM (233), (254).

One of the main problems of this technique is to overcome the aspecific binding. This is actually the main problem to solve when somebody wants to deal with complex matrixes like serum. Some proteins like albumin have an overwhelming presence in blood, that can be more than 6 orders of magnitude higher than the concentration of disease markers. Its physiological concentration is in fact assessed to be 35-50 mg/mL (255), while hepcidin concentration was evaluated to be between 5 and 350 ng/mL considering both sexes (262). The natural proceeding in the method development could therefore be the analysis of serum samples after filtration on a high MW cut-off membrane. Kobold et al, for example, obtained a recovery of hepcidin

between 95 and 100% by filtering serum samples on a 10kDa cut-off cellulose acetate membrane (256).

In conclusion, the system under development here described has the potential to permit an easy and straightforward measurement of hepcidin in body fluids, a highly desired goal of the scientific community.

Chapter 4

GENERAL CONCLUSIONS

Proteomics showed a pivotal role in the process of discovery of new potential biomarkers for diseases (286). The methods are quite well established, but an improvement at all levels are needed if we want to dig in the subproteome (proteins present in picomolar amount). Disease biomarkers are in fact often in this range of concentration in body fluids (287). The detection and quantification of established biomarkers can also take advantage of biosensing techniques, that are emerging as valuable diagnostic tools. Their inner potential lays in the possibility of develop the so-called point-of-care diagnostics, i.e. directly at the patient's bedside (288).

The use proteomics techniques, in particular 2D-PAGE, it has been here applied to discover up- or down-regulated proteins in umbilical cord serum and amniotic fluids of Intrauterine Growth Restricted (IUGR) foetuses. A total of 14 and 11 proteins were found to be modulated in IUGR umbilical cord serum and amniotic fluids respectively. In particular, proteins related to blood pressure, coagulation, immunity, oxidative stress and iron/copper metabolism were found to be involved in the IUGR pathological picture. Proteomics furnishes a snapshot of the whole protein complement in a particular stage of life and/or in a particular condition. This is however just a first step: the data obtained in this study necessitates a further validation on a larger scale and a more deepened analysis to shed light in the pathological mechanisms. The final goal is in fact to detect diagnostic biomarkers which could help a specific and early IUGR diagnosis.

The improvement of the analysis methods is at the basis of the process of biomarkers discovery. Phosphoproteomics is definitely a subject of importance to identify deranged mechanisms, being it involved in so many life processes like signalling, cell duplication and apoptosis. Altered phosphorylation pathways are in fact present in pathologies like cancer, neurodegeneration and diabetes (66).

A little step was made here in the production of Molecularly Imprinted Polymer nanoparticles (nanoMIPs) for the sequestration of phosphoproteins/phosphopeptides from complex protein mixtures. The challenge in the production of nano-MIPs is in fact to create a valid alternative to antibodies, whose cost is nowadays high and stability is low (225). The experiments allowed to definea photoactivated synthesis protocol for the production of nanoMIPs and the first experiments to evaluate the efficiency of the material towards the binding phosphotyrosine were also performed. The loading capacity of thenanoMIPs were assessed. More experiments are needed in order to extend the binding experiments to a wide range of nanoMIPs compositions (229).

The field of biosensors is definitely a sparkling one, being published so many papers in the recent years. Biosensors can give a boost in the process of biomarkers detection, having the potential of miniaturization and thus of being employed directly on the patient's bedside, when not directly implanted under the skin (288). An interesting subject for which to devise a biosensor is hepcidin, the major regulator of systemic iron homeostasis in mammals. Its quantification could be useful in the deepening the knowledge of iron unbalance-related diseases, in stratifying patients but also in monitoring a disease progression (290).

The detection and quantification of hepcidin-25 was here attempted with the employment of Surface Plasmon Resonance as biosensing technique. A protocol for chip preparation was set and a calibration curve in the physiopathological range of concentrations was made. Moreover, the affinity between hepcidin-25 and its binding domain on ferroportin (HBD) was evaluated, assessing the negligible binding of HBD for the competitor hepcidin-20. This part of experiments should be considered as preliminary, and it has to be extended to the analysis of real samples, with the intention of selecting hepcidin as primary analyte to be measured, overcoming the hurdle of aspecific binding, in particular of highly abundant proteins of serum, like albumin (291).

In conclusion, the field of biomarkers discovery and quantification was here explored on three research topics. The results obtained are some steps on the path. More steps need to be taken in order to deepen our knowledge of these subjects in the near future.

BIBLIOGRAPHY

1. **Gardosi J.** *Horm Res.* 2006, Vol. 65: 15-18.
2. **Mandruzzato G, Antsaklis A, Botet F, Chervenak FA, Figueras F, Grunebaum A, Puerto B, Skupski D, Stanojevic M.** *J Perinat Med.* 2008, Vol. 36: 277-281.
3. **Breeze ACG, Lees CC.** Prediction and perinatal outcomes of fetal restriction. *Seminars in Fetal and Neonatal Medicine.* 2007, Vol. 12- 383,397.
4. **Bernstein G.** *American Journal Obstetrics Gynaecology.* 2000.
5. **Hui L, Challis D.** *Best Practice & Research Clinical Obstetrics and Gynaecology.* 2008, Vol. 22: 139-158.
6. **Loue S.** Forensic epidemiology. *Jones and Bartlett publishers 2010 Washington USA.* Vol. ISBN 978-0-7637-3849-5.
7. **Jauniaux E, Jurkovic D, Gulbis B, Collins W P, Zaidi J, Campbell S.** *Am J Obstet Gynecol.* 1994, Vol. 170: 1365–1369.
8. **Kolialexi A, Mavrou A, Tsangaris GT.** *Prot Clin Applic.* 2007, Vol. 1: 853–860.
9. **Brenner.** *Thromb. Res.* 2004, Vol. 114: 409–414.
10. **Vuadens F, Benay C, Crettaz D, Gallot D, Sapin V, Schneider P, Bienvenut WV, Lemery D, Quadroni M, Dastugue B, Tissot JD.** *Proteomics.* 2003, Vol. 3, 1521–1525.
11. **Amarilyo G, Oren A, Mimouni FB, Ochshorn Y, Deutsch V, Mandel D.** *INPG J Perinatol.* 2010, Vol. 1-3.
12. **Neta GI, von Ehrenstein OS, Goldman LR, Lum K, Sundaram R, Andrews W, Zhang J.** *Am J Epidemiol.* 2010, Vol. 171: 859-867.
13. **Gazzolo D, et al.** *Crit Care Med.* 2004, Vol. 32: 131-136.
14. **Hellstrom-Westas L, Rosen I, Svenningsen NW.** *Arch Dis Child.* 1995, Vol. 72: 34–38.
15. **Huang CC, Wang ST, Chang YC,.** *N Engl J Med.* 1999, Vol. 341: 328–335.
16. **Harry JL, Wilkins M R, Herbert B R, Packer N H, Gooley A, Williams K.** *Electrophoresis.* 2000, Vol. 21: 1071-1081.
17. **Neuhoff V, Arold N , Taube D, Ehrhardt W.** *Electrophoresis.* 1988, Vol. 9: 255-262.
18. **Yan JX, Harry RA, Spibey C, Dunn MJ.** *Electrophoresis.* 2000, Vol. 21: 3657-3665.
19. **Shevchenko A, Wilm M, Vorm O, Mann M.** *Anal Chem.* 1996, Vol. 68: 850-858.
20. **Hunt SMN, Thomas MR ,Sebastian LT , Pedersen SK, Harcourt RL, Sloane AJ, Wilkins MR.** *Journal of Proteome Research.* 2005, Vol. 4: 809-819.
21. **Chen, Chung-Hsuan.** *Analytica Chimica Acta.* 2008, Vol. 624: 16–36 .
22. **Bairoch A, Apweiler R.** *Nucleic Acids Res.* 2000, Vol. 28: 45-48.
23. **Cecconi D, Zamo A, Parisi A, Bianchi E.** *J Proteome Res.* 2008, Vol. 7: 2670-2680.
24. **Bellart J, Gilabert R, Fontcuberta J, Carreras E.** *Am J Perinatol.* 1998, Vol. 15: 81-85.
25. **Benedetto C, Marozio L, Tavella A M, Salton L.** *Ann N Y Acad Sci.* 2010, Vol. 1205: 106-117.
26. **Ducloy-Bouthors AS.** *Ann Fr Anesth Reanim.* 2010, Vol. 29: 121-134.
27. **Persson B L, Holmberg L, Astedt B, Nilsson IM.** *Acta Obstet Gynecol Scand.* 1982, Vol. 61: 455-459.
28. **Yu YH, Shen L Y, Zou H, Wang Z J, Gong SP,.** *J Matern Fetal Neonatal Med.* 2010, Vol. 23: 980-987.
29. **Yu YH, Shen L Y, Zhong M, Zhang Y.** *Zhonghua Fu Chan Ke Za Zhi.* 2004, Vol. 39, 793-796.
30. **Camilleri R S, Peebles D, Portmann C, Everington T, Cohen H.** *Blood Coagul Fibrinolysis.* 2004, Vol. 15: 139-147.
31. **von Tempelhoff G F, Velten E, Yilmaz A, Hommel G.** *Clin Hemorheol Microcirc.* 2009, Vol. 42: 127-139.
32. **Cvirn G, Gallistl S, Koestenberger M, Kutschera J.** *Thromb Res.* 2002, Vol. 105: 433-439.

33. **Goldenberg RL, Tamura T, Cliver S P, Cutter GR.** *Obstet Gynecol.* 1991, Vol. 78: 594-599.
34. **Cliver SP, Goldenberg RL, Neel N R, Tamura T.** *Early Hum Dev.* 1993, Vol. 33: 201-206.
35. **Lipinski S, Bremer L, Lammers T, Thieme F.** *Hamostaseologie.* 2010, Vol. 31, Epub ahead of print.
36. **Girardi G.** *Immunol Invest.* 2008, Vol. 37: 645-659.
37. **Richani K, Soto E, Romero R, Espinoza J.** *J Matern Fetal Neonatal Med.* 2005, Vol. 17: 239-245.
38. **Tincani A, Cavazzana I, Ziglioli T, Lojacono A.** *Clin Rev Allergy Immunol.* 2010, Vol. 39: 153-159.
39. **Labarrere C, Manni J, Salas P, Althabe O.** *Am J Reprod Immunol Microbiol.* 1985, Vol. 8: 87-93.
40. **Labarrere CA, Althabe OH.** *Am J Reprod Immunol Microbiol.* 1986, Vol. 12: 4-6.
41. **Lynch AM, Gibbs RS, Murphy JR, Giclas PC.** *Obstet Gynecol.* 2010, Vol. 117: 75-83.
42. **Xia Y, Wen HY, Kellems RE.** *J Biol Chem.* 2002, Vol. 277: 24601-24608.
43. **Zohdi V, Moritz KM, Bubb KJ, Cock ML.** *Am J Physiol Regul Integr Comp Physiol.* 2007, Vol. 293: R1267-1273.
44. **Grigore D, Ojeda NB, Robertson EB, Dawson AS.** *Am J Physiol Regul Integr Comp Physiol.* 2007, Vol. 293: R804-811.
45. **Zhang XQ, Varner M, Dizon-Townson D, Song F, Ward K.** *Obstet Gynecol.* 2003, Vol. 101: 237-242.
46. **Zhang X, Ye J, Jensen ON, Roepstorff P.** *Molecular and Cellular Proteomics.* 2007, Vol. 6: 2032–2042.
47. **Bouba I, Makrydimas G, Kalaitzidis R, Lolis DE.** *Eur J Obstet Gynecol Reprod Biol.* 2003, Vol. 110: 8-11.
48. **Blumenstein M, Prakash R, Cooper G J, North R A.** *Reprod Sci.* 2009, Vol. 16, 1144-1152.
49. **Salas SP, Rosso P, Espinoza R, Robert JA.** *Obstet Gynecol.* 1993, Vol. 81: 1029-1033.
50. **Salas SP, Giacaman A, Romero W, Downey P.** *Hypertension.* 2007, Vol. 50: 773-779.
51. **Gambling L, Danzeisen R, Fosset C, Andersen HS.** *J Nutr.* 2003, Vol. 133: 1554S-1556S.
52. **Andersen HS, Gambling L, Holtrop G, McArdle HJ.** *Br J Nutr.* 2007, Vol. 97: 239-246.
53. **Mando C, Tabano S, Colapietro P, Pileri P.** *Placenta.* 2010, Vol. 32: 44-50.
54. **Soubasi V, Petridou S, Sarafidis K, Tsantali C.** *Diabetes Metab.* 2010, Vol. 36: 58-63.
55. **Wu Y, Sakamoto H, Kanenishi K, Li J.** *Clin Chim Acta.* 2003, Vol. 332: 103-110.
56. **Zadrozna M, Gawlik M, Nowak B, Marcinek A,.** *J Trace Elem Med Biol* . 2009, Vol. 23, 144-148.
57. **Salimonu LS.** *Afr J Med Med Sci.* 1992, Vol. 21: 55-59.
58. **Airede AI.** *Early Hum Dev.* 1998, Vol. 52: 199-210.
59. **Mann M, Jensen ON.** *Nature Biotechnology.* 2003, Vol. 21: 255-261.
60. **Baumann M, Meri S.** *Expert Rev Proteomics.* 2004, Vol. 1: 207-217.
61. **Collins MO, Lu Yu, Choudhary JS.** *Proteomics.* 2007, Vol. 7: 2751–2768.
62. **Graves J, Krebs D.** *Pharmacology & Therapeutics.* 1999, Vol. 82: 111–121.
63. **Hunter T.** *Cell.* 2000, Vol. 100: 113–127.
64. **Sickmann A, Meyer HE.** *Proteomics.* 2001, Vol. 1: 200-206.
65. **Raggiaschi R, Gotta S, Terstappen GC.** *Bioscience Reports.* 2005, Vol. 25: 33-44.
66. **Thingholm TE, Jensen ON, Larsen MR.** *Phospho-Proteomics – Methods and Protocols, Humana Press, Totowa, NJ.* 2009, Vol. Chapter4:47–56.
67. **Nelson L, Cox M.** *Lehninger principles of biochemistry, WHFreeman.* 2004, Vol. 4th edition.
68. **Clevenger CV, et al.** *American Journal of Pathology.* 2004, Vol. 165: 1449–1460.

69. **Zhu X, Lee H, Raina AK, Perry G, Smith RD.** *Neurosignals.* 2002, Vol. 11: 270–281.
70. **Grønborg M, Kristiansen TZ, Stensballe A, Jensen ON, Pandey A.** *Molecular and Cellular Proteimics.* 2002, Vol. 1: 517-527.
71. **Kersten B, Agrawal GK, Iwahashi H, Rakwal R.** Plant phosphoproteomics: A long road ahead. *Proteomics.* 2006, Vol. 6: 5517–5528.
72. **Manning G, Whyte DB, Martinez R, Hunter T, Sudarsanam S.** *Human Genome Science.* 2002, Vol. 298: 1912–1934.
73. **Twyman RM.** *Principles of proteomics, BIOS Scientific Publishers, Taylor and Francis Group* . 2004, Vol. pp273-275.
74. **Venter JC, et al.** *Science.* 2001, Vol. 291: 1304–1351.
75. **Zhang H, Zha X, Tan Y, Hornbeck PV, Mastrangelo AJ, Alessi DR, Polakiewicz RD, Comb MJ.** *Journal of Biological Chemistry.* 2002 , Vol. 277: 39379-39387.
76. **Thingholm TE, Larsen MR, Ingrell CR, Kassem M, Jensen ON.** *Journal of Proteome Research.* 2008, Vol. 7: 3304–3313.
77. **Eymann C, Becher D, Bernhardt J, Gronau K, Klutzny A, Hecker M.** *Proteomics.* 2007, Vol. 7: 3509–3526.
78. **Guy GR, Philip R, Tan YH.** *Electrophoresis.* 1994, Vol. 15: 417–440.
79. **Steen H, Kuster B, Fernandez M, Pandey A, Mann M.** *Journal of Biological Chemistry.* 2001, Vol. 277: 1031–1039.
80. **Hu VW, Heikka DS, Dieffenbach PB, Ha L.** *FASEB J.* 2001, Vol. 15: 1562–1568.
81. **Graham ME, Anggono V, Bache N, Larsen MR, Craft GE, Robinson PJ.** *Journal of Biological Chemistry.* 2007, Vol. 282: 14695–14707.
82. **Magi B, Bini L, Marzocchi B, Liberatori S, Raggiaschi R, Pallini V.** *Methods in Molecular Biology.* 1999, Vol. 112: 431–443.
83. **Schmidt SR, Schweikart F, Andersson ME.** *Journal of Chromatography B.* 2007, Vol. 849: 154-162.
84. **Kaufmann H, Bailey JE, Fussenegger M.** *Proteomics.* 2001, Vol. 1: 194–199.
85. **Steinberg TH, Agnew BJ, Gee KR, Leung WY, Goodman T, Schulenberg B, Hendrickson J, Beechem JM, Haugland RP, Patton WF.** *Proteomics.* 2003, Vol. 3: 1128–1144.
86. **Schulenberg B, Hendrickson J, Beechem JM, Haugland RP, Patton WF.** *Proteomics.* 2003, Vol. 3: 1128–1144.
87. **Kumar Y, Khachane A, Belwal M, Das S, Somsundaram K, Tatu U.** *Proteomics.* 2004, Vol. 4: 1672-1683.
88. **Yamagata A, Kristensen DB, Takeda Y, Miyamoto Y, Okada K, Inamatsu M, Yoshizato K.** *Proteomics.* 2002, Vol. 2 : 1267–1276.
89. **Bodenmiller B, Mueller LN, Mueller M, Domon B, Aebersold R.** *Nature Methods.* 2007, Vol. 4: 231–237.
90. **Stannard C, Soskic V, Godovac-Zimmermann J.** *Biochemistry.* 2003, Vol. 42: 13919–13928.
91. **Ong SE, Blagoev B, Kratchmarova I, Kristensen DB, Steen H, Pandey A, Mann M.** *Molecular and Cellular Proteomics.* 2002, Vol. 1: 376–386.
92. **Blagoev B, Ong SE, Kratchmarova I, Mann M.** *Nature Biotechnology.* 2004, Vol. 22:1139–1145.
93. **Porath J, Carlsson J, Olsson I, Belfrage G.** *Nature.* 1975, Vol. 258: 598–599.
94. **Feng S, Ye M, Zhou H, Jiang X, Jiang X, Zou H, Gong B.** *Molecular and Cellular Proteomics.* 2007, Vol. 6: 1656–1665.
95. **Posewitz MC, Tempst P.** *Chemistry.* 1999, Vol. 71: 2883–2892.
96. **Ficarro SB, Mc Cleland ML, Stukenberg PT, Burke DJ, Ross MM, Shabanowitz J, Hunt DF, White FM.** *Nature Biotechnology.* 2002, Vol. 20: 301–400.
97. **Collins MO, Yu L, Coba MP, Husi H, Campuzano I, Blackstock WP, Choudhary JS, Grant SG.** *Journal of Biological Chemistry.* 2005, Vol. 280: 5972–5982.

98. **Ficarro S, Chertihin O, Westbrook VA, White Shabanowitz J, Herr JC, Hunt DF, Visconti PE.** *Journal of Biological Chemistry.* 2003, Vol. 278: 11579-11589.
99. **Trinidad JC, Specht CG, Thalhammer A, Schoepfer R, Burlingame AL.** *Molecular and Cellular Proteomics.* 2006, Vol. 5: 914–922 .
100. **Nühse TS, Stensballe A, Jensen ON, Peck SC.** *Molecular and Cellular Proteomics.* 2003, Vol. 2: 1234– 1243.
101. **Villen J, Beausoleil SA, Gerber SA, Gygi SP.** *Proceedings National Academy of Science USA.* 2007, Vol. 104: 1488–1493.
102. **Leitner A.** *Trends in Analytical Chemistry.* 2010, Vol. 29: 177-185 .
103. **Ikeguchi Y, Nakamura H.** *Analytical Sciences.* 2000, Vol. 16: 541-543.
104. **Pinkse MW, Uitto PM, Hilhorst MJ, Ooms B, Heck AJ.** *Analytical Chemistry.* 2004, Vol. 76: 3935–3943.
105. **Jensen SS, Larsen MR.** *Rapid Communication in Mass Spectrometry.* 2007, Vol. 21: 3635–3645.
106. **Olsen JV, Macek B, Lange O, Makarov A, Horning S, Mann M.** *Nature Methods.* 2007, Vol. 4: 709–712.
107. **Kweon HK, Hakansson K.** *Analytical Chemistry.* 2006, Vol. 78: 1743–1749.
108. **Sugiyama N, Nakagami H, Mochida K, Daudi A, Tomita M, Shirasu K, Ishihama Y.** *Molecular Systems Biology.* 2008, Vol. 4.
109. **Thingholm TE, Jensen ON, Robinson PJ, Larsen MR.** *Molecular and Cellular Proteomics.* 2008, Vol. 7: 661-671.
110. **Chang Ck, Wu CC, Wang YS , Chang HC.** *Analytical Chemistry.* 2008, Vol. 80: 3791–3797.
111. **Chen CT, Chen YC.** *Analysis.* 2005, Vol. 77: 5912-5919.
112. **Schürenberg M, Dreisewerd K, Hillenkamp F.** *Analytical Chemistry.* 1999, Vol. 71: 221-229.
113. **Qi D, Lu J, Deng C, Zhang X.** *Journal of Physical Chemistry.* 2009, Vol. 113: 15854–15861.
114. **Reynolds EC, Riley PF, Adamson NJ.** *Analytical Biochemistry.* 1994, Vol. 217: 277–284.
115. **Xia QW, Cheng D, Duong DM, Gearing M, Lah JJ, Levey AI, Peng J.** *Journal of Proteome Research.* 2008, Vol. 7: 2845–2851.
116. **Swinkels D, et al.** *PLoS ONE.* 2008, Vol. 3:e2706.
117. **Zhai B, Villen J, Beausoleil SA, Mintseris J, Gygi SP.** *Journal of Proteome Research.* 2008 , Vol. 7: 1675-1682.
118. **Olsen JV, Blagoev B, Gnad F, Macek B, Kumar C, Mortensen P, Mann M.** *Cell.* 2006, Vol. 127: 635–648.
119. **Ficarro S, Parikh JR, Blank NC, Marto JA.** *Anal Chem.* 2008, Vol. 80: 4606–4613 .
120. **Beausoleil SA, Jedrychowski M, Schwartz D, Elias JE, Villen J, Li J, Cohn MA, Cantley LC, Gygi SP.** *Proceedings National Academy Science USA.* 2004, Vol. 101: 560-570.
121. **Mohammed S, Heck AJR.** *Current Opinion in Biotechnology.* 2011, Vol. 22: 9–16.
122. **Han G, Ye M, Zhou H, Jiang X, Tian R, Wan D, Zou H, Gu A.** *Proteomics.* 2008, Vol. 8: 1346-1361.
123. **McNulty DE, Annan RS.** *Molecular and Cellular Proteomics.* 2008, Vol. 7: 971-980.
124. **Albuquerque CP, Smolka MB, Payne SH, Bafna V, Eng J, Zhou H.** *Molecular and Cellular Proteomics.* 2008, Vol. 7: 1389–1396.
125. **Bodenmiller B, Mueller LN, Pedrioli PG, Pflieger D, Jünger MA, Eng JK, Aebersold R, Tao WA.** *Molecular Biosystems.* 2007, Vol. 3: 275-286.
126. **Tao WA, Wollscheid B, O'Brien, R Eng, JK Li XJ, Bodenmiller B, Watts JD, Hood L, Aebersold R.** *Nature Methods.* 2005, Vol. 2: 591-598.
127. **Rush, J, Moritz, A, Lee, KA, Guo, A, Goss, VL, Spek, EJ, Zhang, H, Xiang-Ming Zha, Polakiewicz RD, Comb MJ.** *Nature BiotechnologY.* 2004, Vol. 23.

128. **Heibeck TH, Shi-Jian Ding, Opresko LK,Tolmachev AV, Monroe ME, Camp II DG, Smith RD, Wiley H S, Wei-Jun Qian.** *Cells Journal of Proteome Research.* 2009, Vol. 8: 3852-3861.
129. **Rigbolt KT, Prokhorova TA, Akimov V, Henningsen J, Johansen PT, Kratchmarova I, Kassem M, Mann M, Olsen JV, Blagoev B.** *Science Signaling.* 2011, Vol. 4: rs3.
130. **Zarei M, Sprenger A, Metzger F, Gretzmeier C, Dengjel J.** *Journal of Proteome Research (in press).* 2011.
131. **Zhang K.** *Analytical Biochemistry.* 2006, Vol. 357: 225–231.
132. **Nühse TS, Stensballe A, Jensen ON, Peck SC.** *The Plant Cell.* 2004, Vol. 16: 2394-2405.
133. **Huttlin EL, Jedrychowski MP, Elias JE, Goswami T, Rad R, Beausoleil SA, Villen J, Haas W, Sowa ME, Gygi L.** *Cell.* 2010, Vol. 143: 1174–1189.
134. **Alpert AJ.** *Journal of Chromatography.* 1990, Vol. 499: 177–196.
135. **Alpert AJ, et al.** *Analytical Chemistry.* 2008, Vol. 80: 62-76.
136. **Chen X, Wu D, Zhao Y, Wong BHC, Guo L.** *Journal of Chromatography B.* 2011, Vol. 879: 25-34.
137. **Tiselius A, Hjerten S, Levin O.** *Archives of biochemistry and biophysics.* 1956, Vol. 65: 32–155.
138. **Mamone G, Picariello G, Ferranti P, Addeo F.** *Proteomics.* 2010, Vol. 10: 380–393.
139. **Helling S, Shinde, S Brosseron, F Schnabel, A Müller, T Meyer, HE Marcus K, Sellergren B.** *Analytical Chemistry.* 2011, Vol. 83: 1862–1865.
140. **Nishino H, Huang CS, Shea KJ.** *Angewandte Chemie International Edition.* 2006, Vol. 45: 2392-2396.
141. **Jaffe H.** *Biochemistry.* 1998, Vol. 37: 16211–16224.
142. **Oda Y, Nagasu T, Chait BT.** *Nature Biotechnology.* 2001, Vol. 19: 379–382.
143. **Zhou H, Watts JD, Aebersold R.** *Nature Biotechnology.* 2001, Vol. 19: 375–378.
144. **Knight ZA, Schilling B, Row RH, Kenski DM, Gibson BW, Shokat KM.** *Nature Biotechnology.* 2003, Vol. 21: 1047–1054.
145. **Goto H, Inagaki M.** *Nature Protocols.* 2007, Vol. 2: 2574– 2581.
146. **Domon RB, Aebersold R.** *Science.* 2006, Vol. 312: 212–217.
147. **Biemann K.** *Biomedical Environmental Mass Spectrometry.* 1988, Vol. 16: 99–111.
148. **Roepstorff P, Fohlman J.** *Biomedical Mass Spectrometry.* 1984, Vol. 11: 601.
149. **Perkins DN, Pappin DJ, Creasy DM, Cottrell JS.** *Electrophoresis.* 1999, Vol. 20: 3551–3567.
150. **Ducret A, Van Oostveen, I Eng, JK Yates JRIII, Aebersold R.** *Protein Science.* 1998, Vol. 7: 706–719.
151. **Larsen MR, Thingholm TE, Jensen ON, Roepstorff P, Jorgensen TJ.** *Molecular and Cellular Proteomics.* 2005, Vol. 4: 873–886.
152. **Reinders J, Sickmann A.** *Proteomics.* 2005, Vol. 5: 4052–4061.
153. **Steen H, Kuster B, Mann M.** *Journal Mass Spectrometry.* 2001, Vol. 367: 782–790.
154. **Zubarev RA, Kelleher NL , McLafferty FW.** *Journal of American Chemical Society.* 1998, Vol. 120: 3265–3266.
155. **Kleinnijenhuis AJ, Kjeldsen F, Kallipolitis B, Haselmann KF, Jensen ON.** *Analytical Chemistry.* 2007, Vol. 79: 7450–7456.
156. **Schroeder MJ, Webb DJ, Shabanowitz J, Horwitz AF, Hunt DF.** *Journal of Proteome Research.* 2005, Vol. 4: 1832–184.
157. **Syka JE, Coon JJ, Schroeder MJ, Shabanowitz J, Hunt DF.** *Proceedings National Academy Science USA.* 2004, Vol. 101: 9528–9533.
158. **Molina H, Horn DM, Tang N, Mathivanan S, Pandey A.** *Proceedings National Academy Science USA.* 2007, Vol. 104: 2199–2204.
159. **Kjeldsen F, Giessing AM, Ingrell CR, Jensen ON.** *Analytical Chemistry.* 2007, Vol. 79: 9243-9252.

160. **Kim S, Mischerikow N, Bandeira N, Navarro NJD, Wich L Mohammed, S Heck AJR, Pevzner PA.** *Molecular and Cellular Proteomics.* 2010, Vol. 9: 2840-2852.
161. **Bantscheff M, Schirle M, Sweetman G, Rick Kuster B.** *Analytical Bioanalytical Chemistry.* 2007, Vol. 389: 1017–1031.
162. **Oda Y, Huang K, Cross FR, Cowburn D, Chait BT.** *Proceedings National Academy Science USA.* 1999, Vol. 96: 6591–6596.
163. **Ibarrola N, Kalume DE, Gronborg M, Iwahori A , Pandey A.** *Analytical Chemistry.* 2003, Vol. 75: 6043–6049.
164. **Goss VL, Lee KA, Moritz A, Nardone, J Spek, EJ MacNeill, J Rush, J Comb, MJ Polakiewicz.** *kinase Blood.* 2006, Vol. 107: 4888–4897.
165. **Olsen JV, Vermeulen M, Santamaria A, Kumar C, Miller ML, Jensen LJ, Gnad F, Cox J, Jensen TS, Nigg EA, Brunak S, Mann M.** *Science Signaling.* 2010, Vol. 3: p ra3.
166. **Dengjel J, Akimov V, Olsen JV, Bunkenborg J, Mann M, Blagoev B, Andersen JS.** *Nature Biotechnology.* 2007, Vol. 25: 566–568.
167. **Schmidt A, Kellermann J, Lottspeich F.** *Proteomics.* 2005, Vol. 5: 4–15.
168. **Ross PL, Huang YN, Marchese JN, Williamson B, Parker K, Hattan S, Khainovski N, Pillai S, Dey S, Daniels S, Purkayastha S, Juhasz P, Martin S, Bartlet-Jones M, He F, Jacobson A, Pappin DJ.** *Molecular and Cellular Proteomics.* 2005, Vol. 3: 1154–1169.
169. **Thompson A, Schafer J, Kuhn K, Kienle S, Schwarz J, Schmidt G, Neumann T, Johnstone R, Mohammed AK, Hamon C.** *Analytical Chemistry.* 2003, Vol. 75: 1895–1904.
170. **Zhang X, Jin QK, Carr SA, Annan RS.** *Rapid Communication Mass Spectrometry.* 2002, Vol. 16: 232-2332.
171. **Wolf-Yadlin A, Hautaniemi S, Lauffenburger DA, White FM.** *Proceedings National Academy of Science USA.* 2007, Vol. 104: 5860–5865.
172. **Goodlett DR, Keller A, Watts JD, Newitt R, Yi EC, von Haller P, Aebersold R, Kolker E.** *Rapid Communication Mass Spectrometry.* 2001, Vol. 15: 1214–1221.
173. **Gerber SA, Rush J, Stemman O, Kirschner MW, Gygi SP.** *Proceedings National Academy of Science USA.* 2003, Vol. 100: 6940–6945.
174. **Pan S, Zhang H, Rush J, Eng J, Zhang N, Patterson D, Comb MJ, Aebersold R.** *Molecular and Cellular Proteomics.* 2005, Vol. 4: 182–190.
175. **Kirkpatrick DS, Gerber SA, Gygi SP.** *Methods.* 2005, Vol. 35: 265–273.
176. **Bondarenko PV, Chelius D, Shaler.** *Analytical Chemistry.* 2002, Vol. 74: 4741-4749.
177. **Wang G, Wu WW, Zeng W, Chou CL, Shen RF.** *Journal of Proteome Research.* 2006, Vol. 5: 1214–1223.
178. **Steen H, Jebanathirajah JA, Springer M, Kirschner MW.** *Proceedings National Academy of Science USA.* 2005, Vol. 102: 3948–3953.
179. **Rappsilber J, Ryder U, Lamond AI, Mann M.** *Genome Research.* 2002, Vol. 12: 1231–1245.
180. **Lu P, Vogel C, Wang R, Yao X, Marcotte EM.** *Nature Biotechnology.* 2007, Vol. 25: 117–124.
181. **Belluco C, Mammano E, Petricoin E, Prevedello L, Calvert V, Liotta L, Nitti D, Lise M.** *Clinica Chimica Acta.* 2005, Vol. 357: 99-111.
182. **Schmelzle K, White FM.** *Current Opinion in Biotechnology.* 2006, Vol. 17: 406-414.
183. **Gembitsky DS, Lawlor K, Jacovina A, Yaneva M & Tempst P.** *Molecular and Cellular Proteomics.* 2004, Vol. 3: 1102-1118.
184. **Khan IH, Mendoza S, Rhyne P, Ziman M, Tuscano J, Eisinger D, Kung HJ, Luciw PA.** *Molecular and Cellular Proteomics.* 2006, Vol. 5: 758-768.
185. **Sachs K, Perez O, Pe'er D, Lauffenburger DA, Nolan,GP.** *Science.* 2005, Vol. 308: 523-529.
186. **Jones RB, Gordus A, Krall JA, Mac Beath G.** *Nature.* 2006, Vol. 439: 168-174.
187. **Yaoi T, Chamnongpol S, Jiang X, Li X.** *Molecular Cellular Proteomics.* 2006, Vol. 5: 959-968.

188. **Ptacek J, Devgan G, Michaud G, Zhu H, Zhu X, Fasolo J, Guo H, Jona G, Breitkreutz A, Sopko R, Stern DF, De Virgilio C, Tyers M, Andrews B, Gerstein M, Schweitzer B, Predki PF, Snyder M.** *Nature.* 2005, Vol. 438: 679–684.
189. **Hornbeck PV, Chabra I, Kornhauser JM, Skrzypek E, Zhang B.** *Proteomics.* 2004, Vol. 4: 1551–1561 .
190. **Gnad F, Ren S, Cox J, Olsen JV, Macek B, Oroshi M, Mann M.** *Genome Biology.* 2007, Vol. 8: R250.
191. **Wulff G.** *Reactive Polymers.* 1991, Vol. 15: 233.
192. **Sellergren B, Lepistö M, Mosbach K.** *Reactive Polymers.* 1989, Vol. 10: 306-307.
193. **Mosbach K.** *Trends Biochem Sci.* 1994, Vol. 19: 9.
194. **Mosbach M, Zimmermann H, Laurell JN, Csöregi E, Schuhmann W.** *Biosensors and Bioelectronics.* 2001, Vol. 16: 827-837.
195. **Piletsky SA, Piletska EV, Bossi AM, Karim K, Anthony PL, Turner PF.** *Biosensors and Bioelectronics.* 2001, Vol. 16: 701-707.
196. **Cormack PAG, Haupt K,.** *Mosbach K Encyclopedia of Separation Science.* 2007, Vol. 288-296.
197. **Kempe M, Mosbach K.** *J Chromatogr A.* 1994, Vol. 664-276 .
198. **Ye L, Mosbach K,.** *Reactive & Functional Polymers* . 2001, Vol. 48: 149–157.
199. **Vlatakis G, Andersson LI, Miiller R, Mosbach K.** *Nature (London).* 1993, Vol. 361-645.
200. **Leonhardt A, Mosbach K.** *Reactive Polymers, Ion Exchangers, Sorbents.* 1987, Vol. 6: 285-290.
201. **Wulff G.** *Studies in Surface Science and Catalysis.* 2002, Vol. 141: 35-44.
202. **Sellergren B, Allender CJ,.** *Advanced Drug Delivery Reviews.* 2005, Vol. 57: 1733-1741.
203. **Cunliffe D, Kirby A, Cameron A,.** *Advanced Drug Delivery Reviews.* 2005, Vol. 57: 1836-1853.
204. **Bossi A, Bonini, F, Turner APF, et al.** *Biosensors and Bioelectronics.* 2007, Vol. 22: 1131-1137.
205. **Cecìlia A, Roque A, Christopher R, Lowe G.** *Biotechnology & Bioengineering.* 2005, Vol. 91: 546-555.
206. **Rachkov A, Minoura N.** *Biochimica et Biophysica Acta* . 2001, Vol. 1544: 255-266.
207. **Kempe M, Mosbach K.** *Journal of Chromatography A.* 1995, Vol. 694: 3-13.
208. **Kempe M.** *Letters in peptide science.* 2000, Vol. 7: 27-33.
209. **Klein JU, Whitcombe MJ, Mulholland F, Vulfson EN.** *Angew Chem Int Ed.* 1999, Vol. 38: No 13/14.
210. **Hart BR, Shea KJ.** *Journal of the American Chemical Society.* 2001, Vol. 123: 2072-2073.
211. **Shi HQ, Tsai WB, Garrison MD, et al.** *Nature.* 1999, Vol. 398: 593-597.
212. **Bossi A, Piletsky SA, Piletska EV, et al.** *Analytical Chemistry.* 2001, Vol. 73, 5281-5286.
213. **Shiomi T, Matsui M, Mizukami F, et al.** *Biomaterials.* 2005, Vol. 26: 5564-5571.
214. **Glad M, Norrlöw O, Sellergren B, Siegbahn N, Mosbach K.** *Journal of Chromatography A.* 1985, Vol. 347: 11-23.
215. **Lulka MF, Iqbal SS, Chambers JP, Valdes ER, Thompson RG, Goode MT, Valdes JJ.** *Materials Science and Engineering: C.* 2000, Vol. 11: 101-105.
216. **Valdes TI, Ciridon W , Ratner BD, Bryers JD, Biomaterials.** 2008, Vol. 29: 1356-1366.
217. **Bossi A, Piletsky SA, Piletska EV, et al.** *Analytical Chemistry.* 2000, Vol. 72: 4296-4300.
218. **Rick J, Chou T-C,.** *Biosensors and Bioelectronics.* 2006, Vol. 22: 329-335.
219. **Hjertén S, Liao JL, Zhang R.** *Journal of Chromatography A.* 1989, Vol. 473: 273-275.

220. **Chao GT, Qian ZY, Huang MJ, et al.** *J of biom materials research Part A.* 2008, Vol. 85A: 36-46.
221. **Ou SH, Wu MC, Chou TC, Liu CC.** *Analytica Chimica Acta.* 2004, Vol. 504: 163-166.
222. **Zhu WP, Gou PF, Zhu K et al.** *Journal of applied polymer science.* 2008, Vol. 109: 1968-1973.
223. **Kugimiya∗ A, Takei H.** *Analytica Chimica Acta* . 2008, Vol. 606: 252-256.
224. **Yamazaki T, Yilmaz E, Mosbach K, Sode K.** *Analytica Chimica Acta.* 2001, Vol. 435: 209-214.
225. **Emgenbroich M, Borrell C, Shinde S, Lazraq I, Vilela F, Hall AJ, Oxelbark, J, De Lorenzi E, Courtois J, Simanova A, Sellergren B.** *Chemistry, a European Journal.* 2008, Vol. 14: 9516-9529.
226. **Ye L, Mosbach K.** *Chemistry of Materials.* 2008, Vol. 20(3): 859-868.
227. **Hoshino* Y, Koide H, Urakami T, Kanazawa H, Kodama T, Oku N, Shea KJ.** *J Am Chem Soc.* 2010, Vol. 132: 6644–6645.
228. **Perrault SD.** *Nano Lett.* 2009, Vol. 9: 1909-15.
229. **Müller RH.** *Clinical Nutrition.* 1993, Vol. 12: 298-309.
230. **Wulff G, Liu J.** *Accounts of Chemical research.* 2012, Vol. 45 (2): 239-247.
231. **Lyubimova T, Caglio S, Gelfi C, Righetti PG, Rabilloud T.** *Electrophoresis* . 1993, Vol. 14: 40-50.
232. **Kim D, ALEC Scranton A.** *Journal of Polymer Science: Part A: Polymer Chemistry.* 2004 , Vol. 42: 5863–5871.
233. **Rudenberg HG.** *Rudenberg PG Advances in Imaging and Electron Physics (Elsevier).* 2010, Vol. 160.
234. **Berne BJ, Pecora R.** *Dynamic Light Scattering. Courier Dover Publications.* 2000, Vol. ISBN 0486411559.
235. **Chu B.** *Laser Light scattering: Basic Principles and Practice. Academic Press.* . 1992, Vol. ISBN 0121745511.
236. **Egerton R.** *Physical principles of electron microscopy. Springer.* 2005, Vol. ISBN 0387258000.
237. **Giessibl FJ.** *Reviews of Modern Physics.* 2003, Vol. 75: 949.
238. **Butt H, Cappella B, Kappl M.** *Surface Science Reports.* 2005, Vol. 59: 1–152.
239. **Hinterdorfer P, Dufrêne YF.** *Nature methods.* 2006, Vol. 3 (5): 347–355.
240. **Emgenbroich M, et al.** *Chemistry, a European Journal.* 2008, Vol. 14: 9516-9529.
241. **Karlgard CCS, Wong NS, Jones LW, Moresoli C.** *International Journal of Pharmaceutics.* 2003, Vol. 257: 141-151.
242. **Brahima S, Narinesingh D, Guiseppi-Elie A.** *Journal of Molecular Catalysis B: Enzymatic.* 2002, Vol. 18: 69–80.
243. **Kryscio DR, Peppas NA.** *Acta Biomaterialia.* 2012, Vol. 8(2): 461-473.
244. **Righetti PG.** *Encyclopedia of Analytical Science.* 2005: , Vol. (Second Edition):396-407.
245. **Kirat KE, Bartkowski M, Haupt K.** *Biosensors and Bioelectronics.* 2009 , Vol. 24: 2618-2624.
246. **Rabilloud T.** *Journal of Proteomics.* 2010 , Vol. 73: 1562–1572 .
247. **Tamayo FG, Turiel E, Martìn-Esteban A.** *Journal of Chromatography A* . 2007, Vol. 1152: 32-40.
248. **Matsui J, Miyoshi Y, Doblhoff-Dier O, Takeuchi T.** *Anal Chem.* 1995, Vol. 67: 4404-4408.
249. **Hochstrasser DF, et a.** *Analytical Biochemistry.* 1988, Vol. 173: 412-23.
250. **Piletska EV, et al.** *Analytica Chimica ACTA.* 2008, Vol. 607: 54–60.
251. **Yoshimatsu K, Yamazaki T, Ioannis S, Chronakis IS, Ye L.** *Journal of Applied Polymer Science* . 2012, Vol. 124: 1249–1255.

252. **Weisenhornt AL, Khorsandit M, Kasast S, Gotzost V, Butt HJ.** *Nanotechnology* . 1993, Vol. 4: 106-113.
253. **Andrews NC, et al.** *N Engl J Med.* 1999, Vol. 1986-1995.
254. **Pigeon C, et al.** J Biol Chem. 2001, Vol. 276: 7811-7819.
255. **Nemeth E, Tuttle MS , PowelsonJ , et al.** *Science.* 2004, Vol. 306: 2090–2093.
256. **Gagliardo B, N Kubat, A Faye, et al.** *J Hepatol.* 2009, Vol. 50: 394–401.
257. **Park CH, Valore EV , Waring AJ, Ganz T.** *J Biol Chem.* 2001, Vol. 276: 7806–7810.
258. **Krause A, Neitz S, Magert HJ, et al.** *FEBS Lett.* 2000, Vol. 480: 147-150.
259. **Kemna EHJM, Tjalsma H, Willems HL, Swinkels DW.** *Haematologica.* 2008, Vol. 93(1): 90-97.
260. **Frazer DM, Anderson GJ.** *Am J Clin Nutr.* 2009, Vol. 89: 475–476.
261. **Ganz T, Olbina D, Girelli D, Nemeth E, Westerman M.** *Blood.* 2008, Vol. 112: 4292–4297.
262. **Koliaraki V, Marinou M, Vassilakopoulos TP, Vavourakis E, Tsochatzis E, Pangalis GA, et al.** *PLoS ONE.* 2009, Vol. 4: e4581.
263. **Schwarz P, Strnad P, von Figura G, Janetzko A, Krayenbu P, Adler G, Hasan Kulaksiz H.** *J Gastroenterol.* 2011, Vol. 46: 648–656.
264. **Ward DG, Roberts K , Stonelake P , et al.** *Proteome Sci.* 2008, Vol. 6: 28.
265. **Bozzini C, Campostrini N , Trombini P , et al.** *Blood Cells Mol Dis.* 2008, Vol. 40: 347–352.
266. **Kemna E, Tjalsma H, Laarakkers C, Nemeth E, Willems H, Swinkels D.** *Blood.* 2005, Vol. 106: 3268–3270.
267. **Kemna EH, Tjalsma H , Podust VN , Swinkels DW.** *Clin Chem.* 2007, Vol. 53: 620–628.
268. **Tomosugi N, Kawabata H , Akatabe RW , et al.** *Blood.* 2006, Vol. 108: 1381–1387.
269. **Altamura S, Kiss J , Blattmann C , Gilles W , Muckenthaler MU.** *Biochimie.* 2009, Vol. 91: 1335-1338.
270. **I De Domenico, E Nemeth, J M Nelson, J D Phillips, R S Ajioka, MS Kay, J P Kushner, T Ganz, D M Ward, and J Kaplan.** *Cell Metabolism.* 2008, Vol. 8: 146–156.
271. **XLiu, F Yangc, D J Haile.** *Blood Cells, Molecules, and Diseases.* 2005, Vol. 35: 133-146.
272. **Lowe CR.** *Trends in Biotechnology.* 1984, Vol. 2 (3): 59-65.
273. **Cooper MA.** *Label-Free Biosensors: techniques and applications Cambridge University Press, New York.* 2009.
274. **Cochran S, Cai Ping Li, Ferro V.** *Glycoconjugate Journal.* 2009, Vol. 26 (5): 577-587.
275. **Kaneko Y, et al.** *J Gastroenterol.* 2010, Vol. 45:1163-1171.
276. **Lasocki S, et al.** *Intensive care med.* 2010, Vol. 36:1044-1048.
277. **Simonis G, et al.** *Peptides.* 2010, Vol. 31:1786-1790.
278. **Nemeth E, Rivera et al.** *J Clin Invest* . 2004, Vol. 113:1271-1276.
279. **Ashby DR, et al.** *Kidney int.* 2009, Vol. 75:976-981.
280. **Kroot T.** *Clin Chem.* 2010, Vol. 56:10.
281. **Anderson DS, Heeney MM, Roth U, Menzel C, Fleming MD, Steen H.** *Anal Chem.* 2010, Vol. 82(4):1551-1555.
282. **Galesloot TE, Vermuelen SH, Geurst-Moespot AJ, Klaver SM, Kroot JJ, van Tienoven D, Wtzels JFM, Kiemeney LALM, Sweep FC, den Heijer M, Swinkels DW.** *Blood.* 2011, Vol. 117 (25): e218-e225.
283. **Anderson NL, Anderson NG.** *Molecular and Cellular Proteomics.* 2002, Vol. 1: 845-867.
284. **Kobold U, et al.** *Clinical Chemistry.* 2008, Vol. 54: 1584-1586.
285. **Calligaris D, Villard C, Lafitte D.** *Journal of proteomics* . 2011, Vol. 74 (7): 920-934.

286. **Righetti PG, Castagna A, Antonucci F, Piubelli C, Cecconi D, Campostrini N, Rustichelli C, Antonioli P, Zanusso G, Monaco S, Lomas L, Boschetti E.** *Clinica Chimica Acta.* 2005, Vol. 357: 123-139.
287. **Mascini M, Tombelli S.** *Biomarkers.* 2008, Vol. 13(7): 637-657.
288. **Lowe CR.** *International Review of Neurobiology.* 2011, Vol. 101: 375–400.
289. **Castagna A, Campostrini N, Zaninotto F, Girelli D.** *Journal of Proteomics* . 2010, Vol. 73: 527-536.
290. **Righetti PG, et al.** *Clin Chem Lab Med.* 2003, Vol. 41: 425-438.

PUBLICATIONS DURING THE PHD STUDIES

RINGRAZIAMENTI

Al termine di questo triennio mi sento innanzitutto di ringraziare le mie tutor italiane, **Alessandra Bossi** e **Daniela Cecconi**.

Rita Polati merita poi senza dubbio un ringraziamento particolare, per essermi stata sempre di supporto, specialmente nei momenti difficili.

Di tutte le persone che ho poi conosciuto ed avuto modo di conoscere durante il triennio alcune hanno senza dubbio lasciato il segno: **Iva Chianella** per la sua disponibilità ed allegria, Dhana Lakshmi per la sua amicizia, Sergey Piletsky per la sua leadership e Michael Withcombe per la sua competenza. Queste persone sono state per me ottimi esempi.

La lista delle persone da ringraziare sarebbe sicuramente molto lunga, mi limito perciò a menzionare alcuni amici conosciuti in questo percorso: Antonio Lapenna, col quale ho condiviso momenti spensierati a Cranfield, e Piyush Sindhu Sharma che è stato ed è tuttora per me un grande amico.

Ma il grazie più grande vorrei rivolgerlo alla mia famiglia, che mi è stata sempre vicino, ed ovviamente al mio angelo custode: sai che parlo di te.